ANALYSIS OF PROPELLER SHAFT TRANSVERSE VIBRATIONS

RAMAN WARIKOO, B.Eng.(Hons.)

ANALYSIS OF

PROPELLER SHAFT TRANSVERSE VIBRATIONS

By

©Raman Warikoo, B.Eng. (Hons.)

A thesis submitted to the School of Graduate Studies
in partial fulfillment of the
requirements for the degree of
Master of Engineering

Faculty of Engineering and Applied Science
Memorial University of Newfoundland
August 1989

St. John's Newfoundland Canada

ISBN 0-315-59221-4

ABSTRACT

The aim of this project was to find a simple, practical and sufficiently accurate method for finding the natural frequencies of a propeller shaft assembly. The need for such methods is felt at the early design stages when sufficient data about the system is not available and the need to restrict the cost of analysis is of importance. Due to these facts it is clear that the methods based on the discretization of the continuum, which can estimate the natural frequencies accurately may not be advisable to go in for in the initial stages.

In the class of approximate methods, to which this work belongs, investigations done so far have crudely modelled the propeller, which was avoided in the present work. The propeller was considered to be a flexible rotor mounted with blades.

To solve the problem analysis was carried out in three parts. First the blade was studied for the natural frequencies, mode shapes, static deflections and the steady state stresses. The blade was assumed to be a cantilever and the results were cross-checked by a preliminary finite element analysis using beam elements. The assumption was found to be quite valid after doing the finite element analysis using 3-D isoparametric 20 noded elements. For the airfoil blade effects of rotation, shear deflection, rotary inertia, pitch setting angle were taken into consideration. Second the shaft-rotor system was studied and the equation for the transverse vibrations was derived in the complex plane which was solved for the natural frequencies. Effects of forward and reverse whirl, fixed and simply supported forward bearing end conditions, tail shaft length variation, rotary inertia and shear deflection were investigated. Lastly the natural frequencies of the blades and the shaft-rotor system were coupled to give the resultant natural frequency of the propeller shaft assembly. The hydrodynamic effect has been taken into consideration by incorporating the added mass effects for the propeller. Two approximations for the natural frequency

of the assembly were arrived at, the zeroth order and the first order. The true value of the frequency is supposed to lie in between the two limits. Effects due to change in the number of blades, blade geometry and the shaft parameters on the propeller shaft assembly were checked for. Agreement between the results obtained from the present work and with those available in the literature was found to be excellent. Finite element analysis comparisons also were very satisfactory.

ACKNOWLEDGEMENTS

I am grateful to Dr. M.R. Haddara for his guidance and encouragement during the course of my research work.

I feel indebted to dean graduate school for providing me with fellowship and NSERC Canada for providing me with financial assistance during the period of my studies. I am thankful to Dr. G.R. Peters, dean of engineering and Dr. T.R. Chari, associate dean of engineering for extending their cooperation and necessary help during my masters program.

A word of praise for Mervin Goodyear for typing the thesis efficiently.

To *Vidyasagaram* (Ocean of Knowledge)

and

My Parents

Contents

List of Figures

List of Tables

NOMENCLATURE

Ω_1	angular velocity of coordinate system xyz
u_s	deflection of the shaft center line along x axis due to vibrations
v_s	deflection of the shaft center line along y axis due to vibrations
ϕ	slope of the deflection along y axis
θ	slope of the deflection along x axis
$\vec{r}$	coordinates of a point on the vibrating shaft center line, in a non-rotating coordinate frame
$\vec{r'}$	coordinates of a point on the vibrating shaft center line, in a rotating coordinate frame
XYZ	global coordinate frame
xyz	frame fixed to the shaft center line.
$\vec{r}_p$	coordinates of a point on the blade
$\vec{r}_o$	coordinates of a point on the blade root
$\vec{r}_{po}$	coordinates of a point on the blade with respect to its root
u'_s	deflection of the shaft center line along x axis, in a rotating coordinate frame, to vibrations
v'_s	deflection of the shaft center line along y axis, in a rotating coordinate frame, due to vibrations
Ω	angular velocity of coordinate system $x_2y_2z_2$
I, J, K	unit vectors along X, Y, Z axes
$\hat{i}, \hat{j}, \hat{k}$	unit vectors along x, y, z axes
$\hat{i}_2, \hat{j}_2, \hat{k}_2$	unit vectors along x_2, y_2, z_2 axes
$\hat{e}_1, \hat{e}_2, \hat{e}_3$	unit vectors along ξ, η, ζ axes
u_b	deflection of the blade along ξ axis due to vibrations
w_b	deflection of the blade along ζ axis due to vibrations
R	hub radius
ψ	pitch angle

$\vec{a}_\xi$	acceleration of a point on the blade along ξ axis
$\vec{a}_\eta$	acceleration of a point on the blade along η axis
$\vec{a}_\zeta$	acceleration of a point on the blade along ζ axis
V	shear force
N	centrifugal force
θ	slope due to both bending moment and shear force
M	bending moment
k_N	nondimensional factor for centrifugal force
l	blade length
K	shape factor constant
A	area of cross-section
E	elastic modulus
G	shear modulus
ρ	density
τ	nondimensional time parameter
ϵ_1	nondimensional constant
ϵ_2	nondimensional constant
$\bar{A}$	nondimensional area
$\bar{I}$	nondimensional area moment of inertia
$\bar{\omega}$	nondimensional eigenvalue
q_k	assumed solution for transverse displacement
p_k	assumed solution for slope of the bending moment
ω_k	eigenvalue of the blade vibrations
ϵ	error incorporated due to assumed solutions
p_{KA}, p_{KB}	explicit expressions for p_k
p_{K1A}, p_{K1B}	explicit expressions for p'_k
λ	eigenvalue of the system
β_k	eigenvalue index

σ_k	a constant
$f(x)$	spatial function of the force on the blade
$g(t)$	time function of the force on the blade
$[\bar{K}]$	global stiffness matrix of a uniform cantilever
$[\bar{M}]$	global mass matrix of a uniform cantilever
$[K]$	global stiffness matrix of the blade
$[M]$	global mass matrix of the blade
$\{F\}$	force vector
$\{q\}$	displacement vector
φ_r	rth nondimensional mode shape of the blade
T	blade thickness
u, v, w	components of generalized displacement vector
$[N]$	shape function matrix
$\{c\}$	nodal coordinate vector
$[m^e]$	element mass matrix
$[k^e]$	element stiffness matrix
$[k_\sigma^e]$	element stress stiffness matrix
$[B]$	strain displacement matrix
$\{\delta\}$	derivative of the nodal displacement vector, w.r.t. x, y, z
$\{\delta'\}$	derivative of the nodal displacement vector, w.r.t. ξ, η, ζ
$[k^e]$	element stress stiffness matrix
$[s]$	stress matrix
ν	poissons ratio
$[J]$	jacobian matrix
$[\Gamma]$	inverse of jacobian matrix
W_i	Gauss weights
$\{\epsilon_L\}$	linear strains
$\{\epsilon_{NL}\}$	nonlinear strains

$\{U_{NL}\}$	strain energy due to nonlinear strains
$[T]$	transformation matrix for condensed displacements
$[K_R]$	reduced stiffness matrix of the system
$[M_R]$	reduced mass matrix of the system
H	angular momentum of the rotor
I_{mx}, I_{my}, I_{mz}	x, y, z components of the mass moment of inertia of the rotor
V_x, V_y	shear force along x, y axis of the rotor
M_x, M_y	bending moment along x, y axis of the rotor
w_r	rotor transverse displacement in the complex plane
w_s	overhang transverse displacement in the complex plane
w_t	tail shaft transverse displacement in the complex plane
a, b, c	rotor, overhang, tail shaft lengths respectively
ξ_1, ξ_r, ξ_s	constants for the rotor and tail shaft
$A_1 \sim A_4$	constants for the displacement function of the rotor
$P_1 \sim P_4$	constants for the displacement function of the overhang
$Q_1 \sim Q_4$	constants for the displacement function of the tail shaft
k	fixity of the forward end bearing
P_i	natural frequency of an isolated system composed of mass and one of the restoring elements
δ_{ij}	perturbation parameter
δ_s	sum of the perturbation parameter for various combinations of inertia and restoring elements
R_{ND}	nondimensional radius of the hub
$A_{11} \sim A_{14}$	nondimensional coefficients of the area polynomial

Chapter 1

INTRODUCTION AND LITERATURE REVIEW

Propeller shaft is an important part of the ship propulsion system and the recent failures of the propeller shafts due to fatigue make it imperative to have an accurate estimate of the propeller shaft natural frequencies early in the design stage to avoid resonance, which of course is one of the prime factors of fatigue failures. This can prove useful in the selection of the engine speed and reduction ratios. Modal analysis not only helps in predicting critical speeds but also in assessing the dynamic stresses in the propeller blade, which are of equal importance, especially at the blade root.

For the propeller shaft the main exciting force comes from the blade excitations, which are caused by the non-uniform wake around the ship propeller. There can be other exciting forces due to mass imbalance, hysteresis damping, fluid friction in the bearings etc., but such effects have not been found to be of predominant effect. It is important to note that the propeller exciting forces can be expressed in a series, whose frequencies bear a ratio of multiples of N to the rotational speed of the propeller shaft, where N is the number of the blades.

1.1 Scope of the Investigation

The main aim of this project was to find a simple, practical and sufficiently accurate method for finding the natural frequencies of the propeller shaft, which can prove

quite reliable and handy in the early stages of design and allows for the study of the effect of propeller shaft geometry on the natural frequencies. The analysis was carried out in two parts: first the blade was analyzed and then the shaft-rotor system. The fundamental frequency of the propeller shaft assembly was estimated by suitably coupling those obtained for the blade and that for the shaft-rotor system.

The natural frequencies of the transverse vibration of a propulsion shafting system can be accurately predicted using numerical methods such as finite element analysis as in Kuo, (1965), Holzer's scheme or Myklestad-Prohl method as in Toms and Martin, (1972). The use of such methods usually requires detailed information which may not be available at the early stages of design process. In addition, the cost of using such programs does not warrant their use when we just need an approximate estimate of the natural frequencies. This clearly highlights the importance of the approximate methods which are by no means complicated and still are not a compromise in their accuracy. The present work falls in this category and satisfies the above mentioned qualities besides taking into consideration some other important characteristics of the propeller shaft which are not available in the existing literature, like the airfoil cross-sectional area of the blades, considering the propeller to be a flexible hub mounted with blades.

1.2 Literature Survey

1.2.1 Propeller Shaft Analysis

In the early fifties two well-known approximate methods for determining critical propeller shaft speeds with respect to lateral vibrations were developed. The first one was formulated by Panagopulos (1950) wherein the momentum of the rotating propeller is ignored, whereas Jasper (1952) ignores the shaft mass and considers the rotor as a thin disc; the rotor is an approximate modelling for the propeller. These two researchers are considered to be the pioneers in the field of determining the natural frequencies of the propeller shaft by such approximate approaches.

Beek (1976) in early seventies improved the existing methods by considering the effects of propeller moment and inertia force, however, the propeller was treated as a disc. He considers a non-rotating shaft on two supports with an overhung mass. Starting from the differential equation governing the dynamic behaviour of a beam, propeller moment and inertia force are applied as boundary conditions at the end of the overhung beam.

In an attempt to solve the problem of finding the natural frequencies of a propeller shaft Woytowich (1979) employed Dunkerley's method for this purpose. The propeller is approximated as a thin disc attached to a massless elastic shaft. An equation of motion, derived by Den Hartog (1956) giving the whirling natural frequencies of a disc on a rotating shaft is used to get the whirling natural frequencies of the overhung portion of the propeller shaft. The frequencies of the exciting forces bear the ratio N to the shaft rotation speed, where N is the number of propeller blades. For the tail shaft, transverse natural frequencies are calculated from the conventional Euler-Bernoulli equation. Dunkerley's formula is used to couple the two natural frequencies to get the combined natural frequency of the system similar work can also be found in Yagoda and Ketchman (1982). In this formulation Den-Hartog's equation gives two values for critical speeds one for forward whirl and another for reverse whirl; it also accounts for the propeller shaft forward bearing end conditions which can be assumed to be fixed or simply supported. The forward and reverse whirl correspond respectively to the conditions where the propeller shaft excitation frequency equals plus or minus times the product of blade number and rotational speed.

Haddara (1988) treats the whole propeller shaft simultaneously and finds the coupled transverse vibration of the shafting in the horizontal and vertical planes. The propeller is appropriately modeled as a rotor. The shaft is considered in three parts: first the rotor is taken wherein the coupled natural frequencies are obtained by taking into consideration the rotary inertia. The other two parts are the overhung

shaft and the tail shaft. The three segments are linked by the boundary conditions. In this work the effect of propeller mass on the whirling natural frequencies of the propeller shaft can be clearly seen; for the shafts having small tail shafts the values of forward and reverse whirl are found to be distinct unlike for the shafts with long tail shafts, wherein the tail shaft mass has an overriding effect.

1.2.2 Blade Analysis

As stated before the problem of finding natural frequencies of propeller shaft was solved by coupling the corresponding natural frequencies of the blades and the shaft. The blades assumed for the present work are of airfoil section. This problem has not been dealt with in the existing literature. Subrahmanyam et.al. (1982) used the Reissner and the potential energy method for the analysis of lateral vibrations of a rotating blade taking shear deflection and rotary inertia into account; this study has been done only for beams of uniform cross-sectional area.

Fox (1985) in his work on rotating cantilevers considers a general case of compact beams wherein the flexural stiffness in the two perpendicular directions are both finite and of the same order so that the assumption that the flexural vibration is confined to a single plane is no longer valid. This leads to a pair of coupled equations of motion which can be decoupled for some special cases of pitch angle or cross-section; the results obtained for these special cases have been compared with those available in the literature. The solution of the equations has been carried out using Galerkin's technique.

More recently, the bending vibrations of a class of rotating beams has been dealt with by Storti et.al. (1987). The method depends on factoring the fourth-order differential operator, which appears in the equation of motion, into a pair of commuting second-order operators. These two second-order differential equations are then solved in terms of hypergeometric functions. The factorization of the fourth order operator can be achieved only in case of selected blade profile geometry.

Moreover, the effects of shear deflection and rotary inertia have not been taken into consideration.

1.3 Description Of The Investigation

The work of this investigation was carried out in stages which serve us in studying the different aspects of the system. The stages are given as:

1. The modal analysis of the propeller blade. The blade has been idealised as a non uniform cantilever beam with an airfoil section. The effects of blade rotation, blade pitch angle setting, shear deflection and rotary inertia have been taken into consideration while solving for the natural frequencies and the mode shapes of the blade. The method employed to solve the problem is based on an improvisation over Galerkin's technique. The assumed displacement function is adjusted in iterations till the extracted eigenvalues become fairly constant in their magnitudes. As a preliminary check finite element analysis using tapered beam elements was carried out, which gave very close comparisons.
2. The analysis of the blade static deflections and stresses.
3. The 3-D finite element analysis of the blade to check the validity of the assumption of blade as a cantilever beam. 20-noded isoparamateric brick elements have been employed for the analysis.
4. The modal analysis of the shaft-rotor system. The shaft was considered to consist of a rotor as an overhang with the forward end bearing of variable fixity. The effects of rotary inertia and shear deflection for the rotor have been considered. In this type of a system the transverse vibrations take place in two perpendicular planes and the equation of motion governing them has been obtained in the complex plane. The critical speeds obtained thus correspond to the forward and reverse whirl of the shaft.
5. After having evaluated the respective frequencies of the two sub-systems of the propeller shaft, namely the blades and the shaft-rotor system, an extended Southwell-Dunkerley method given by Endo and Taniguchi,

(1976) is employed to estimate the natural frequencies of the assembly. For employing this method a criterion has been satisfied, which justifies the use of this approximation for our system.

6. For a marine propeller it is necessary to consider added mass and added moment of inertia in the determination of the natural frequencies. However, the solution of the hydrodynamic problem is beyond the scope of this work. Recourse to empirical values was made as given by Haddara (1988), Brooks (1980) and Toms (1972). A sensitivity analysis was carried out to investigate the importance of calculating the added mass of the propeller accurately.

Chapter 2

BLADE ANALYSIS

2.1 Acceleration Analysis

2.1.1 Introduction

In this section the expressions for acceleration of a point on the shaft center line and on the blade, in the rotating coordinate system have been derived. The effects of shaft bending and shaft vibrations have been taken into account. The coordinate systems fixed to the shaft center line and blade have been described in appendix A

2.1.2 Acceleration of a Point on the Shaft Center Line

The angular velocity of the coordinate system xyz, fixed to the shaft center line, with respect to the fixed reference frame XYZ,is given as:(refer appendix A)

$$\vec{\Omega}_1 = \dot{\phi} I + \dot{\theta} \hat{j}_1 \tag{2.1}$$

The coordinates of a point on the vibrating shaft center line, which is aligned with z axis are given as:

$$\vec{r} = u_s I + v_s J \tag{2.2}$$

where:

$$\varphi = -\frac{\partial v_s}{\partial z} \tag{2.3}$$

$$\theta = \frac{\partial u_s}{\partial z} \tag{2.4}$$

u_s = deflection of the shaft center line along X axis, due to vibrations

v_s = deflection of the shaft center line along Y axis, due to vibrations

dots represent differentiation w.r.t time

After the transformation of coordinate axes and under the assumption:

$$\cos\theta \approx \cos\phi \approx 1$$

$$\sin\theta \approx \theta, \sin\phi \approx \phi$$

we get:(refer to appendix B)

$$\vec{\Omega}_1 = \dot{\phi}\hat{\imath} + \dot{\theta}\hat{\jmath}$$

$$\vec{r} = u_s\hat{\imath} + v_s\hat{\jmath} \tag{2.5}$$

The velocity of a point on the shaft center line as in Torby (1984) is given as:

$$\dot{\vec{r}} = \dot{u}_s\hat{\imath} + \dot{v}_s\hat{\jmath} + \vec{\Omega}_1 \times \vec{r}$$

The last term appears since the shaft center line has an angular velocity $\vec{\Omega}_1$

$$\vec{\Omega}_1 \times \vec{r} = \begin{vmatrix} \hat{\imath} & \hat{\jmath} & \vec{k} \\ \dot{\phi} & \dot{\theta} & 0 \\ u_s & v_s & 0 \end{vmatrix} = (v_s\dot{\phi} - u_s\dot{\theta})\hat{k}$$

$$\cong 0$$

(product of two small quantities is negligible).

$$\dot{\vec{r}} = \dot{u}_s\hat{\imath} + \dot{v}_s\hat{\jmath} \tag{2.6}$$

$$\ddot{\vec{r}} = \ddot{u}_s\hat{\imath} + \ddot{v}_s\hat{\jmath} + \vec{\Omega}_1 \times \dot{\vec{r}}$$

$$= \ddot{u}_s\hat{\imath} + \ddot{v}_s\hat{\jmath} \tag{2.7}$$

2.1.3 Acceleration of a Point on the Blade

As given in the fig 2.1, coordinates of a point on the propeller blade can be written as:

$$\vec{r}_p = \vec{r}_o + \vec{r}_{po} \tag{2.8}$$

From equation (2.5) the coordinates of a point on the shaft center line are:

$$\vec{r} = u_s\hat{\imath} + v_s\hat{\jmath}$$

In the rotating coordinate system it takes the form $\vec{r'} = u'_s\hat{\imath}_2 + v'_s\hat{\jmath}_2$, such that

$$\left\{ \begin{array}{c} u'_s \\ v'_s \end{array} \right\} = \left[\begin{array}{cc} \cos\Omega t & \sin\Omega t \\ -\sin\Omega t & \cos\Omega t \end{array} \right] \left\{ \begin{array}{c} u_s \\ v_s \end{array} \right\} \tag{2.9}$$

where:

u'_s = shaft deflections in the x_2 direction in the rotating frame $x_2y_2z_2$

v'_s = shaft deflections in the y_2 direction in the rotating frame $x_2y_2z_2$

Ω = rotational speed of coordinate frame $x_2y_2z_2$

The coordinates of a point at the blade root are given as:

$$\begin{aligned} \vec{r}_o &= \vec{r'} + R\hat{\jmath}_2 \\ &= (u'_s\hat{\imath}_2 + v'_s\hat{\jmath}_2) + R\hat{\jmath}_2 \\ &= u'_s\hat{\imath}_2 + (v'_s + R)\hat{\jmath}_2 \end{aligned} \tag{2.10}$$

Consider a point P on the blade at a distance η from the blade root, as shown in fig.2.1. The position vector of P in the blade local coordinate system can be given as:

$$\vec{r}_{po} = u_b\hat{e}_1 + \eta\hat{e}_2 + w_b\hat{e}_3 \tag{2.11}$$

using equation (2.10) and (2.11) in equation (2.8) we obtain:

$$\vec{r}_p = u'_s\hat{\imath}_2 + (v'_s + R)\hat{\jmath}_2 + u_b\hat{e}_1 + \eta\hat{e}_2 + w_b\hat{e}_3 \tag{2.12}$$

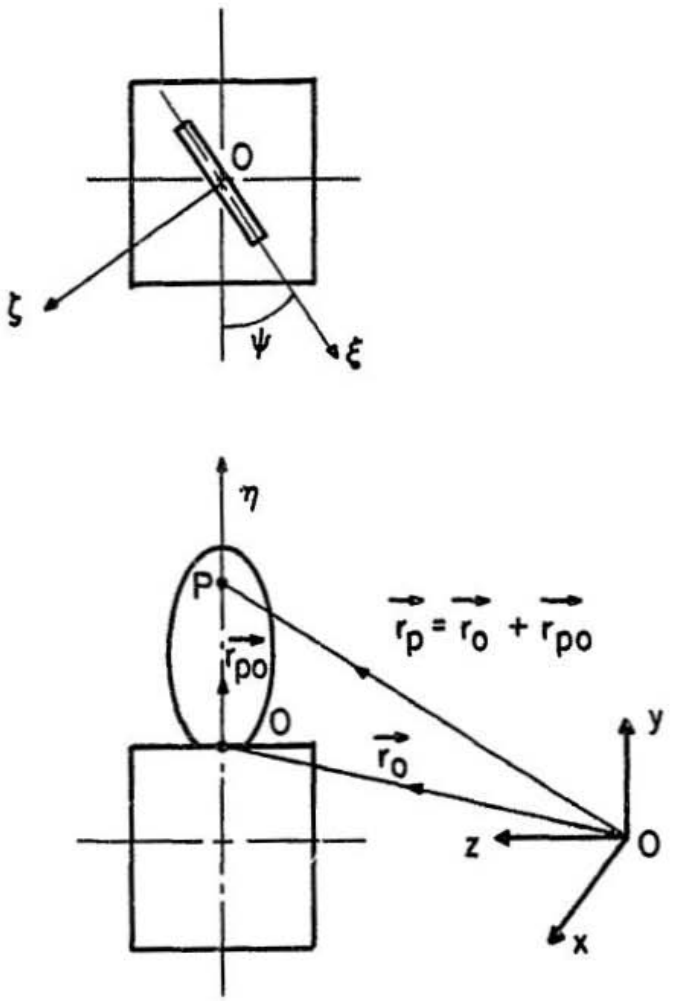

Figure 2.1: Blade coordinate system

where:

R = hub radius

u_b = transverse deflection of point P in ξ direction

w_b = transverse deflection of point P in ζ direction

e_1, e_2, e_3 = unit vectors of the blade local coordinate frame along ξ, η, ζ respectively.

Equation (2.12) gives the absolute displacement of a point on the blade in the rotating coordinate system, which when transformed to blade local coordinate frame, takes the form: (see appendix B)

$$\vec{r}_p = (u'_s \cos\psi + u_b)\hat{e}_1 + (v'_s + R + \eta)\hat{e}_2 + (u'_s \sin\psi + w_b)\hat{e}_3 \qquad (2.13)$$

where ψ is the pitch setting angle of the blade on the hub.

The angular velocity of the reference frame $x_2y_2z_2$ rotating at Ω is given as: (refer appendix A)

$$\vec{\Omega}_2 = \dot{\phi}\hat{\imath} + \dot{\theta}\hat{\jmath} + \Omega\hat{k}$$

Since the coordinate frame fixed to the root of blade has time invariant transformations R and ψ from $x_2y_2z_2$ reference frame, the angular velocity of $\xi\eta\zeta$ coordinate frame is given as: (see appendix B for details)

$$\begin{aligned}
\vec{\Omega}_3 &= \dot{\phi}\hat{\imath} + \dot{\theta}\hat{\jmath} + \Omega\hat{k} \\
&= e_1\left[\dot{\phi}\cos\Omega t\cos\psi + \dot{\theta}\sin\Omega t\cos\psi - \Omega\sin\psi\right] \\
&\quad + e_2\left[-\dot{\phi}\sin\Omega t + \dot{\theta}\cos\Omega t\right] \\
&\quad + e_3\left[\dot{\phi}\cos\Omega t\sin\psi + \dot{\theta}\sin\Omega t\sin\psi + \Omega\cos\psi\right] \qquad (2.14)
\end{aligned}$$

from equation (2.13), we have

$$\begin{aligned}
\dot{\vec{r}}_p &= (\dot{u}'_s\cos\psi + \dot{u}_b)\hat{e}_1 + \dot{v}'_s\hat{e}_2 + (\dot{u}'_s\sin\psi + \dot{w}_b)\hat{e}_3 + \vec{\Omega}_3 \times \vec{r}_p \\
&= \left[(\dot{u}'_s\cos\psi + \dot{u}_b) - (R+\eta)(\dot{\phi}\cos\Omega t + \dot{\theta}\sin\Omega t)\sin\psi - \Omega(v'_s + R + \eta)\cos\psi\right]\hat{e}_1 \\
&\quad + [\dot{v}'_s + \Omega(u'_s\sin\psi + w_b)\sin\psi + \Omega(u'_s\cos\psi + u_b)\cos\psi]\hat{e}_2 \\
&\quad + \left[(\dot{u}'_s\sin\psi + \dot{w}_b) + (R+\eta)(\dot{\phi}\cos\Omega t + \dot{\theta}\sin\Omega t)\cos\psi - \Omega(v'_s + R + \eta)\sin\psi\right]\hat{e}_3
\end{aligned}$$

from the above expression, $\ddot{\vec{r}}_p$ is given as:

$$\begin{aligned}
\ddot{\vec{r}}_p &= [(\ddot{u}'_s\cos\psi + \ddot{u}_b) - (R+\eta)(\ddot{\phi}\cos\Omega t + \ddot{\theta}\sin\Omega t)\sin\psi \\
&\quad -(R+\eta)(-\dot{\phi}\sin\Omega t + \dot{\theta}\cos\Omega t)\Omega\sin\psi - \Omega\dot{v}'_s\cos\psi]\hat{e}_1 \\
&\quad + [\ddot{v}'_s + \Omega(\dot{u}'_s\sin\psi + \dot{w}_b)\sin\psi + \Omega(\dot{u}'_s\cos\psi + \dot{u}_b)\cos\psi]\hat{e}_2 \\
&\quad +[(\ddot{u}'_s\sin\psi + \ddot{w}_b) + (R+\eta)(\ddot{\phi}\cos\Omega t + \ddot{\theta}\sin\Omega t)\cos\psi \\
&\quad +(R+\eta)(-\dot{\phi}\sin\Omega t + \dot{\theta}\cos\Omega t)\Omega\cos\psi - \Omega\dot{v}'_s\sin\psi]\hat{e}_3 \\
&\quad +\vec{\Omega}_3 \times \dot{\vec{r}}_p \\
&= [\ddot{u}_b - \Omega^2(w_b\sin\psi\cos\psi + u_b\cos^2\psi) + (\ddot{u}'_s - 2\Omega\dot{v}'_s - \Omega^2 u'_s)\cos\psi \\
&\quad -(R+\eta)(\ddot{\phi}\cos\Omega t + \ddot{\theta}\sin\Omega t)\sin\psi \\
&\quad +2\Omega(R+\eta)(\dot{\phi}\sin\Omega t - \dot{\theta}\cos\Omega t)\sin\psi]\hat{e}_1 \\
&\quad + [\ddot{v}'_s + \dot{u}'_s + \Omega(2\dot{w}_b\sin\psi + 2\dot{u}_b\cos\psi + \dot{u}'_s - v'_s - R - \eta)]\hat{e}_2 \\
&\quad +[\ddot{w}_b - \Omega^2(u_b\sin\psi\cos\psi + w_b\sin^2\psi) + (\ddot{u}'_s - 2\Omega\dot{v}'_s - \Omega^2 u'_s)\sin\psi \\
&\quad +(R+\eta)(\ddot{\phi}\cos\Omega t + \ddot{\theta}\sin\Omega t)\cos\psi \\
&\quad -2\Omega(R+\eta)(\dot{\phi}\sin\Omega t - \dot{\theta}\cos\Omega t)\cos\psi]\hat{e}_3 \qquad (2.15) \\
&= a_\xi\hat{e}_1 + a_\eta\hat{e}_2 + a_\zeta\hat{e}_3 \qquad (2.16)
\end{aligned}$$

where:

$\vec{a}_\xi$ = acceleration of a point on the blade along ξ axis in the $\xi\eta\zeta$ local coordinate system of the blade

$\vec{a}_\eta$ = acceleration of a point on the blade along η axis in the $\xi\eta\zeta$ local coordinate system of the blade

$\vec{a}_\zeta$ = acceleration of a point on the blade along ζ axis in the $\xi\eta\zeta$ local coordinate system of the blade

(for details refer to appendix C)

Equation (2.16) gives the expression for absolute acceleration of a point on the blade at a distance η from the blade root.

Using equations (2.3),(2.4)and(2.9) we have:

$$\begin{aligned}\ddot{\phi}\cos\Omega t + \ddot{\theta}\sin\Omega t &= \frac{\partial^3}{\partial z \partial t^2}[-v_s\cos\Omega t + u_s\sin\Omega t] \\ &= -\frac{\partial^3 v_s'}{\partial z \partial t^2} \qquad (2.17)\end{aligned}$$

$$\begin{aligned}\dot{\phi}\sin\Omega t - \dot{\theta}\cos\Omega t &= \frac{\partial^2}{\partial z \partial t}[-v_s\sin\Omega t - u_s\cos\Omega t] \\ &= -\frac{\partial^2 u_s'}{\partial z \partial t} \qquad (2.18)\end{aligned}$$

using equations (2.17) and (2.18) in equation (2.16) we have:

$$\begin{aligned}\vec{a}_\zeta &= \ddot{w}_b - \Omega^2(u_b\cos\psi + w_b\sin\psi)\sin\psi \\ &\quad +(\ddot{u}_s' - 2\Omega\dot{v}_s' - \Omega^2 u_s')\sin\psi \\ &\quad -(R+\eta)\left[\frac{\partial^3 v_s'}{\partial z\partial t^2} - 2\Omega\frac{\partial^2 u_s'}{\partial z\partial t}\right]\cos\psi \qquad (2.19)\end{aligned}$$

2.2 Equation of Motion

2.2.1 Introduction

In this section the equation of motion of a rotating blade, having a non-uniform cross-sectional area and moment of inertia, has been derived using Newtonian approach. The effects of centrifugal force due to rotation, pitch setting angle, shear deformation and rotary inertia have been taken into consideration. The propeller blade has been treated as a cantilever with bending stiffness about the major principle axis sufficiently large to ignore bending about this axis. The acceleration of the blade is considered purely due to blade vibrations and excitations due to the

shaft vibrations have been ignored since we are interested in the isolated natural frequencies of the blade. The blade is assumed to have a vanishing thickness at the tip (which simplifies the treatment of boundary conditions) and a coincident mass and elastic axes (doubly symmetric), so that the torsional coupling can be eliminated.

2.2.2 Mathematical Formulation

Consider the free-body diagram of a blade element in $\zeta\eta$ plane, as given in fig.2.2, where in the coordinate system $\xi\eta\zeta$ is rotating with the blade and has its origin at the blade root. The acceleration of the element is obtained from equation (2.19) after ignoring the shaft displacements due to vibrations, blade deflection along ξ axis being very small in magnitude has been neglected.

Equilibrium of forces in the ζ direction yields:

$$V\cos\phi - (V+dV)\cos\phi + (N+dN)\sin\theta - N\sin\theta = (md\eta)\ddot{\zeta} \tag{2.20}$$

$$m\ddot{\zeta} = -\frac{dV}{\partial\eta} + \frac{\partial}{\partial\eta}(N\sin\theta) \tag{2.21}$$

Equilbrium of moments in the $\eta - \zeta$ plane yields :

$$(M+dM) - (V+dV)d\eta - M = \rho I d\eta \frac{\partial^2\phi}{\partial t^2} \tag{2.22}$$

$$\rho I\ddot{\phi} = \frac{\partial M}{\partial\eta} - V \tag{2.23}$$

where:

$$M = EI\frac{\partial\phi}{\partial\eta} \tag{2.24}$$

$$\ddot{\zeta} = \ddot{w}_b - \Omega^2 w_b \sin^2\psi \tag{2.25}$$

$$N = \rho\Omega^2 k_N l^4 \tag{2.26}$$

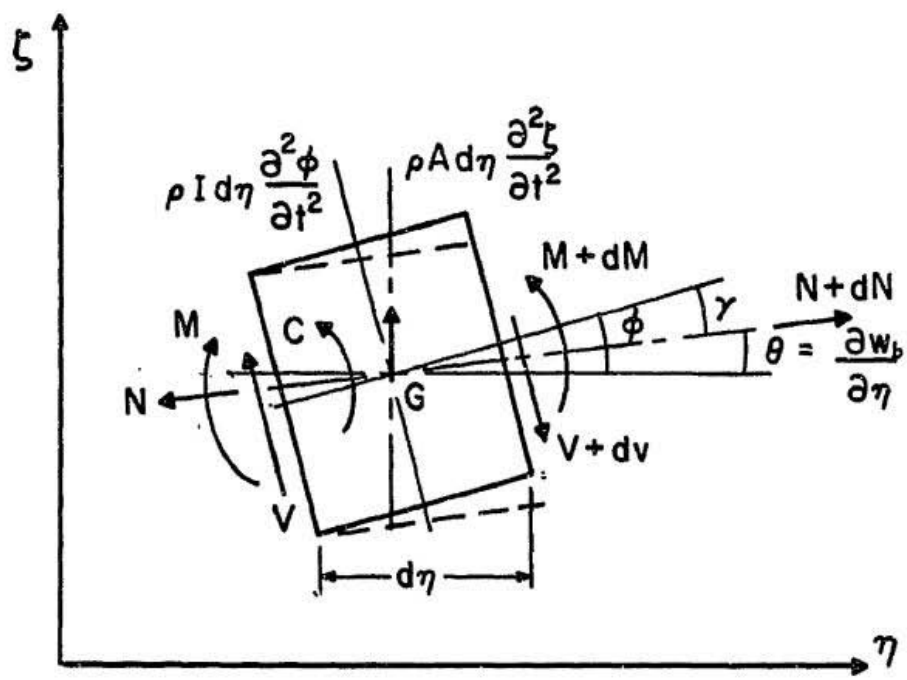

Figure 2.2: Free body diagram of the blade element

V = shear force
ϕ = slope due to bending alone
N = centrifugal force, (refer to appendix I)
θ = slope due to bending and shear
m = total virtual mass per unit length of the blade
M = bending moment
ρ = density
I = area moment of inertia
E = modulus of elasticity
w_b = transverse displacement along ζ axis
Ω = hub rotation rate
dots over the variable denote differentiation with respect to time.

As can be seen in Rao (1986) the shear force V decreases the slope of the deflection curve by an angle γ. Now the slope of the deflection curve due to both bending and shear is given by $\phi - \gamma$, hence :

$$\frac{\partial w_b}{\partial \eta} = \phi - \gamma \tag{2.27}$$

shear angle γ is given as :

$$\gamma = \frac{V}{KAG} \tag{2.28}$$

$$V = \left(\phi - \frac{\partial w_b}{\partial \eta}\right) KAG \tag{2.29}$$

where:

γ = shear angle
K = shape constant, depending on the cross-section of the element
A = cross-sectional area
G = shear modulus
from equation (2.21) we have :

$$m(\ddot{w}_b - \Omega^2 w_b \sin^2\psi) = -\frac{\partial}{\partial \eta}\left[KAG(\phi - \frac{\partial w_b}{\partial \eta})\right] + \frac{\partial}{\partial \eta}(N \sin\theta) \tag{2.30}$$

since θ is small

$$\sin\theta \approx \tan\theta \approx \frac{\partial w_b}{\partial \eta}$$

$$m(\ddot{w}_b - \Omega^2 w_b \sin^2\psi) = -KG[A(\phi - w_b')]' + (N w_b')' \tag{2.31}$$

where a dash over the variable represents differentiation w.r.t. η.

Substituting (2.24) and (2.29) into (2.23), we get:

$$\rho I\ddot{\phi} = \frac{\partial}{\partial\eta}[EI\phi'] - KGA\left(\phi - \frac{\partial w_b}{\partial\eta}\right) \tag{2.32}$$

2.2.3 Non-Dimensionalization

For non-dimensionalization w.r.t. space and time variables, we define the following non-dimensional parameters:

$$z = \frac{w_b}{l}$$

$$\tau = \Omega t$$

$$y = \frac{\eta}{l}$$

$$k_N = \frac{1}{l^4}\int_\eta^l A(\eta + R)d\eta$$

$$\epsilon_1 = \frac{KG}{\rho\Omega^2 l^2}$$

$$\epsilon_2 = \frac{E}{\rho\Omega^2 l^2}$$

$$\overset{*}{A} = \frac{A}{l^2}$$

$$\overset{*}{I} = \frac{I}{l^4}$$

where :

l = blade length
R = hub radius

Equations (2.31) and (2.32) can be written in the following non-dimensional form :

$$\overset{*}{A}\,\ddot{z} - \overset{*}{A}\,z\sin^2\psi = -\epsilon_1[\overset{*}{A}\,(\phi - z')]' + (k_N z')' \tag{2.33}$$

$$\overset{*}{I}\,\ddot{\phi} = \epsilon_2(\overset{*}{I}\,\phi')' - \epsilon_1\,\overset{*}{A}\,(\phi - z') \tag{2.34}$$

where the boundary conditions are given as:

$$z, z' = 0 \quad \text{at} \quad y = 0$$

$$\overset{**}{I}, \overset{*}{A}, k_N = 0 \quad \text{at} \quad y = 1$$

Equations (2.34) and (2.33) are two coupled partial differential equations in two variables z and ϕ. The coefficients of the equations are functions of the independent variable y. Since the exact solution of the problem is difficult to obtain, a numerical technique based on Galerkin's method as explained in Meirovitch (1967) has been used.

2.2.4 Solution of the Equations

We assume a series solution for the variables z and ϕ in terms of the comparison functions q_k and p_k respectively, where q_k and p_k satisfy the boundary conditions of the system.

$$z = \sum_{k=1}^{n} q_k e^{i\omega_k t}$$

$$\phi = \sum_{k=1}^{n} p_k e^{i\omega_k t}$$

using the above expressions in equations (2.33) and (2.34) we get :

$$\sum_{k=1}^{n} \left\{ -\omega_k^2 \overset{*}{A}\, q_k - \overset{*}{A}\, q_k \sin^2 \psi \right\} = \sum_{k=1}^{n} \left\{ -\epsilon_1 [\overset{*}{A}\, (p_k - q_k')]' + (k_N q_k')' \right\} \tag{2.35}$$

and

$$\sum_{k=1}^{n} \left\{ -\omega_k^2 \overset{**}{I}\, p_k \right\} = \sum_{k=1}^{n} \left\{ \epsilon_2 (\overset{*}{I}\, p_k')' - \epsilon_1 \overset{*}{A}\, (p_k - q_k') \right\} \tag{2.36}$$

Galerkin's method of weighted residuals states that the error ϵ incorporated in the above two equations, due to the assumed solution integrated over the domain should vanish.

ie.

$$\int_D \epsilon q_r \, dD = 0$$

and for $r = 1, 2, 3 \cdots n$

$$\int_D \epsilon p_r dD = 0 \tag{2.37}$$

where the domain D for the present case is the length of the blade varying from 0 to 1.

For equation (2.35)

$$\epsilon = \sum_{k=1}^{n} \left\{ -\omega_k^2 \, \overset{\bullet}{A} \, q_k - \overset{\bullet}{A} \, q_k \sin^2 \psi + \epsilon_1 [\overset{\bullet}{A} \, (p_k - q_k')]' - (k_N q_k')' \right\} \tag{2.38}$$

For equation (2.36)

$$\epsilon = \sum_{k=1}^{n} \left\{ -\omega_k^2 \, \overset{\bullet}{I} \, p_k - \epsilon_2 (\overset{\bullet}{I} \, p_k')' + \epsilon_1 \, \overset{\bullet}{A} \, (p_k - q_k') \right\} \tag{2.39}$$

using equation (2.37) we get :

$$\int \sum_{k=1}^{n} \left\{ -\omega_k^2 \, \overset{\bullet}{A} \, q_k - \overset{\bullet}{A} \, q_k \sin^2 \psi + \epsilon_1 [\overset{\bullet}{A} \, (p_k - q_k')]' - (k_N q_k')' \right\} q_r dy = 0 \tag{2.40}$$

and for $r = 1, 2, 3 \cdots n$

$$\int \sum_{k=1}^{n} \left\{ -\omega_k^2 \, \overset{\bullet}{I} \, p_k - \epsilon_2 (\overset{\bullet}{I} \, p_k')' + \epsilon_1 \, \overset{\bullet}{A} \, (p_k - q_k') \right\} p_r dy = 0 \tag{2.41}$$

for $r = 1, 2, 3 \cdots n$

Boundary conditions for the blade are :

at

$$y = 0 \quad q_r = 0$$

at

$$y = 1 \quad \overset{\bullet}{A}, k_N = 0 \tag{2.42}$$

On the application of boundary conditions, the above equations take the following form:(as explained in appendix D)

$$-\omega_k^2 \sum_{k=1}^{n} \int_0^1 \overset{\bullet}{A} \, q_r q_k dy - \sin^2 \psi \sum_{k=1}^{n} \int_0^1 \overset{\bullet}{A} \, q_r q_k dy$$

$$= \epsilon_1 \sum_{k=1}^{n} \int_0^1 \overset{\bullet}{A} \, q_r' (p_k - q_k') dy - \sum_{k=1}^{n} \int_0^1 k_N q_r' q_k' dy \tag{2.43}$$

for $r = 1, 2, 3 \cdots n$

and

$$\omega_k^2 \sum_{k=1}^{n} \int_0^1 \overset{*}{I}\, p_k p_r dy - \epsilon_2 \sum_{k=1}^{n} \int_0^1 \overset{*}{I}\, p_r' p_k' dy - \epsilon_1 \sum_{k=1}^{n} \int_0^1 \overset{*}{A}\, p_r (p_k - q_k') dy = 0 \quad (2.44)$$

equations (2.43) and (2.44) reduce to the form:

$$\omega_k^2 \sum_{k=1}^{n} \int_0^1 \overset{*}{A}\, q_r q_k dy + \sin^2 \psi \sum_{k=1}^{n} \int_0^1 \overset{*}{A}\, q_r q_k dy$$

$$= -\epsilon_1 \sum_{k=1}^{n} \int_0^1 \overset{*}{A}\, q_r' (p_k - q_k') dy + \sum_{k=1}^{n} \int_0^1 k_N q_r' q_k' dy \quad (2.45)$$

for $r = 1, 2, 3 \cdots n$

and

$$\omega_k^2 \sum_{k=1}^{n} \int_0^1 \overset{*}{I}\, p_k p_r dy = \epsilon_2 \sum_{k=1}^{n} \int_0^1 \overset{*}{I}\, p_r' p_k' dy + \epsilon_1 \sum_{k=1}^{n} \int_0^1 \overset{*}{A}\, p_r (p_k - q_k') dy \quad (2.46)$$

for $r = 1, 2, 3 \cdots n$

adding the above two equations, we get :

$$\omega_k^2 \sum_{k=1}^{n} \int_0^1 [\overset{*}{A}\, q_r q_k + \overset{*}{I}\, p_k p_r] dy + \sin^2 \psi \sum_{k=1}^{n} \int_0^1 \overset{*}{A}\, q_r q_k dy$$

$$= -\epsilon_1 \sum_{k=1}^{n} \int_o^1 \overset{*}{A}\, [q_r' (p_k - q_k') - p_r (p_k - q_k') dy$$

$$+ \epsilon_2 \sum_{k=1}^{n} \int_0^1 \overset{*}{I}\, p_r' p_k' dy + \sum_{k=1}^{n} \int_0^1 k_N q_r' q_k' dy$$

$$= \epsilon_2 \sum_{k=1}^{n} \int_0^1 \overset{*}{I}\, p_r' p_k' dy + \sum_{k=1}^{n} \int_0^1 k_N q_r' q_k' dy$$

$$+ \epsilon_1 \int_o^1 \overset{*}{A}\, [(p_k - q_k')(p_r - q_r') dy \quad (2.47)$$

for $r = 1, 2, 3 \cdots n$

from equation (2.35), we have : (see appendix E)

$$\sum_{k=1}^{n} p_k = \frac{\lambda}{\epsilon_1 \dot{A}} \sum_{k=1}^{n} \int_0^1 \dot{A}\, q_k dy + \frac{\sin^2 \psi}{\dot{A}\, \epsilon_1} \sum_{k=1}^{n} \int_0^1 \dot{A}\, q_k dy$$

$$+ \sum_{k=1}^{n} q_k' + \frac{1}{\dot{A}\, \epsilon_1} \sum_{k=1}^{n} [k_N q_k']$$

or

$$\sum_{k=1}^{n} p_k = \lambda \sum_{k=1}^{n} P_{KA} + \sum_{k=1}^{n} P_{KB} \tag{2.48}$$

where:

$$\lambda = \omega_k^2$$

$$P_{KA} = \frac{1}{\epsilon_1 \dot{A}} \int_0^1 \dot{A}\, q_k dy$$

$$P_{KB} = \frac{\sin^2 \psi}{\dot{A}\, \epsilon_1} \int_0^1 \dot{A}\, q_k dy + q_k' + \frac{1}{\dot{A}\, \epsilon_1} k_N q_k' \tag{2.49}$$

similarly we have:(refer appendix E)

$$\sum_{k=1}^{n} p_k' = \lambda \sum_{k=1}^{n} P_{K1A} + \sum_{k=1}^{n} P_{K1B} \tag{2.50}$$

where :

$$P_{K1A} = \frac{q_k}{\epsilon_1} - \frac{\dot{A}'}{\dot{A}} P_{KA}$$

$$P_{K1B} = \frac{\sin^2 \psi}{\epsilon_1} q_k + \frac{(\dot{A}\, q_k')'}{\dot{A}} + \frac{1}{\dot{A}\, \epsilon_1} (k_N q_k'' + k_N' q_k') - \frac{\dot{A}'}{\dot{A}} P_{KB} \tag{2.51}$$

Equation (2.47) represents n equations for n values of r, on adding these n equations, we get :

$$\omega_k^2 \sum_{r=1}^{n} \sum_{k=1}^{n} \int_0^1 [\dot{A}\, q_r q_k + \dot{I}\, p_k p_r] dy + \sin^2 \psi \sum_{r=1}^{n} \sum_{k=1}^{n} \int_0^1 \dot{A}\, q_r q_k dy$$

$$= \epsilon_2 \sum_{r=1}^{n}\sum_{k=1}^{n} \int_0^1 \dot{I}\, p'_r p'_k dy + \sum_{r=1}^{n}\sum_{k=1}^{n} k_N q'_r q'_k dy$$
$$+\epsilon_1 \sum_{r=1}^{n}\sum_{k=1}^{n} \int_0^1 \dot{A}\,[(p_k - q'_k)(p_r - q'_r)]dy \qquad (2.52)$$

On further simplification and application of boundary conditions the above equations as given in Warikoo and Haddara (1989) can be written as : (see appendix F).

$$\lambda \sum_{r=1}^{n}\sum_{k=1}^{n} \Big[\int_0^1 \dot{A}\, q_r q_k dy + \int_0^1 \dot{I}\, P_{RB} P_{KB} dy - \epsilon_2 \int_0^1 \dot{I}\,(P_{R1A} P_{K1B} + P_{R1B} P_{K1A})dy$$
$$- \epsilon_1 \int_0^1 \dot{A}\,(P_{RB} P_{KA} + P_{RA} P_{KB})dy + c_1 \int_0^1 \dot{A}\,(P_{RA} q'_k + P_{KA} q'_r)dy \Big]$$

$$= \sum_{r=1}^{n}\sum_{k=1}^{n} \Big[- \sin^2\psi \int_0^1 \dot{A}\, q_r q_k dy + \epsilon_2 \int_0^1 \dot{I}\, P_{R1B} P_{K1B} dy + \int_0^1 k_N q'_r q'_k dy$$
$$+ \epsilon_1 \int_0^1 \dot{A}\,(P_{KB} P_{RB} - P_{RB} q'_k - P_{KB} q'_r + q'_r q'_k)dy \Big] \qquad (2.53)$$

or

$$\lambda [M] = [K] \qquad (2.54)$$

Boundary conditions are applied to the third term on the mass side, which state that $\dot{I} = 0$ at $y = 1$ and $q_r = 0$ at $y = 0$ (details given in appendix II).

2.2.5 Sample Problem

The software developed was used to find the natural frequencies and mode shapes of two blades having airfoil sections NACA 16-018 and NACA $63_3 - 018$ as shown in fig. 2.3 and fig. 2.4, wherein the cord ratios for the blades are given in table 2.1.

The blades have been assumed to be of length 2.8m mounted on a hub of diameter 1.4m for a .7m diameter tail shaft. Fig. 2.5 to fig. 2.7 and fig. 2.8 to fig. 2.10 show the variation of natural frequencies with respect to the hub rotation speed, for these two blades for the pitch angle settings of 0,30,45 degrees respectively. The decrease in the natural frequencies due to shear deformation and rotary inertia can be clearly seen.

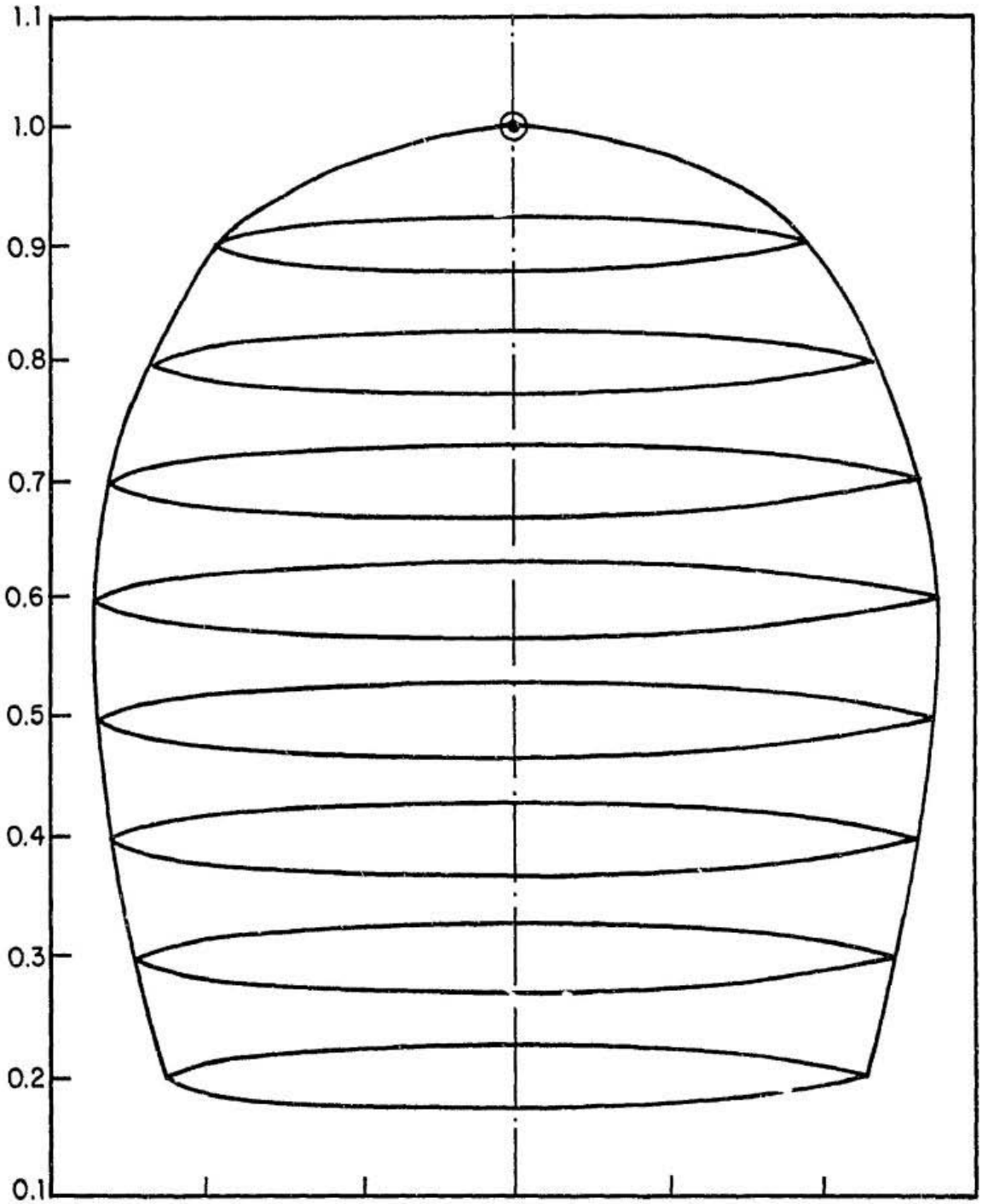

Figure 2.3: Blade profile at various sections NACA 16-018

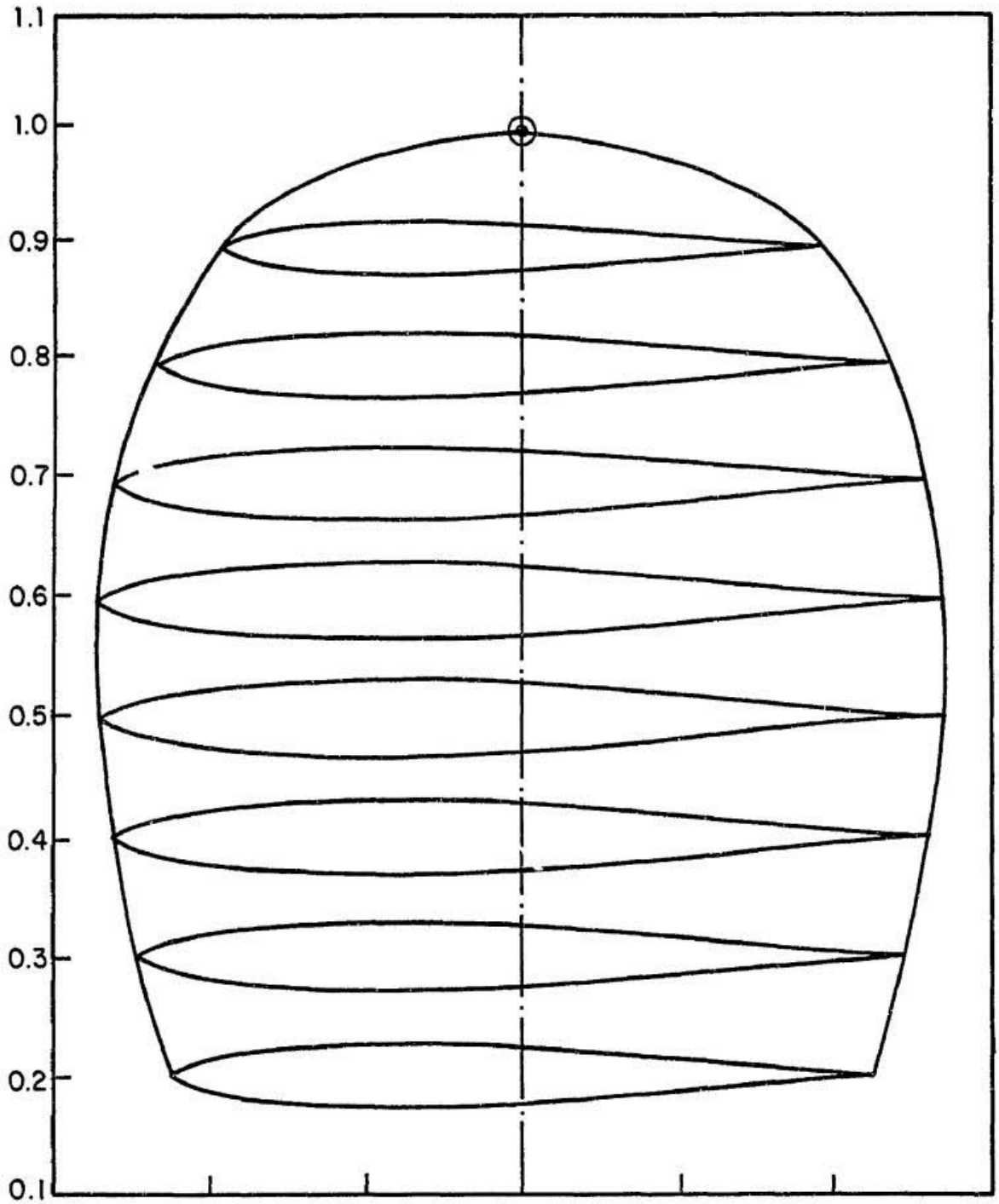

Figure 2.4: Blade profile at various sections NACA $63_3 - 018$

Table 2.1: Cord lengths at various blade sections

Blade length	*Cord length/Diameter*
0	.325
.125	.35
.25	.375
.375	.387
.5	.39
.625	.375
.75	.333
.875	.275
.937	.2
1.	0.

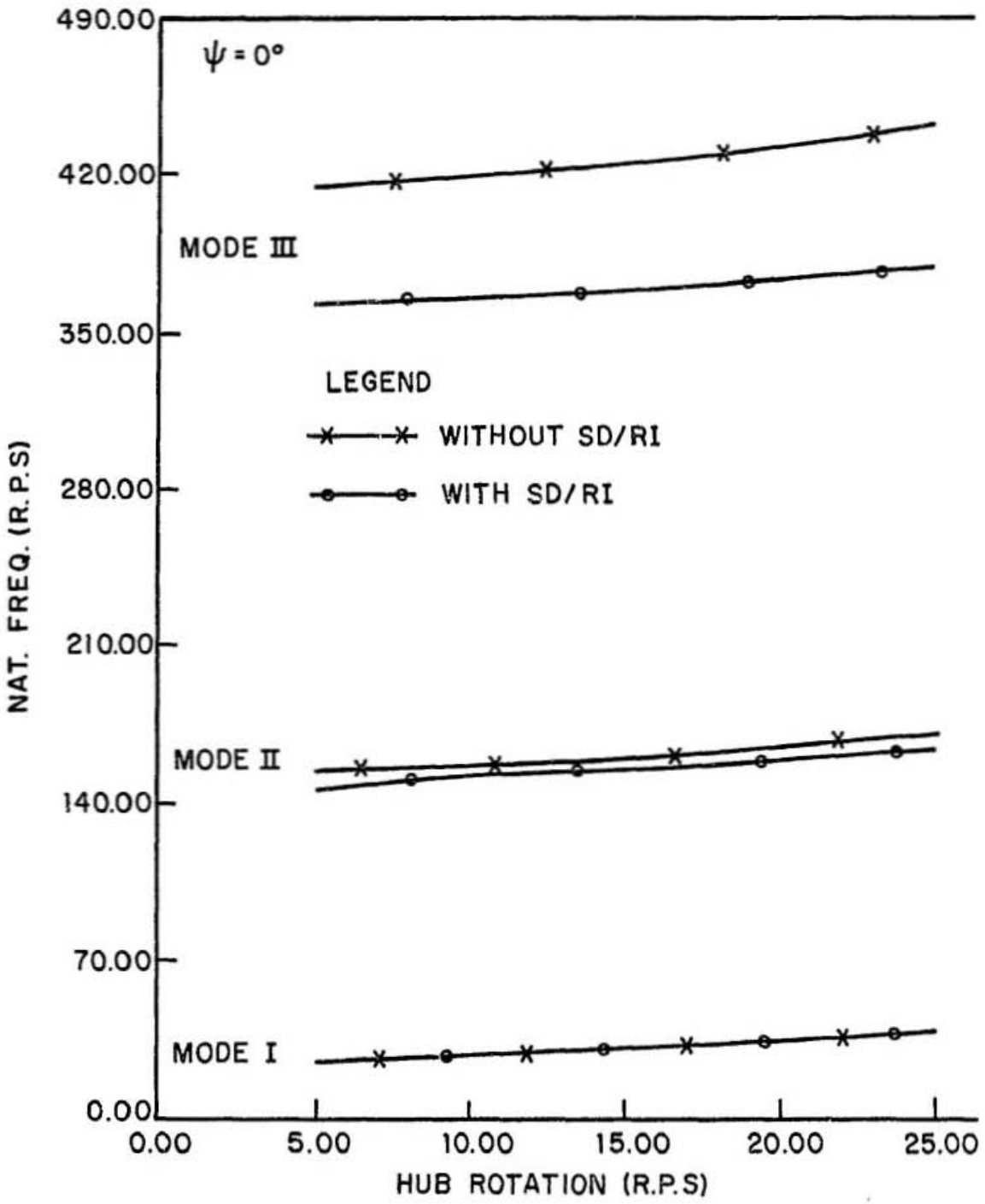

Figure 2.5: Variation of natural frequency for NACA 16-018, pitch angle = 0 deg.

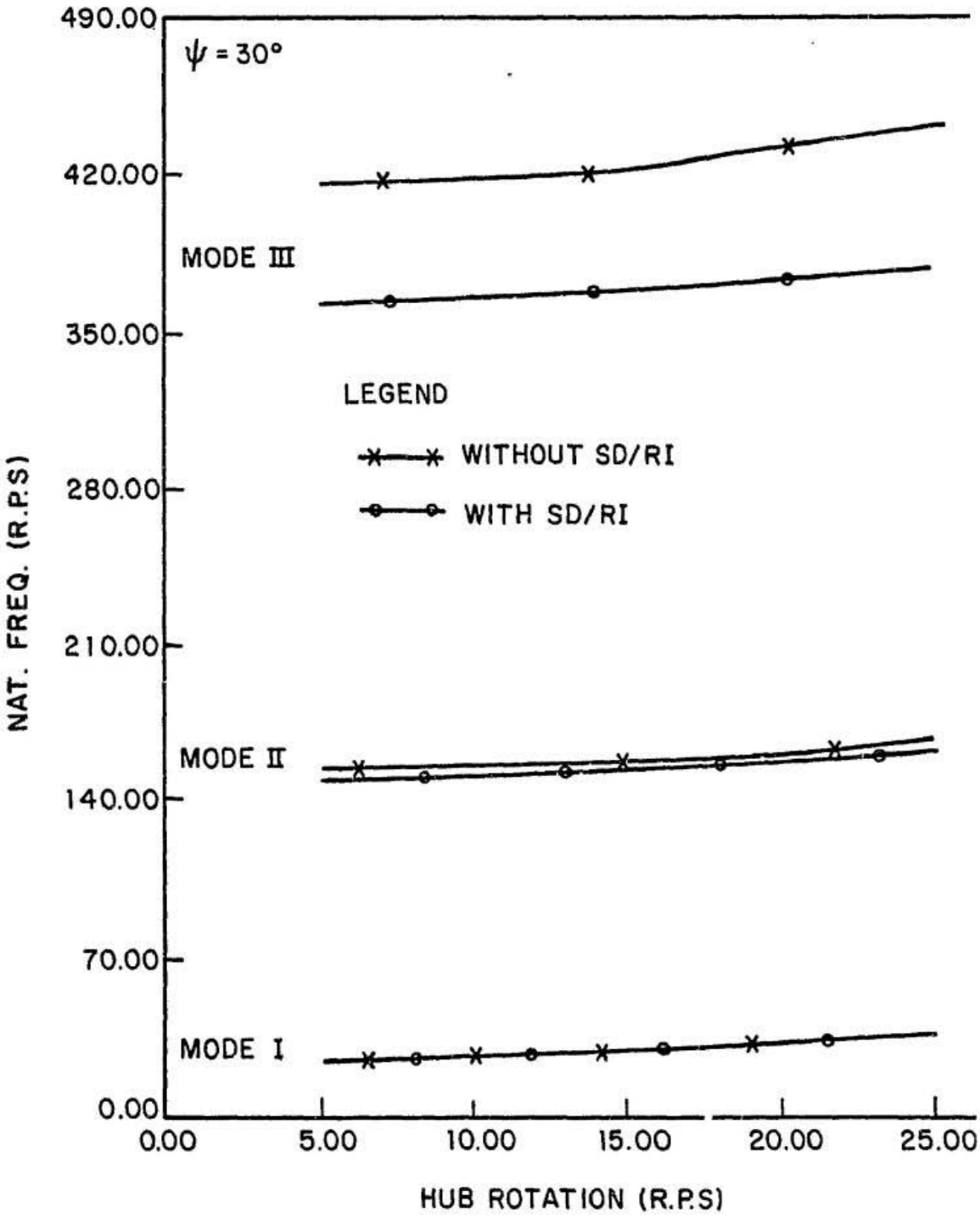

Figure 2.6: Variation of natural frequency for NACA 16-018, pitch angle = 30 deg.

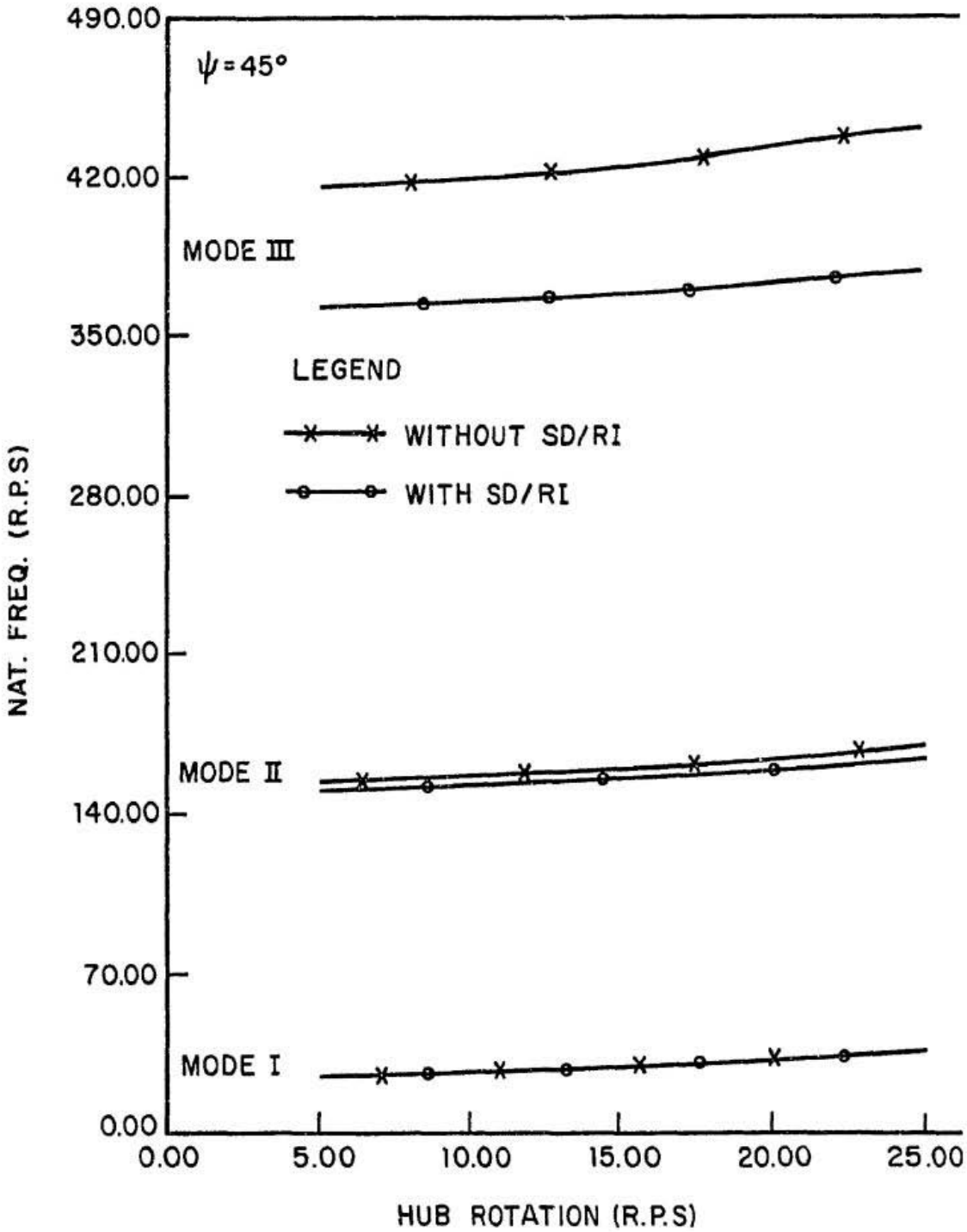

Figure 2.7: Variation of natural frequency for NACA 16-018, pitch angle = 45 deg.

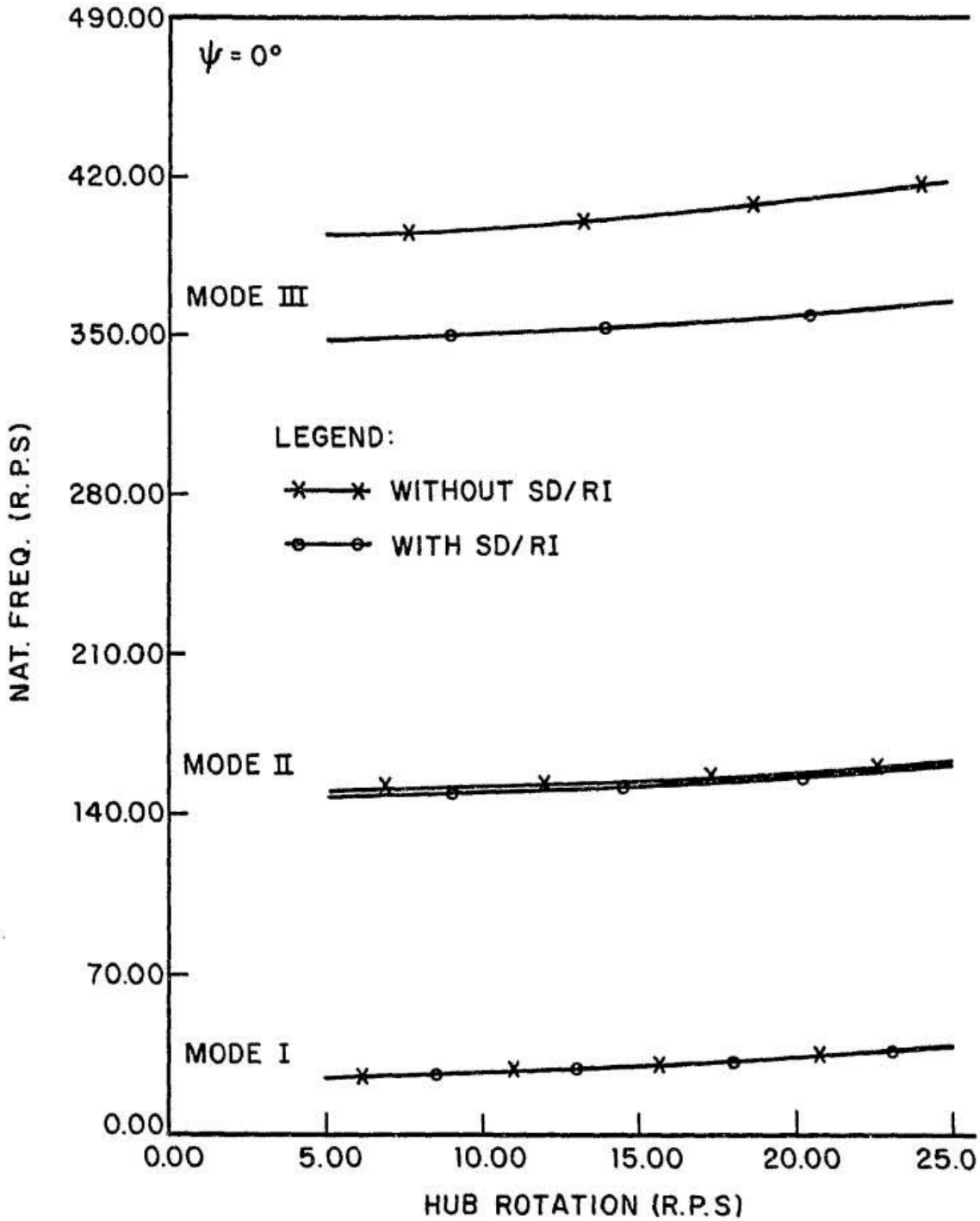

Figure 2.8: Variation of natural frequency for NACA $63_3 - 018$, pitch angle = 0 deg.

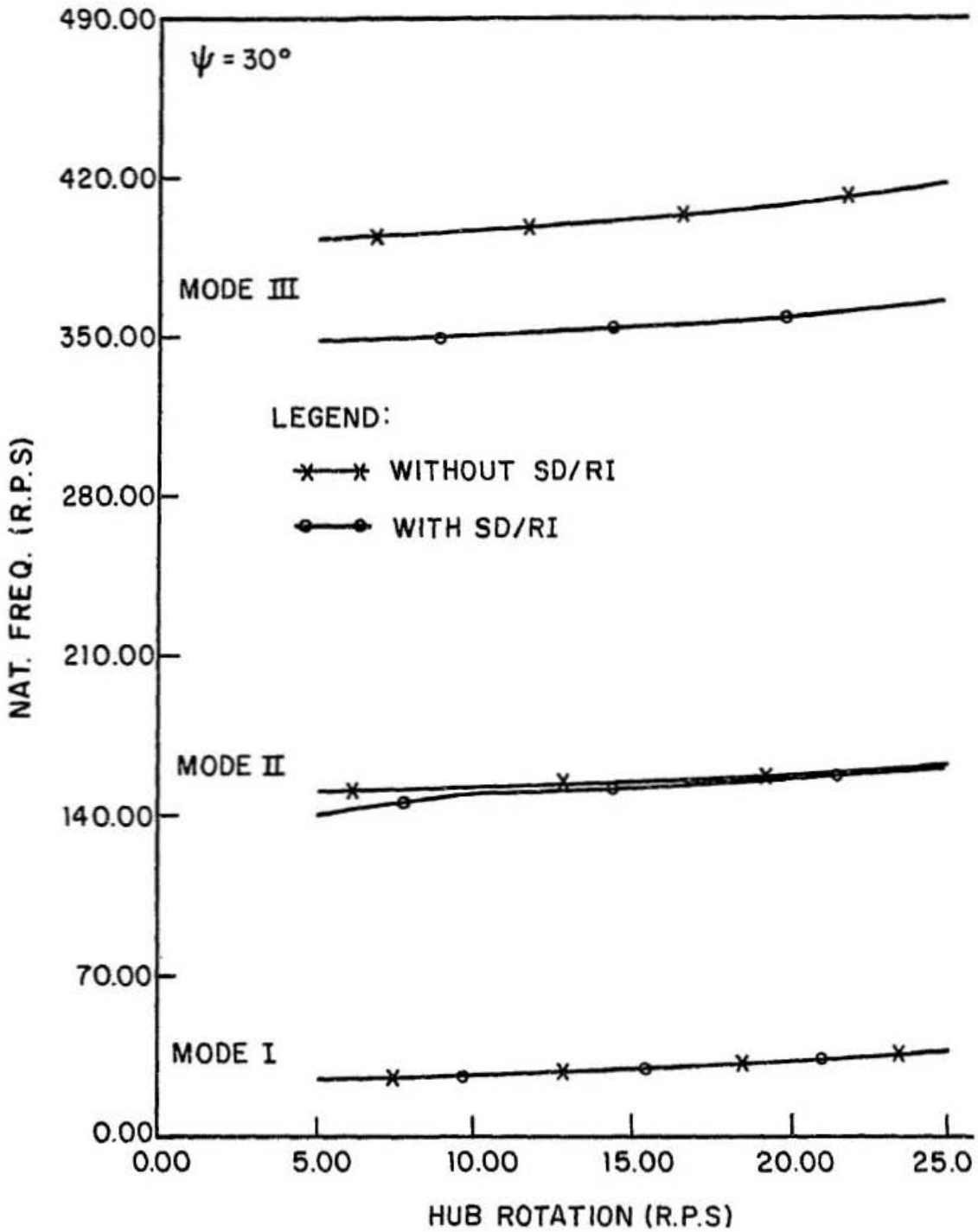

Figure 2.9: Variation of natural frequency for NACA $63_3 - 018$, pitch angle = 30 deg.

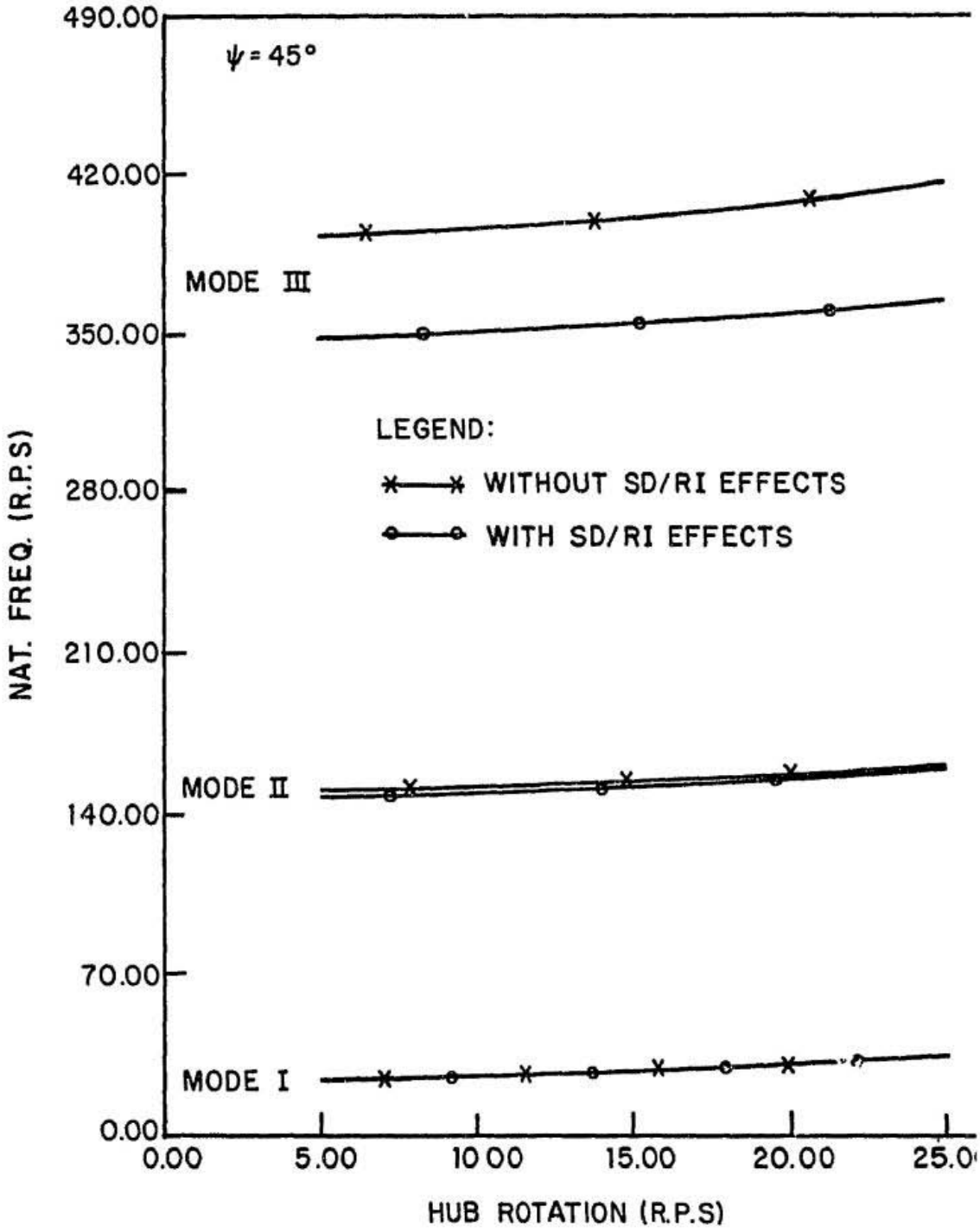

Figure 2.10: Variation of natural frequency for NACA $63_3 - 018$, pitch angle = 45 deg.

2.2.6 Hydrodynamic Effects

As mentioned before, for marine applications of the propeller shaft, hydrodynamic effects have been taken into consideration by taking into account the added mass and added moment of inertia effects of the propeller. The effects were incorporated by increasing the mass of the propeller blades by a factor of 25% as can be seen in Haddara (1988). It is worth mentioning here that the formulation presented for finding the natural frequencies of the propeller blade can take into consideration any empirical factor assumed for a particular case. To check the sensitivity of this factor it was observed that a 10% change in this factor results only in a 1% change in the values of the natural frequencies. This implies that the factor assumed gives fairly close values for the natural frequencies of propeller blades in water.

2.2.7 Comparisons

The effects of rotary inertia and shear deflection on the natural frequencies of a rotating uniform beam have been dealt with by Subrahmanyam, et.al. (1982). On checking the example given in the paper as a special case for our study, the results matched quite close as are given in table 2.2. However, the effects of pitch angle on the natural frequencies as given in the reference were seen to contradict the results obtained from the analysis of the present work, which was confirmed from the findings of Storti (1987).

Storti studied the beams of a non-uniform cross-section but the method of solution has been applied only to a particular class of cross-sections for it gets complicated in the case of arbitary beam profiles. Table 2.3 gives the comparison of the frequencies with the example taken by Storti, wherein the discrepancy for the first mode is not more than .5%, which highlights the accuracy of the method investigated in this work, in estimating the natural frequencies and mode shapes of beams, having non-uniform cross-sectional area.

Table 2.2: Comparison of natural frequencies with the case taken in Subrahmanyam, 1982

Hub Rotation = $540.35 rad/sec$

		Without S.D&R.I		*With S.D&R.I*	
Mode No.	$\cos^2\psi$	Reference	Calculated	Reference	Calculated
I	0	5800.04	5776.75	5576.83[1]	5710.79
II	0	35565.0	35573.87	33832	32618.07
III	0	99365.6	99391	89677.6	82754.56
I	.45	5788.73	5788.16	5746.09	5721.6
II	.45	35563.3	35576.43	33832.0	32619.98
III	.45	99365.6	99393.49	89677.6	82755.04

1 seems to be erroneous

Table 2.3: Comparison of natural frequencies with the case taken in Storti, 1987

Hub Rot.	*1st Mode(HZ)*			*2nd Mode(HZ)*		
(HZ)	Reference	Calculated	%error	Reference	Calculated	%error
5	241.5	242.76	.5	783	793.62	1.3
10	242	243.29	.5	785.6	794.18	1.0
15	243	244.1	.4	787	795.24	1.0
20	244	245.4	.5	789.2	796.7	.9
25	247.5	246.97	.2	795.5	798.58	.3

2.3 Mode Shapes

The ith mode shape for the propeller blade is given by:

$$\phi_i = \sum_{k=1}^{4} a_{ik} q_k \qquad \text{for } i = 1 \sim 4$$

where :

$a_{ik}(k = 1 \sim 4)$	=	eigenvector for a given value of i
q_k	=	$\cos\beta_k y - \cosh\beta_k y + \sigma_k(\sinh\beta_k y - \sin\beta_k y)$
σ_k	=	$\dfrac{\cos\beta_k l + \cosh\beta_k l}{\sin\beta_k l + \sinh\beta_k l}$
β_k^4	=	$\dfrac{M\omega^2}{EI}$
M	=	average total virtual mass per unit length of the blade
I	=	average area moment of inertia of the blade
ω	=	natural frequency of the blade

The mode shapes obtained using the present technique were checked for the case considered by Storti (1987) and the fig. 2.11 shows their close agreement.

2.4 Preliminary Check Using Finite Element Formulation

For checking the accuracy of the method presented earlier in this chapter, finite element analysis of the blade using beam elements was carried out. The analysis was done using the finite element analysis package ANSYS.

2.4.1 Element Selection

To accomodate the non-uniform area of the blade, 3-D tapered unsymmetrical beam elements were used. The blade was discretized into 40 such elements.

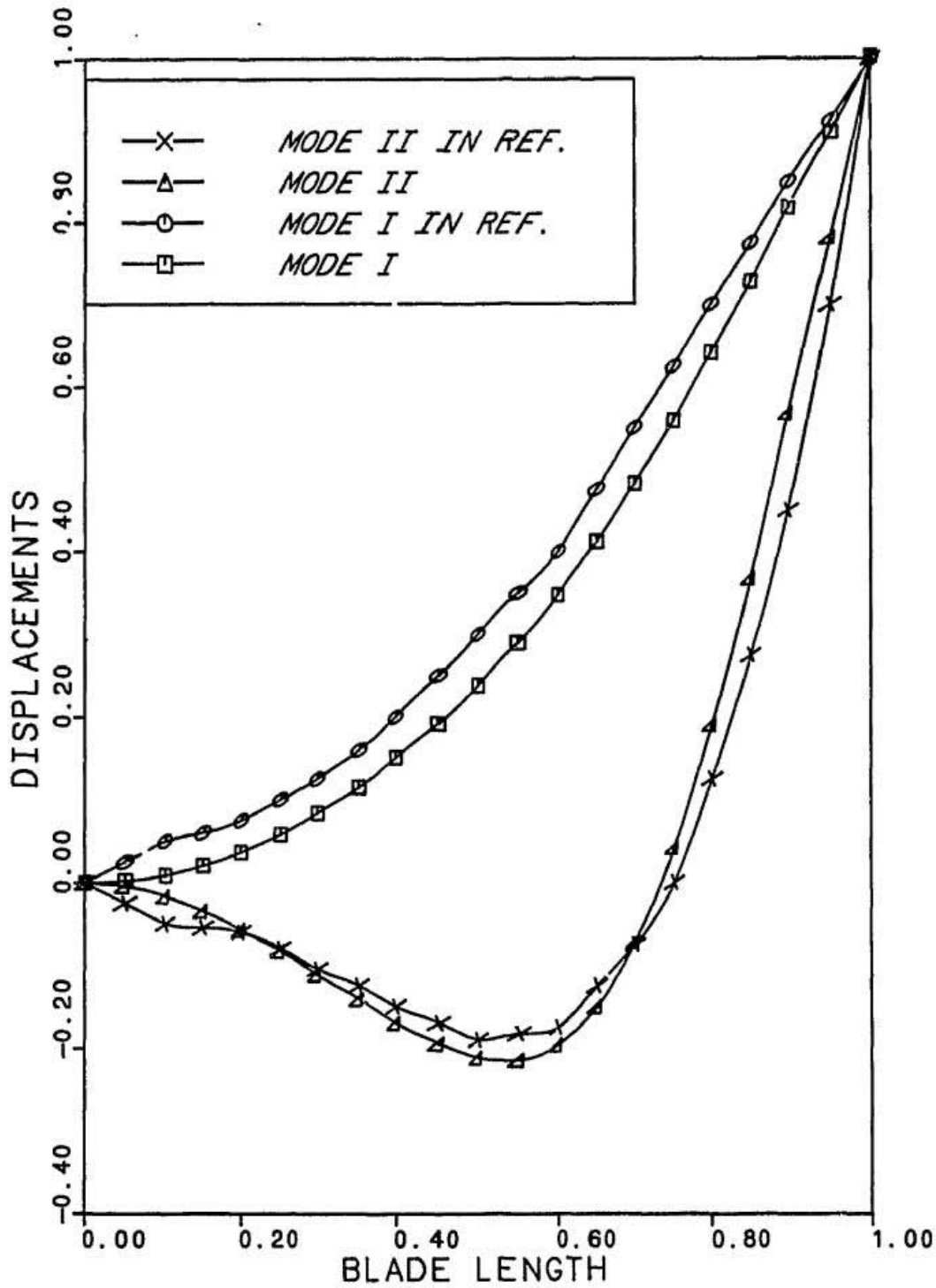

Figure 2.11: Comparison of mode shapes with the case taken in Storti, 1987

2.4.2 Element Properties

The beam element is defined by two nodes I, J as can be seen in the fig. 2.12. I and J represent the nodes at the ends of the element. Six degrees of freedom , three rotational and three translational, are defined at nodes I and J.

Other parameters that are defined for each element are :

i. Area at nodes I and J

ii. Area moment of inertia at nodes I and J

iii. Shear deflection constant depending on the cross-section of the element.

The computer program is run in two stages, in the first stage it generates the stress stiffness matrix from the nodal forces exerted due the blade rotation. In the second stage the stress stiffness matrix is used to find the eigenvalues and eigenvectors of the system.

The comparison of the natural frequencies computed with the method presented in this work with those obtained from beam finite element analysis is shown in Fig. 2.13. The mode shapes given in fig. 2.14 also match well.

2.5 Blade Deflection and Stresses

2.5.1 Introduction

The propeller blades should satisfy the strength requirements to withstand long periods of arduous service without suffering failure or permanent distortions; also the deflections under the load should not alter the geometric shape of the blade. At the same time, propellers should not be excessively strong incurring high weight and cost and possibly prejudicing good hydrodynamic design. In view of this it becomes imperative to determine blade deflections and stresses. The method presented in this section for determining the static blade deflections and steady state stresses is based on the mode summation procedure. For giving a sufficiently accurate value

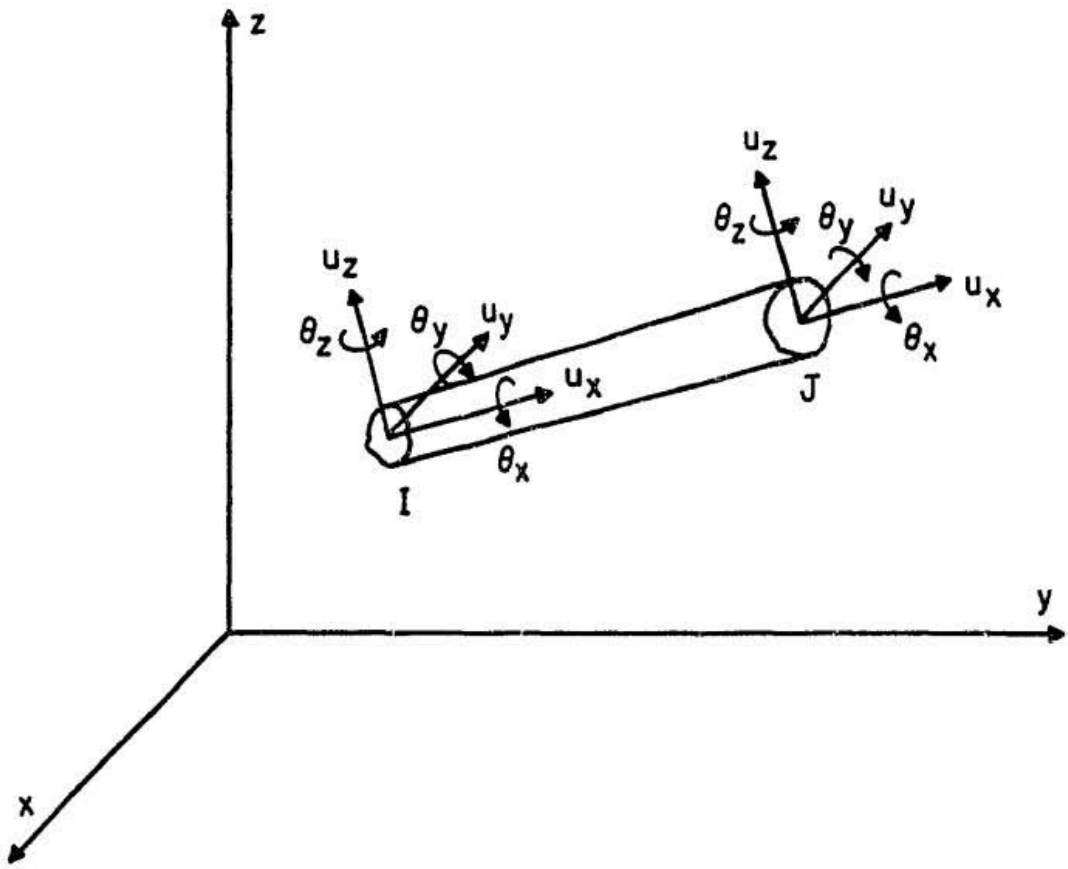

Figure 2.12: 3-D tapered beam element

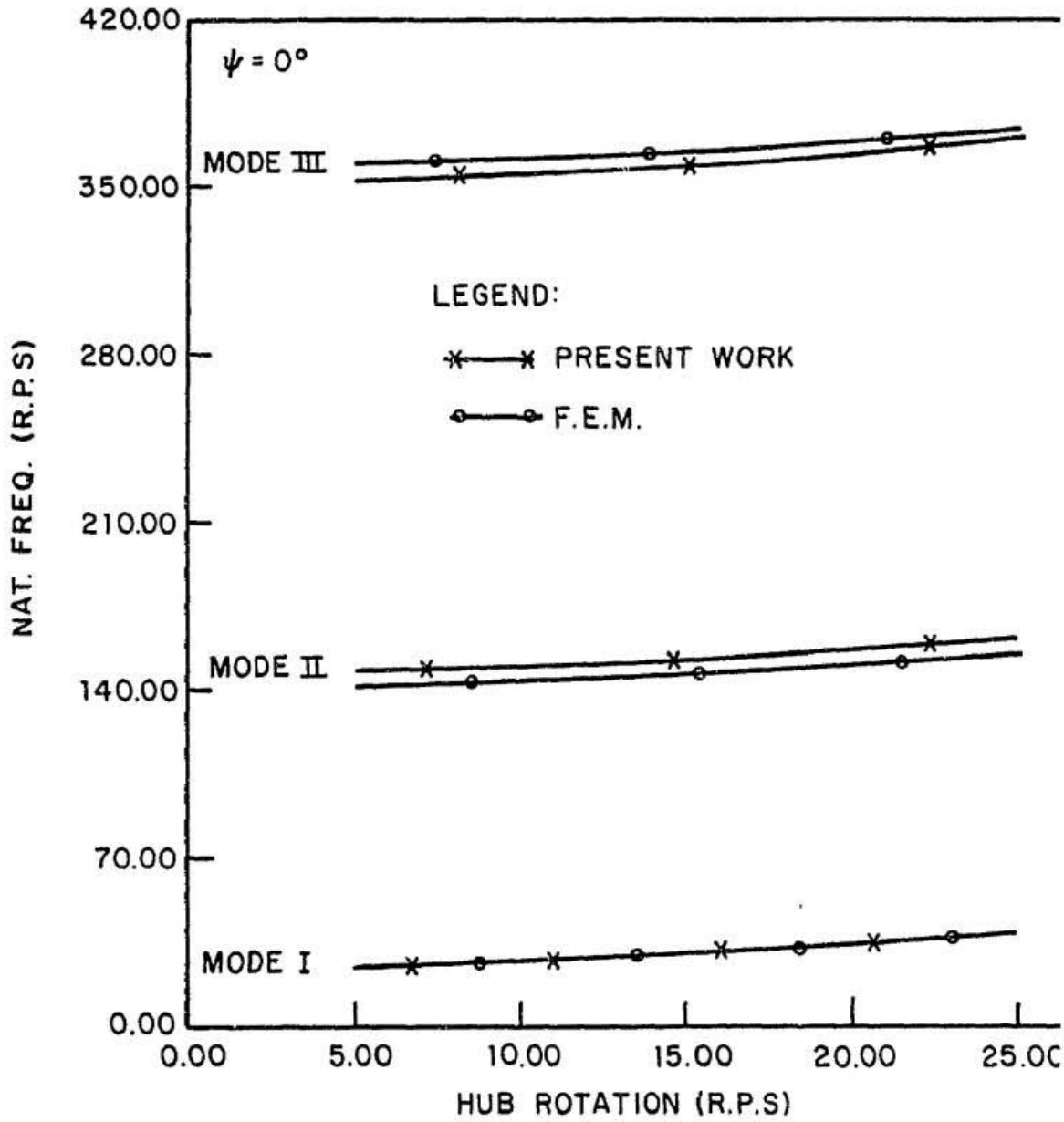

Figure 2.13: Comparison of natural frequencies with finite element analysis using tapered beam elements

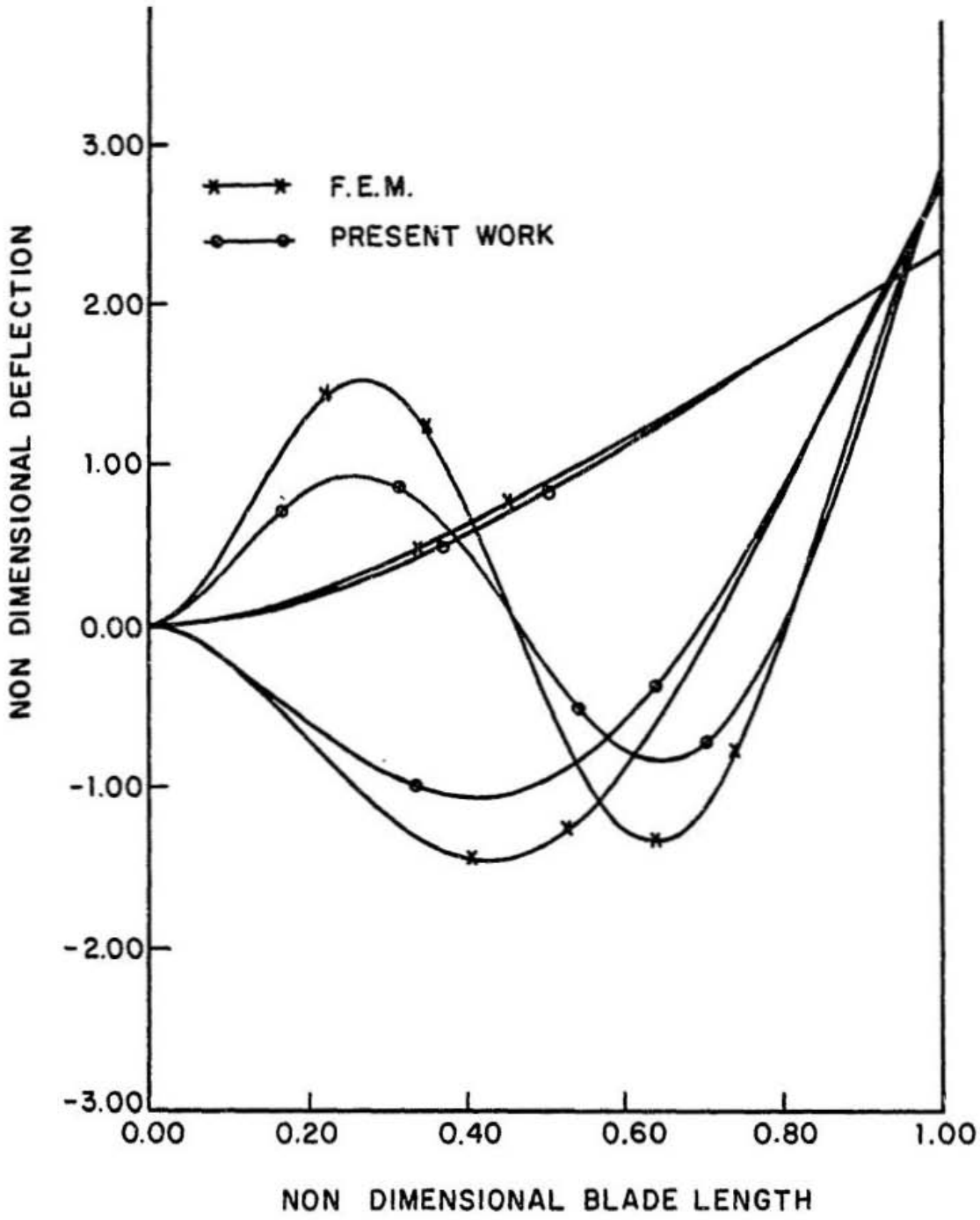

Figure 2.14: Comparison of mode shapes with finite element analysis using tapered beam elements

for the displacement the first four mode shapes obtained from the modal analysis were taken for the summation.

2.5.2 Formulation

We consider the case of a cantilever loaded by a distributed force $F(x,t)$, whose equation of motion describing the transverse displacement is :

$$[EIy''(x,t)]'' + m(x)\ddot{y}(x,t) = F(x,t) = Pf(x)g(t) \tag{2.55}$$

where :

E	=	modulus of elasticity
I	=	area moment of inertia
y	=	transverse displacement
x	=	spatial coordinate along the length of the blade
m	=	total virtual mass per unit length of the blade
$'$ and $\cdot$		represent differentiation w.r.t. space and time variables respectively
$f(x)$	=	spatial function of the force
$f(t)$	=	time function of the force
P	=	a constant

We assume y to be the sum of the first n modes.

$$y(x,t) = \sum_{i=1}^{n} \phi_i(x) q_i(t) \tag{2.56}$$

where :

ϕ_i	=	ith mode shape for the blade
q_i	=	time function associated with ith mode shape

Using in equation(2.55) we have :

$$\left[EI \sum_{i=1}^{n} \phi_i'' q_i\right]'' + m \sum_{i=1}^{n} \phi_i \ddot{q}_i = Pf(x)g(t)$$

multiplying by ϕ_j and integrating

$$\sum_{i=1}^{n} \int_0^l EI\phi_i'''' \phi_j q_i dx + \sum_{i=1}^{n} \int_0^l m\phi_i\phi_j\ddot{q}_i dx = \int_0^l Pf(x)\phi_j g(t) dx$$

for $j = 1 \sim n$

using the boundary condition for the cantilever we have :

$$\sum_{i=1}^{n} \int_0^l EI\phi_i''\phi_j'' q_i dx + \sum_{i=1}^{w} \int_0^l m\phi_i\phi_j\ddot{q}_i dx = \int_0^l Pf(x)\phi_j g(t) dx \qquad (2.57)$$

for $j = 1 \sim n$

The normal modes ϕ_i and ϕ_j are known to satisfy the condition of orthogonality given by :

$$\int_0^l m\phi_i\phi_j dx = \begin{cases} 0 \ for \ j \neq i \\ m_{ii} \ for \ j = i \end{cases} \qquad (2.58)$$

$$\int_0^l EI\phi_i''\phi_j'' dx = \begin{cases} 0 \ for \ j \neq i \\ k_{ii} \ for \ j = i \end{cases} \qquad (2.59)$$

using equations (2.58) and (2.59), equation (2.57) takes the form

$$\begin{bmatrix} \bar{k_{11}} & 0 & \cdots & 0 \\ 0 & \bar{k_{22}} & & 0 \\ \vdots & & \ddots & \\ 0 & 0 & & \bar{k_{nn}} \end{bmatrix} \begin{Bmatrix} q_1 \\ q_2 \\ \vdots \\ q_n \end{Bmatrix} + \begin{bmatrix} \bar{m_{11}} & 0 & \cdots & 0 \\ 0 & \bar{m_{22}} & & 0 \\ \vdots & & \ddots & \\ 0 & 0 & & \bar{m_{nn}} \end{bmatrix} \begin{Bmatrix} \ddot{q}_1 \\ \ddot{q}_2 \\ \vdots \\ \ddot{q}_n \end{Bmatrix} = \begin{Bmatrix} f_1 \\ f_2 \\ \vdots \\ f_n \end{Bmatrix} \qquad (2.60)$$

or :

$$[\bar{K}]\{q\} + [\bar{M}]\{\ddot{q}\} = \{F\} \qquad (2.61)$$

where

$[\bar{K}]$ = stifness matrix of the cantilever
$[\bar{M}]$ = mass matrix of the cantilever
$\{F\}$ = force vector
$\{q\}$ = displacement vector

In the case of propeller blade, idealized as a cantilever of non-uniform area, the normal modes we arrive at are approximate and hence the equations (2.58) and (2.59) are not satisfied fully.

This is clear from equation (2.54) which states that :

$$[K] = \lambda[M]$$

where $[K]$ and $[M]$ are the stiffness and the mass matrices of the system respectively having non zero off-diagonal terms.

Ignoring the off-diagonal elements of $[K]$ and $[M]$ matrices, which are negligible as compared to the diagonal elements, we can write an equation for the propeller blade similar to equation (2.60). Taking the first four modes into consideration equation (2.60) reduces to the following nondimensional form.

$$\begin{bmatrix} k_{11} & 0 & 0 & 0 \\ 0 & k_{22} & 0 & 0 \\ 0 & 0 & k_{33} & 0 \\ 0 & 0 & 0 & k_{44} \end{bmatrix} \begin{Bmatrix} q_1 \\ q_2 \\ q_3 \\ q_4 \end{Bmatrix} + \begin{bmatrix} m_{11} & 0 & 0 & 0 \\ 0 & m_{22} & 0 & 0 \\ 0 & 0 & m_{33} & 0 \\ 0 & 0 & 0 & m_{44} \end{bmatrix} \begin{Bmatrix} \ddot{q}_1 \\ \ddot{q}_2 \\ \ddot{q}_3 \\ \ddot{q}_4 \end{Bmatrix} = \begin{Bmatrix} f_1 \\ f_2 \\ f_3 \\ f_4 \end{Bmatrix} \tag{2.62}$$

where :

$f_i = \epsilon_3 g(t) \int_0^1 f_y \varphi_r dy = \Theta_i$

$\epsilon_3 = \dfrac{P}{\rho \Omega^2 l^3}$

φ_r = rth nondimensional mode shape of blade

f_y = non-dimensional force distribution along the blade length

Upon solving the four equations given by (2.62) the steady state deflection can be given as :

$$q_i = \frac{\Theta_i}{k_i i} = \frac{\Theta_i}{m_{ii}\omega_i^2}$$

where ω_i is the ith eigenvalue.

Using in equation (2.56) the steady state displacement of the blade can be given as :

$$y = q_1\phi_1 + q_2\phi_2 + q_3\phi_3 + q_4\phi_4 \tag{2.63}$$

The maximum bending stress at a section in the blade is given as :

$$\sigma = Ey''\frac{T}{2}$$

where :

y'' = $q_1\phi_1'' + q_2\phi_2'' + q_3\phi_3'' + q_4\phi_4''$
T = blade thickness at the section

Fig. 2.15 and fig. 2.16 show the variation of the static deflections and steady state stresses for the blade NACA 16-018 taken as a sample example in this work. The pressure distribution assumed for the study is given in Fig. 2.17.

The formulation derived for the blade deflections and stresses was used to check these parameters for a 10 feet diameter propeller spinning at 300 r.p.m. with a h.p. of 18,000 given in Conolly (1960). The experimental values in the reference were predicted from the measurements on a model. Blade deflections matched quite close as given in Fig. 2.18, while as blade stresses at mid-sections compared well and are given in Table 2.4.

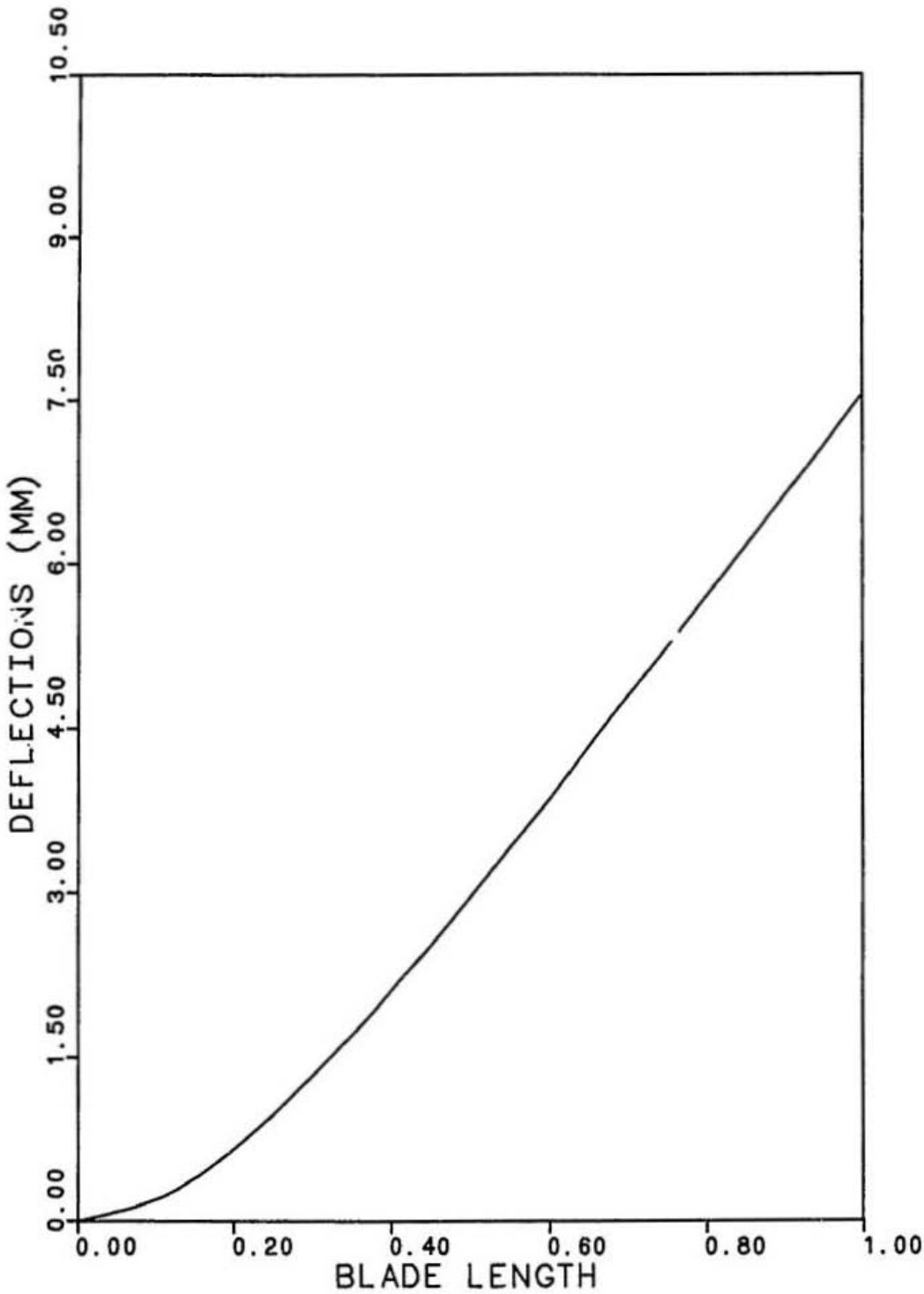

Figure 2.15: Variation of static blade deflections

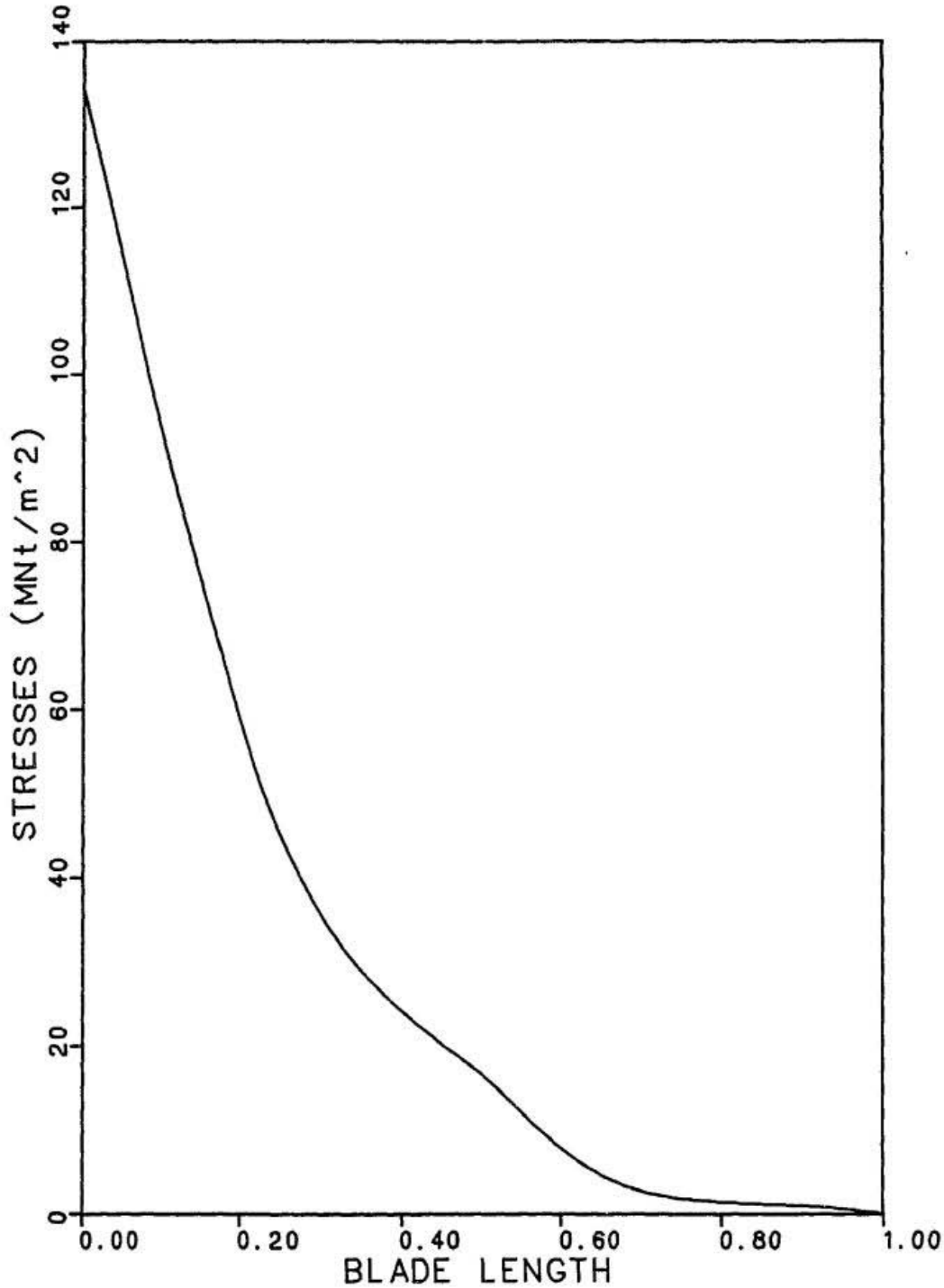

Figure 2.16: Variation of steady state stresses

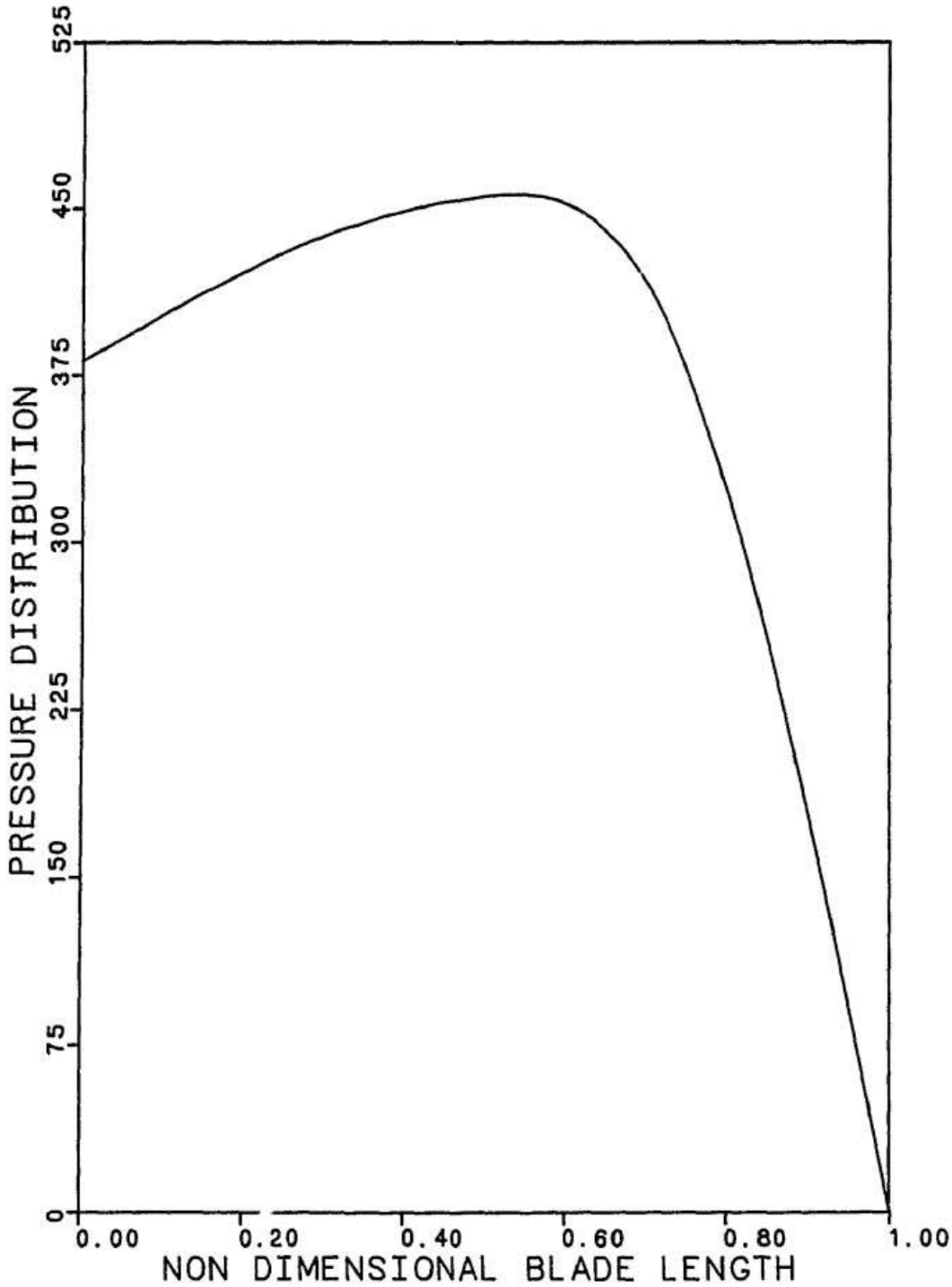

Figure 2.17: Load variation of the blade

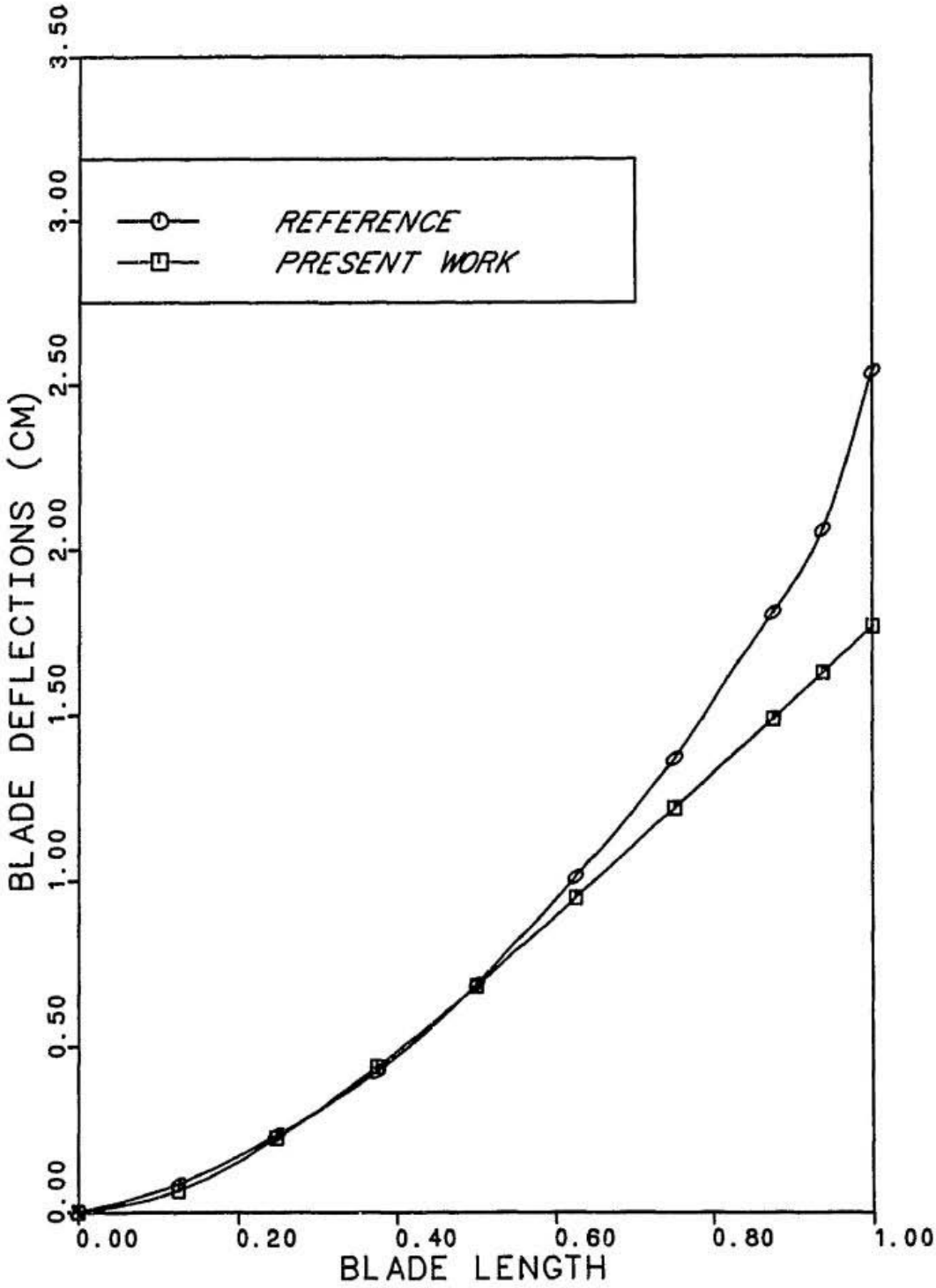

Figure 2.18: Comparison of static blade deflections with the case taken in Conolly, 1960.

Table 2.4: Comparison of static blade stresses with the case taken in Conolly, 1960.

Blade length	*Stress (Pa)*	
	Reference	Calculated
.375	1.115×10^8	1.399×10^8
.625	6.81×10^7	4.621×10^7
.875	2.23×10^7	2.2×10^7

Chapter 3

ISOPARAMETRIC FINITE ELEMENT FORMULATION OF THE BLADE

3.1 Introduction

In the preceeding chapter formulation for finding the natural frequency of the propeller blade was based on the assumption that the blade can be considered as a cantilever of varying cross section. Since we are primarily interested in finding the fundamental mode of vibration the assumption is supposed to be quite valid. To check this, finite element analysis of the blade was carried out using 20 noded, serendipity, solid isoparametric elements. The analysis takes into account the increase in the stiffness of the structure due to rotation as well as the added mass of the propeller. For the eigenvalue extraction, dynamic condensation was carried out to reduce the C.P.U. time consumed.

3.2 Element Selection

Blade geometry being quite complicated, selection of isoparametric elements was thought to be appropriate, for the fact that in such elements the generalized coordinates and the generalized displacements are related to the nodal coordinates and nodal displacements respectively by the same shape function. Twenty noded

element was chosen to give a non linear displacement field, which in turn takes care of the non linear geometry as can be seen in Bahree (1987). The degrees of freedom at the nodes of the element are translational in nature along all the three axes, hence the element is a C^0 continuity element. By choosing the degrees of freedom for displacements at the nodes along all the three axes, we are able to get the other modes of vibration also, besides that for the transverse deflection, obtained with the beam formulation. The element characteristics are given in Fig. 3.1

3.3 Mathematical Formulation

The chosen element is associated with a local coordinate system $\xi\eta\zeta$ (shown in Fig 3.1), where in the values of ξ, η and ζ vary from -1 to 1 in the element. The coordinate system XYZ is the global cartesian coordinate system.

The displacement vector at a point in the element, as in Rao (1982), is given by:

$$\begin{Bmatrix} u \\ v \\ w \end{Bmatrix} = [N]\{d\} \tag{3.1}$$

The global coordinate vector of a point in the element is given as :

$$\begin{Bmatrix} x \\ y \\ z \end{Bmatrix} = [N]\{c\} \tag{3.2}$$

where :

u = generalized displacement along global X - axis
v = generalized displacement along global Y - axis
w = generalized displacement along global Z - axis
x = generalized coordinates along global X - axis
y = generalized coordinates along global Y - axis
z = generalized coordinates along global Z - axis
d = nodal displacement vector
N = shape function matrix
c = nodal coordinate vector

For getting the eigenvalues and the eigenvectors of the system we need to get the stiffness and the mass matrices of the system.

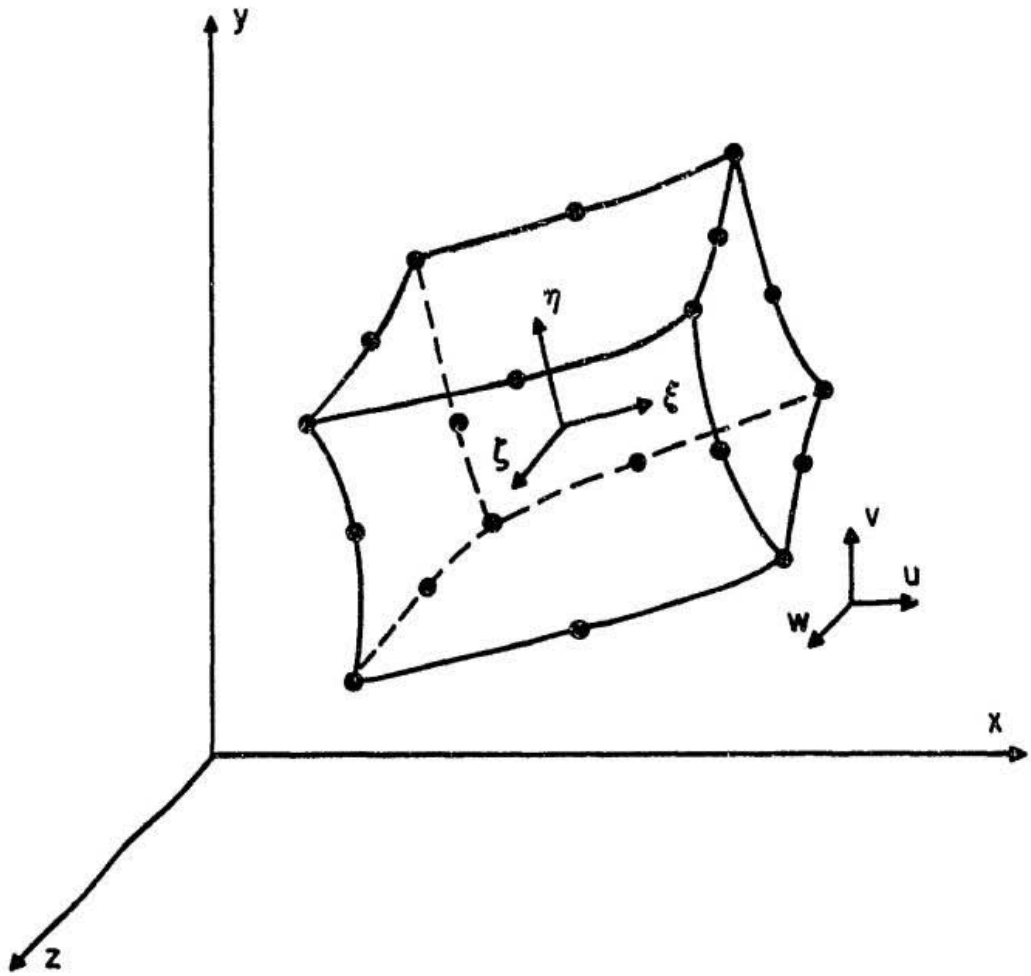

Figure 3.1: 3-D, 20 noded isoparametric element

The stiffness of the system consists of two matrices :

1. $[k^e]$ the element stiffness matrix depending on the material properties and given as :

$$[k^e] = \int_v [B]^T [D][B] dv \tag{3.3}$$

2. $[k_\sigma^e]$ the element stiffness matrix resulting due to the rotation of the blade. This matrix is called the stress stiffness matrix and is independent of the material properties. This matrix is given as :

$$[k_\sigma^e] = \int_v [G]^T \begin{bmatrix} s & 0 & 0 \\ 0 & s & 0 \\ 0 & 0 & s \end{bmatrix} [G] dv \tag{3.4}$$

The element mass matrix of the system is given as

$$[m^e] = \int_v [N]^T \rho [N] dv \tag{3.5}$$

where :

$[B]$ = strain displacement matrix

v = volume of the element

ρ = density of the material

$\{\delta\} = [G]\{d\}$

$\{\delta\} = \{u_{,x}\ u_{,y}\ u_{,z}\ v_{,x}\ v_{,y}\ v_{,z}\ w_{,x}\ w_{,y}\ w_{,z}\}$

$$[s] = \begin{bmatrix} \sigma_{xo} & \tau_{xy0} & \tau_{zx0} \\ \tau_{xy0} & \sigma_{y0} & \tau_{yz0} \\ \tau_{zx0} & \tau_{yz0} & \sigma_{z0} \end{bmatrix}$$

$[D]$ = material property matrix whose expression is given as:

$$\frac{E(1-\nu)}{(1+\nu)(1-2\nu)}\begin{bmatrix} 1 & \frac{\nu}{1-\nu} & \frac{\nu}{1-\nu} & 0 & 0 & 0 \\ & 1 & \frac{\nu}{1-\nu} & 0 & 0 & 0 \\ & & 1 & 0 & 0 & 0 \\ & & & \frac{1-2\nu}{2(1-\nu)} & 0 & 0 \\ & symmetric & & & \frac{1-2\nu}{2(1-\nu)} & 0 \\ & & & & & \frac{1-2\nu}{2(1-\nu)} \end{bmatrix}$$

The eigenvalue equation for the system takes the form :

$$[K] + [K_\sigma] = \lambda[M] \tag{3.6}$$

where :

$[K]$	=	conventional global stiffness matrix of the system
$[K_\sigma]$	=	global stress stiffness matrix of the system
$[M]$	=	global mass matrix of the system
λ	=	is the eigenvalue.

3.4 Formulation of $[N]$ Matrix

The shape function or the interpolation function matrix for the 20 noded isoparametric solid element is given as :

$$N = \begin{bmatrix} N_1 & 0 & 0 & N_2 & 0 & 0 & \ldots & N_{20} & 0 & 0 \\ 0 & N1 & 0 & 0 & N_2 & 0 & \ldots & 0 & N_{20} & 0 \\ 0 & 0 & N_1 & 0 & 0 & N_2 & \ldots & 0 & 0 & N_{20} \end{bmatrix}$$

where $N_1, N_2 \ldots N_{20}$ are the interpolation functions of the nodes $1, 2 \ldots 20$ of the element, and in the natural coordinate system are given as :(refer to Cook, 1987)

$N_i = \frac{1}{8}(1+\xi\xi_i)(1+\eta\eta_i)(1+\zeta\zeta_i)(\xi\xi_i+\eta\eta_i+\zeta\zeta_i-2)$ for a corner node and $N_i = \frac{1}{4}(1-\xi^2)(1+\eta\eta_i)(1+\zeta\zeta_i)$ for a typical midside node given by $\xi_i = 0, \eta_i = \overset{+}{-} 1, \zeta_i = \overset{+}{-} 1.$

From (3.1) and (3.2), we have

$$\begin{Bmatrix} u \\ v \\ w \end{Bmatrix} = \begin{bmatrix} N_1 & 0 & 0 & N_2 & 0 & 0 & \dots & N_{20} & 0 & 0 \\ 0 & N_1 & 0 & 0 & N_2 & 0 & \dots & 0 & N_{20} & 0 \\ 0 & 0 & N_1 & 0 & 0 & N_2 & \dots & 0 & 0 & N_{20} \end{bmatrix} \begin{Bmatrix} u_1 \\ v_1 \\ w_1 \\ u_2 \\ v_2 \\ w_2 \\ \vdots \\ u_{20} \\ v_{20} \\ w_{20} \end{Bmatrix} \tag{3.7}$$

$$\begin{Bmatrix} x \\ y \\ z \end{Bmatrix} = \begin{bmatrix} N_1 & 0 & 0 & N_2 & 0 & 0 & \dots & N_{20} & 0 & 0 \\ 0 & N_1 & 0 & 0 & N_2 & 0 & \dots & 0 & N_{20} & 0 \\ 0 & 0 & N_1 & 0 & 0 & N_2 & \dots & 0 & 0 & N_{20} \end{bmatrix} \begin{Bmatrix} x_1 \\ y_1 \\ z_1 \\ x_2 \\ y_2 \\ z_2 \\ \vdots \\ x_{20} \\ y_{20} \\ z_{20} \end{Bmatrix} \tag{3.8}$$

3.5 Formulation of Strain Displacement Matrix $[B]$

Matrix $[B]$ relates the strain in the element to the nodal displacements.

$$\{\epsilon\} = [B]\{d\} \tag{3.9}$$

3.5.1 Strain Vector

The strain vector $\{\epsilon\}$ for a 3D element is given as :

$$\epsilon = \begin{Bmatrix} \epsilon_{xy} \\ \epsilon_{yy} \\ \epsilon_{zz} \\ \gamma_{xy} \\ \gamma_{yz} \\ \gamma_{zx} \end{Bmatrix} = \begin{Bmatrix} u_{,x} \\ v_{,y} \\ w_{,z} \\ u_{,y} + v_{,x} \\ v_{,z} + w_{,y} \\ u_{,z} + w_{,x} \end{Bmatrix}$$

$$= \begin{bmatrix} 1 & 0 & 0 & 0 & 0 & 0 & 0 & 0 & 0 \\ 0 & 0 & 0 & 0 & 1 & 0 & 0 & 0 & 0 \\ 0 & 0 & 0 & 0 & 0 & 0 & 0 & 0 & 1 \\ 0 & 1 & 0 & 1 & 0 & 0 & 0 & 0 & 0 \\ 0 & 0 & 0 & 0 & 0 & 1 & 0 & 1 & 0 \\ 0 & 0 & 1 & 0 & 0 & 0 & 1 & 0 & 0 \end{bmatrix} \begin{Bmatrix} u_{,x} \\ u_{,y} \\ u_{,z} \\ v_{,x} \\ v_{,y} \\ v_{,z} \\ w_{,x} \\ w_{,y} \\ w_{,z} \end{Bmatrix}$$

or

$$\{\epsilon\} = [C]\{\delta\} \tag{3.10}$$

from equation (3.7) it is clear that u is a function of the interpolation functions, which are given in terms of the natural coordinates ξ, η, ζ. In order to evaluate $\{\delta\}$ we have to get the derivatives of u, v, w w.r.t. ξ, η, ζ and then use the Jacobian transformation.

3.5.2 Jacobian Matrix

From differential calculus :

$$u_{,x} = u_{,\xi}\xi_{,x} + u_{,\xi}\xi_{,y} + u_{,\xi}\xi_{,z}$$

we can write :

$$\begin{Bmatrix} u_{,\xi} \\ u_{,\eta} \\ u_{,\zeta} \end{Bmatrix} = \begin{bmatrix} x_{,\xi} & y_{,\xi} & z_{,\xi} \\ x_{,\eta} & y_{,\eta} & z_{,\eta} \\ x_{,\zeta} & y_{,\zeta} & z_{,\zeta} \end{bmatrix} \begin{Bmatrix} u_{,x} \\ u_{,y} \\ u_{,z} \end{Bmatrix}$$

or

$$\begin{Bmatrix} u_{,\xi} \\ u_{,\eta} \\ u_{,\zeta} \end{Bmatrix} = [J] \begin{Bmatrix} u_{,x} \\ u_{,y} \\ u_{,z} \end{Bmatrix}$$

or

$$\begin{Bmatrix} u_{,x} \\ u_{,y} \\ u_{,z} \end{Bmatrix} = [J]^{-1} \begin{Bmatrix} u_{,\xi} \\ u_{,\eta} \\ u_{,\zeta} \end{Bmatrix}$$
$$= [\Gamma] \begin{Bmatrix} u_{,\xi} \\ u_{,\eta} \\ u_{,\zeta} \end{Bmatrix} \tag{3.11}$$

where $[J]^{-1} = [\Gamma]$

using equation (3.11) we can write $\{\delta\}$ vector as :

$$\begin{Bmatrix} u_{,x} \\ u_{,y} \\ u_{,z} \\ v_{,x} \\ v_{,y} \\ v_{,z} \\ w_{,x} \\ w_{,y} \\ w_{,z} \end{Bmatrix} = \begin{bmatrix} \Gamma_{11} & \Gamma_{12} & \Gamma_{13} & 0 & 0 & 0 & 0 & 0 & 0 \\ \Gamma_{21} & \Gamma_{22} & \Gamma_{23} & 0 & 0 & 0 & 0 & 0 & 0 \\ \Gamma_{31} & \Gamma_{32} & \Gamma_{33} & 0 & 0 & 0 & 0 & 0 & 0 \\ 0 & 0 & 0 & \Gamma_{11} & \Gamma_{12} & \Gamma_{13} & 0 & 0 & 0 \\ 0 & 0 & 0 & \Gamma_{21} & \Gamma_{22} & \Gamma_{23} & 0 & 0 & 0 \\ 0 & 0 & 0 & \Gamma_{31} & \Gamma_{32} & \Gamma_{33} & 0 & 0 & 0 \\ 0 & 0 & 0 & 0 & 0 & 0 & \Gamma_{11} & \Gamma_{12} & \Gamma_{13} \\ 0 & 0 & 0 & 0 & 0 & 0 & \Gamma_{21} & \Gamma_{22} & \Gamma_{23} \\ 0 & 0 & 0 & 0 & 0 & 0 & \Gamma_{31} & \Gamma_{32} & \Gamma_{33} \end{bmatrix} \begin{Bmatrix} u_{,\xi} \\ u_{,\eta} \\ u_{,\zeta} \\ v_{,\xi} \\ v_{,\eta} \\ v_{,\zeta} \\ w_{,\xi} \\ w_{,\eta} \\ w_{,\zeta} \end{Bmatrix}$$

or

$$\{\delta\} = [AJ]\{\delta'\} \tag{3.12}$$

3.5.3 $\{\delta'\}$ Vector

From equation (3.7) we have

$$u = u_1N_1 + u_2N_2 + u_3N_3 + ...u_{20}N_{20}$$
$$v = v_1N_1 + v_2N_2 + v_3N_3 + ...v_{20}N_{20}$$
$$w = w_1N_1 + w_2N_2 + w_3N_3 + ...w_{20}N_{20}$$

Differentiating w.r.t. the natural coordinates, we have :

$$u_{,\xi} = u_1N_{1,\xi} + u_2N_{2,\xi} + u_3N_{3,\xi} + ...u_{20}N_{20,\xi}$$
$$u_{,\eta} = u_1N_{1,\eta} + u_2N_{2,\eta} + u_3N_{3,\eta} + ...u_{20}N_{20,\eta}$$
$$u_{,\zeta} = w_1N_{1,\zeta} + w_2N_{2,\zeta} + w_3N_{3,\zeta} + ...w_{20}N_{20,\zeta}$$

and so on.

$\{\delta'\}$ vector can thus be written as :

$$\begin{Bmatrix} u_{,\xi} \\ u_{,\eta} \\ u_{,\zeta} \\ v_{,\xi} \\ v_{,\eta} \\ v_{,\zeta} \\ w_{,\xi} \\ w_{,\eta} \\ w_{,\zeta} \end{Bmatrix} = \begin{bmatrix} N_{1,\xi} & 0 & 0 & N_{2,\xi} & 0 & 0 & \cdots & N_{20,\xi} & 0 & 0 \\ N_{1,\eta} & 0 & 0 & N_{2,\eta} & 0 & 0 & \cdots & N_{20,\eta} & 0 & 0 \\ N_{1,\zeta} & 0 & 0 & N_{2,\zeta} & 0 & 0 & \cdots & N_{20,\zeta} & 0 & 0 \\ 0 & N_{1,\xi} & 0 & 0 & N_{2,\xi} & 0 & \cdots & 0 & N_{20,\xi} & 0 \\ 0 & N_{1,\eta} & 0 & 0 & N_{2,\eta} & 0 & \cdots & 0 & N_{20,\eta} & 0 \\ 0 & N_{1,\zeta} & 0 & 0 & N_{2,\zeta} & 0 & \cdots & 0 & N_{20,\zeta} & 0 \\ 0 & 0 & N_{1,\xi} & 0 & 0 & N_{2,\xi} & \cdots & 0 & 0 & N_{20,\xi} \\ 0 & 0 & N_{1,\eta} & 0 & 0 & N_{2,\eta} & \cdots & 0 & 0 & N_{20,\eta} \\ 0 & 0 & N_{1,\zeta} & 0 & 0 & N_{2,\zeta} & \cdots & 0 & 0 & N_{20,\zeta} \end{bmatrix} \begin{Bmatrix} u_1 \\ v_1 \\ w_1 \\ u_2 \\ v_2 \\ w_2 \\ \vdots \\ u_{20} \\ v_{20} \\ w_{20} \end{Bmatrix}$$

or

$$\{\delta'\} = [DS]\{d\} \tag{3.13}$$

using equations (3.10), (3.12) and (3.13) we can write :

$$\{\epsilon\} = [C][AJ][DS]\{d\} \tag{3.14}$$

comparing (3.9) and (3.14), we have :

$$[B] = [C][AJ][DS]$$

3.6 Formulation of Element Stiffness Matrix $[k^e]$

As given in the equation (3.3)

$$[k^e] = \int_v [B]^T[D][B]dv$$

$$= \int_v [B]^T[D][B]dxdydz$$

since $[B]$ matrix is in terms of the variables ξ, η, ζ we can transform the above expression to $\xi\eta\zeta$ system as :

$$[k^e] = \int_v [B]^T[D][B]Jd\xi d\eta d\zeta$$

where J = Det $[J]$.

The natural coordinate axes $\xi\eta\zeta$ vary from -1 to 1 in the element, so $[k^e]$ can be expressed as :

$$[k^e] = \int_{-1}^{1}\int_{-1}^{1}\int_{-1}^{1} [B]^T[D][B]Jd\xi d\eta d\zeta \tag{3.15}$$

3.6.1 Integration Scheme

To integrate the equation (3.15) Gauss quadrature procedure was used wherein two points along each axis are selected as Gauss points. (refer Scarborough 1987).

Since we selected a quadratic interpolation function, the expression for the element stiffness matrix is also quadratic. Two Gauss points yield the exact area under the curve of the form $\phi = a + c\xi^2$. We know that a curve $\phi = b\xi$ will integrate to zero in this kind of integration, as it has equal positive and negative area about ξ axis; hence for a general second degree polynomial $\phi = a + b\xi + c\xi^2$ (as in our case) two point Gauss quadrature integeration scheme should give an accurate solution (refer Cook 1987).

The expression is represented by a summation given as: (see appendix J)

$$[k^e] = \sum_{i=1}^{n}\sum_{j=1}^{n}\sum_{k=1}^{n} W_i W_j W_k \phi_s(\xi_i, \eta_j, \zeta_k)$$

where :

W_i	=	weight at the ith Gauss point along ξ axis.
n	=	no. of Gauss points chosen along an axis, which in this case is 2 for all axes.
$\phi_s(\xi_i, \eta_j, \zeta_k)$	=	function to be integrated.

3.7 Formulation of Element Mass Matrix $[m^e]$

From equation (3.5) we have :

$$\begin{aligned}
[m^e] &= \int_v [N^T]\rho[N]dv \\
&= \int_{-1}^{1}\int_{-1}^{1}\int_{-1}^{1} [N^T]\rho[N]Jd\xi d\eta d\zeta \\
&= \sum_{i=1}^{n}\sum_{j=1}^{n}\sum_{k=1}^{n} W_i W_j W_k \phi_m(\xi_i, \eta_j, \zeta_k)
\end{aligned}$$

The integration of the above expression can be done on similar lines as done for getting the element stiffness matrix $[k^e]$.

3.8 Formulation of Element Stress Stiffness Matrix $[k_\sigma^e]$

The element stress stiffness matrix is derived by adding higher - order terms to the strain - displacement relations. In linear problems only the simplest of the higher - order terms are used.

Strains can be written as :

$$\{\epsilon\} = \{\epsilon_L\} + \{\epsilon_{NL}\} \tag{3.16}$$

where $\{\epsilon_L\}$ contains the strain terms linear in the displacement derivatives and $\{\epsilon_{NL}\}$ contains the higher-order terms.

Strain energy stored in a system, subjected to uniform stresses $\{\sigma_0\}$ can be given as:

$$\begin{aligned} U = \int_v \{\epsilon\}^T \{\sigma_0\} dv &= \int_v \{\epsilon_L\}^T \{\sigma_0\} dv + \int_v \{\epsilon_{NL}\}^T \{\sigma_0\} dv \\ &= U_L + U_{NL} \end{aligned} \tag{3.17}$$

$[k_\sigma^e]$ is produced by stress acting through displacements associated with higher - order contributions to strain. Accordingly, we extract $[k_\sigma]$ from U_{NL} (see appendix K).

$\{\epsilon\}$ for a three-dimensional element is given as :

$$\begin{Bmatrix} \epsilon_x \\ \epsilon_y \\ \epsilon_z \\ \gamma_{xy} \\ \gamma_{yz} \\ \gamma_{zx} \end{Bmatrix} = \begin{Bmatrix} u_{,x} + \frac{1}{2}(u_{,x}^2 + v_{,x}^2 + w_{,x}^2) \\ u_{,y} + \frac{1}{2}(u_{,y}^2 + v_{,y}^2 + w_{,y}^2) \\ u_{,z} + \frac{1}{2}(u_{,z}^2 + v_{,z}^2 + w_{,z}^2) \\ u_{,y} + v_{,x} + (u_{,x}u_{,y} + v_{,x}v_{,y} + w_{,x}w_{,y}) \\ v_{,z} + w_{,y} + (v_{,y}v_{,z} + w_{,y}w_{,z} + u_{,y}u_{,z}) \\ w_{,x} + u_{,z} + (w_{,z}w_{,x} + u_{,z}u_{,x} + v_{,z}v_{,x}) \end{Bmatrix}$$

$$= \begin{Bmatrix} u_{,x} \\ u_{,y} \\ u_{,z} \\ u_{,y} + v_{,x} \\ v_{,z} + w_{,y} \\ w_{,x} + u_{,z} \end{Bmatrix} + \begin{Bmatrix} \frac{1}{2}(u_{,x}^2 + v_{,x}^2 + w_{,x}^2) \\ \frac{1}{2}(u_{,y}^2 + v_{,y}^2 + w_{,y}^2) \\ \frac{1}{2}(u_{,z}^2 + v_{,z}^2 + w_{,z}^2) \\ (u_{,x}u_{,y} + v_{,x}v_{,y} + w_{,x}w_{,y}) \\ (v_{,y}v_{,z} + w_{,y}w_{,z} + u_{,y}u_{,z}) \\ (w_{,z}w_{,x} + u_{,z}u_{,x} + v_{,z}v_{,x}) \end{Bmatrix} \tag{3.18}$$

comparing equation (3.16) and (3.18) we can write :

$$\{\epsilon_{NL}\} = \frac{1}{2}[Q][G]\{d\} \tag{3.19}$$

where :

$$[Q] = \begin{bmatrix} u_{,x} & 0 & 0 & v_{,x} & 0 & 0 & w_{,x} & 0 & 0 \\ 0 & u_{,y} & 0 & 0 & v_{,y} & 0 & 0 & w_{,y} & 0 \\ 0 & 0 & u_{,z} & 0 & 0 & v_{,z} & 0 & 0 & w_{,z} \\ u_{,y} & u_{,x} & 0 & v_{,y} & v_{,x} & 0 & w_{,y} & w_{,x} & 0 \\ 0 & u_{,z} & u_{,y} & 0 & v_{,z} & v_{,y} & 0 & w_{,z} & w_{,y} \\ u_{,z} & 0 & u_{,x} & v_{,z} & 0 & v_{,x} & w_{,z} & 0 & w_{,x} \end{bmatrix}$$

$$\{\delta\} = [G]\{d\}$$

from equation (3.17) we have.

$$\begin{aligned} U_{NL} &= \frac{1}{2}\int_v ([Q][G]\{d\})^T\{\sigma_0\}dv \\ &= \frac{1}{2}\int_v ([G]\{d\})^T[Q]^T\{\sigma_0\}dv \\ &= \frac{1}{2}\{d\}^T\int_v [G]^T[Q]^T\{\sigma_0\}dv \\ &= \frac{1}{2}\{d\}^T\int_v [G]^T\begin{bmatrix} s & 0 & 0 \\ 0 & s & 0 \\ 0 & 0 & s \end{bmatrix}\{\delta\}dv \end{aligned} \tag{3.20}$$

where :

$$[Q]^T_{9\times6}\{\sigma_0\}_{6\times1} = \begin{bmatrix} s & 0 & 0 \\ 0 & s & 0 \\ 0 & 0 & s \end{bmatrix}_{9\times9} \{\delta\}_{9\times1}$$

$$[s]_{3\times3} = \begin{bmatrix} \sigma_{x0} & \tau_{xy0} & \tau_{xz0} \\ \tau_{xy0} & \sigma_{y0} & \tau_{yz0} \\ \tau_{xz0} & \tau_{yz0} & \sigma_{z0} \end{bmatrix}$$

Noting that $\{\delta\} = [G]\{d\}$, from equation (3.20), which relates strain energy to displacement and stiffness, we can write :

$$U_{NL} = \frac{1}{2}\{d\}^T[k^e_\sigma]\{d\} \tag{3.21}$$

where:

$$[k^e_\sigma] = \int_v [G]^T \begin{bmatrix} s & 0 & 0 \\ 0 & s & 0 \\ 0 & 0 & s \end{bmatrix} [G]dv$$

The element stress stiffness matrix $[k^e_\sigma]$ is a symmetric matrix like the conventional stiffness matrix and the global $[K_\sigma]$ is obtained by the usual assembly of element $[k^e_\sigma]$ matricies.

3.8.1 [s] Matrix

The stress matrix [s] after simplifications can be written in the following form, in terms of the known quantities : (refer to appendix L)

$$[s] = \begin{bmatrix} \sigma_{x0} & \tau_{xy0} & \tau_{xz0} \\ \tau_{xy0} & \sigma_{y0} & \tau_{yz0} \\ \tau_{xz0} & \tau_{yz0} & \sigma_{z0} \end{bmatrix}$$

$$= \begin{bmatrix} E\epsilon_{xx} & (u_{,y} + v_{,x})G & (u_{,z} + w_{,x})G \\ (u_{,y} + v_{,x})G & E\epsilon_{yy} & (v_{,z} + w_{,y})G \\ (u_{,z} + w_{,x})G & (v_{,z} + w_{,y})G & E\epsilon_{zz} \end{bmatrix}$$

$$= \begin{bmatrix} E & 0 & 0 & 0 & 0 & 0 & 0 & 0 & 0 \\ 0 & G & 0 & G & 0 & 0 & 0 & 0 & 0 \\ 0 & 0 & G & 0 & 0 & 0 & G & 0 & 0 \end{bmatrix} \begin{Bmatrix} u_{,x} \\ u_{,y} \\ u_{,z} \\ v_{,x} \\ v_{,y} \\ v_{,z} \\ w_{,x} \\ w_{,y} \\ w_{,z} \end{Bmatrix} \begin{bmatrix} 1 & 0 & 0 \end{bmatrix}$$

$$+$$

$$\begin{bmatrix} 0 & G & 0 & G & 0 & 0 & 0 & 0 & 0 \\ 0 & 0 & 0 & 0 & E & 0 & 0 & 0 & 0 \\ 0 & 0 & 0 & 0 & 0 & G & 0 & G & 0 \end{bmatrix} \begin{Bmatrix} u_{,x} \\ u_{,y} \\ u_{,z} \\ v_{,x} \\ v_{,y} \\ v_{,z} \\ w_{,x} \\ w_{,y} \\ w_{,z} \end{Bmatrix} \begin{bmatrix} 0 & 1 & 0 \end{bmatrix}$$

$$+$$

$$\begin{bmatrix} 0 & 0 & G & 0 & 0 & 0 & G & 0 & 0 \\ 0 & 0 & 0 & 0 & 0 & G & 0 & G & 0 \\ 0 & 0 & 0 & 0 & 0 & 0 & 0 & 0 & E \end{bmatrix} \begin{Bmatrix} u_{,x} \\ u_{,y} \\ u_{,z} \\ v_{,x} \\ v_{,y} \\ v_{,z} \\ w_{,x} \\ w_{,y} \\ w_{,z} \end{Bmatrix} \begin{bmatrix} 0 & 0 & 1 \end{bmatrix}$$

3.9 Solution of The Eigenvalue Problem

After assembling all the element mass and stiffness matrices into the global form, we get the following eigenvalue equation for the free vibration analysis :

$$[K]_{(n\times n)}\{x\}_{(n\times 1)} - \lambda[M]_{(n\times n)}\{\ddot{x}\}_{(n\times 1)} = \{0\}$$

The model under study had 1086 degrees of freedom and hence the size of $[K]$ and $[M]$ matrices was (1086×1086), which was quite large so far as the C.P.U. time consumed is concerned. In order to reduce the size of the matrices, "Dynamic Condensation" of the system was carried out.

3.9.1 Dynamic Condensation

In this technique usually known as Guyan Reduction, as given in Guyan (1965), we retain important degrees of freedom of the system, called "master d.o.f." and the remaining degrees of freedom called "slave d.o.f." are either neglected because of their neglegible influence or obtained in terms of master d.o.f. The criterion for selection of master d.o.f. is that the ratio K_{ii}/M_{ii} should be least for such a d.o.f.

In our case we selected all the degrees of freedom in the z direction of the system as master d.o.f., since the ratio of the stiffness to the mass in the other two directions is quite high. The master degrees of freedom numbered 362 and hence we had to solve the reduced system of $[K]$ and $[M]$ matrices having a size of (362×362).

The procedure is described briefly as fo.lows :

$$\left\{ \begin{bmatrix} K_{mm} & \vdots & K_{ms} \\ \cdots & \cdots & \cdots \\ K_{sm} & \vdots & K_{ss} \end{bmatrix} - \lambda \begin{bmatrix} M_{mm} & \vdots & M_{ms} \\ \cdots & \cdots & \cdots \\ M_{sm} & \vdots & M_{ss} \end{bmatrix} \right\} \begin{Bmatrix} x_m \\ \cdots \\ x_s \end{Bmatrix} = \begin{Bmatrix} 0 \\ \cdots \\ 0 \end{Bmatrix} \quad (3.22)$$

The above system can be partioned into two systems as shown, where :

x_m = displacement associated with master d.o.f.
x_s = displacement associated with slave d.o.f.
m = refers to master d.o.f.
s = refers to slave d.o.f.

from (3.22) we get:

$$(K_{mm} - \lambda M_{mm})x_m + (K_{ms} - \lambda M_{ms})x_s = 0 \quad (3.23)$$

$$(K_{sm} - \lambda M_{sm})x_m + (K_{ss} - \lambda M_{ss})x_s = 0 \quad (3.24)$$

Neglecting M_{sm} and M_{ss}, we get from (3.24) :

$$\{x_s\} = -[K_{ss}^{-1}][K_{sm}]\{x_m\}$$

Hence :

$$\begin{Bmatrix} x_m \\ x_s \end{Bmatrix} = \begin{bmatrix} I \\ -[K_{ss}^{-1}][K_{sm}] \end{bmatrix} \{x_m\}$$

$$= [T]\{x_m\}$$

where $[T]$ is the transformation matrix.

Since the total energy of the system is conserved, we have

$$P.E. = \frac{1}{2}\{x\}^T[K]\{x\} = \frac{1}{2}\{x_m\}^T[T]^T[K][T]\{x_m\}$$

$$= \frac{1}{2}\{x_m\}^T[K_R]\{x_m\}$$

$$K.E. = \frac{1}{2}\{\dot{x}\}^T[M]\{\dot{x}\} = \frac{1}{2}\{\dot{x}_m\}^T[T]^T[M][T]\{\dot{x}_m\}$$

$$= \frac{1}{2}\{\dot{x}_m\}^T[M_R]\{\dot{x}_m\}$$

the above two equations indicate that the reduced stiffness and mass matrices of the system are given as:

$$[K_R]_{m\times m} = [T]^T[K][T]$$

$$[M_R]_{m\times m} = [T]^T[M][T] \qquad \text{where } m < n$$

Fig. 3.2 shows the close comparison between the natural frequencies obtained with this analysis and those computed by assuming the propeller blade to be a cantilever, as given in the previous chapter.

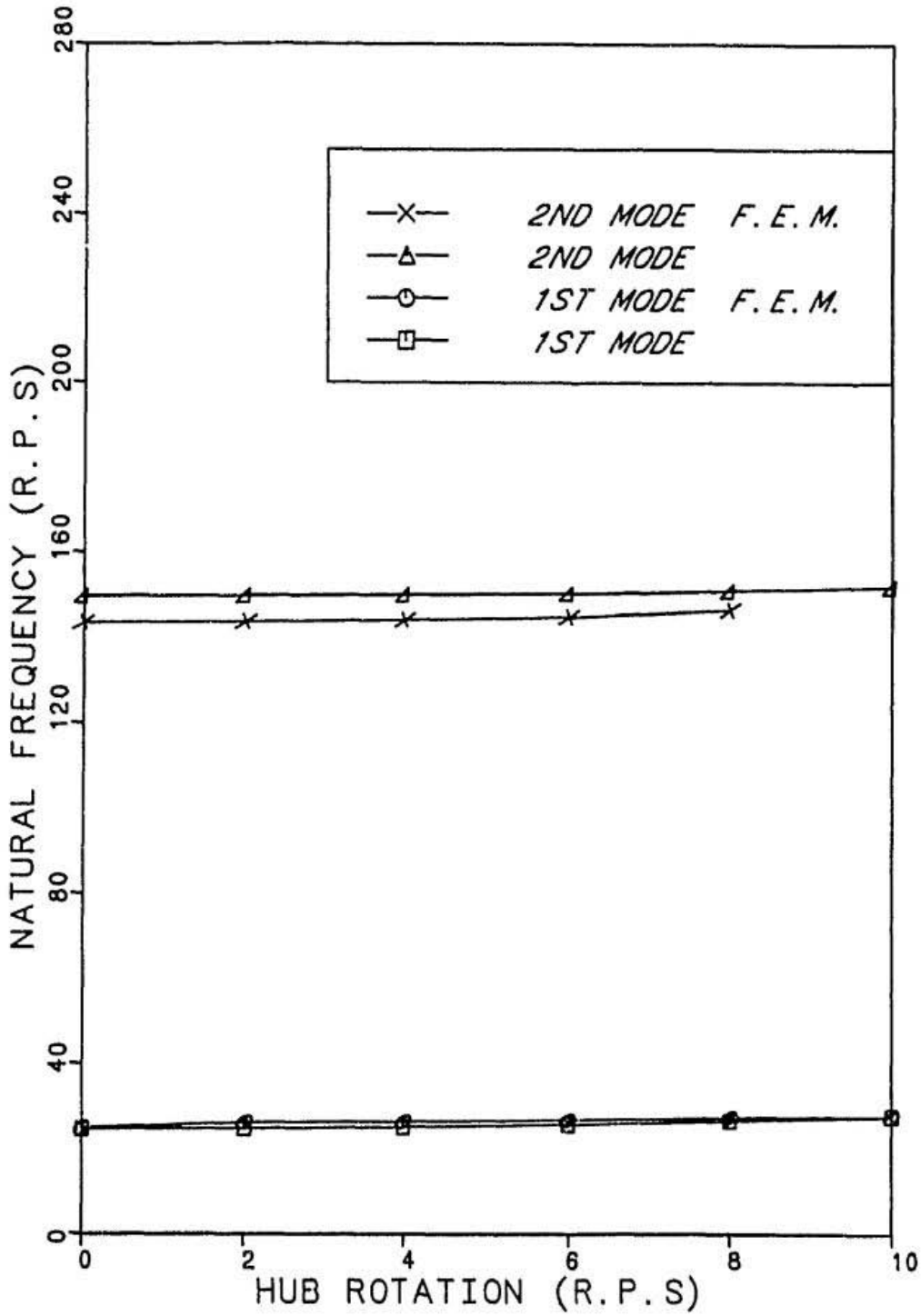

Figure 3.2: Comparison of natural frequencies, against those obtained using 3-D finite element analysis.

Chapter 4

FREQUENCY ANALYSIS OF SHAFT-ROTOR SYSTEM

4.1 Introduction

In this chapter the equation of motion, describing the transverse vibrations, of the propeller shaft without the blades has been derived using Newtonian approach. The hub of the propeller has been treated as a flexible rotor and thus the whole shafting can be considered as a shaft-rotor system. The system has been considered in three parts: tail shaft, over hang and rotor, as can be seen in Fig. 4.1.

Equations of motion have been derived separately for the three segments as can be seen in Haddara (1988). After applying the boundary conditions we get the characteristic equation of the whole system. For the propulsion shafting under consideration, coupled transverse vibrations in the horizontal and vertical planes are known to occur as a result of propeller gyroscopy, bearing properties, shaft properties and shaft unbalance. For this fact equations of motion of the shaft segments in two perpendicular planes have been derived, which when coupled give the final equation (see Chivens, 1975). Shear deflection and rotary inertia effects have been considered for the rotor since it has a larger diameter as compared to the tail shaft.

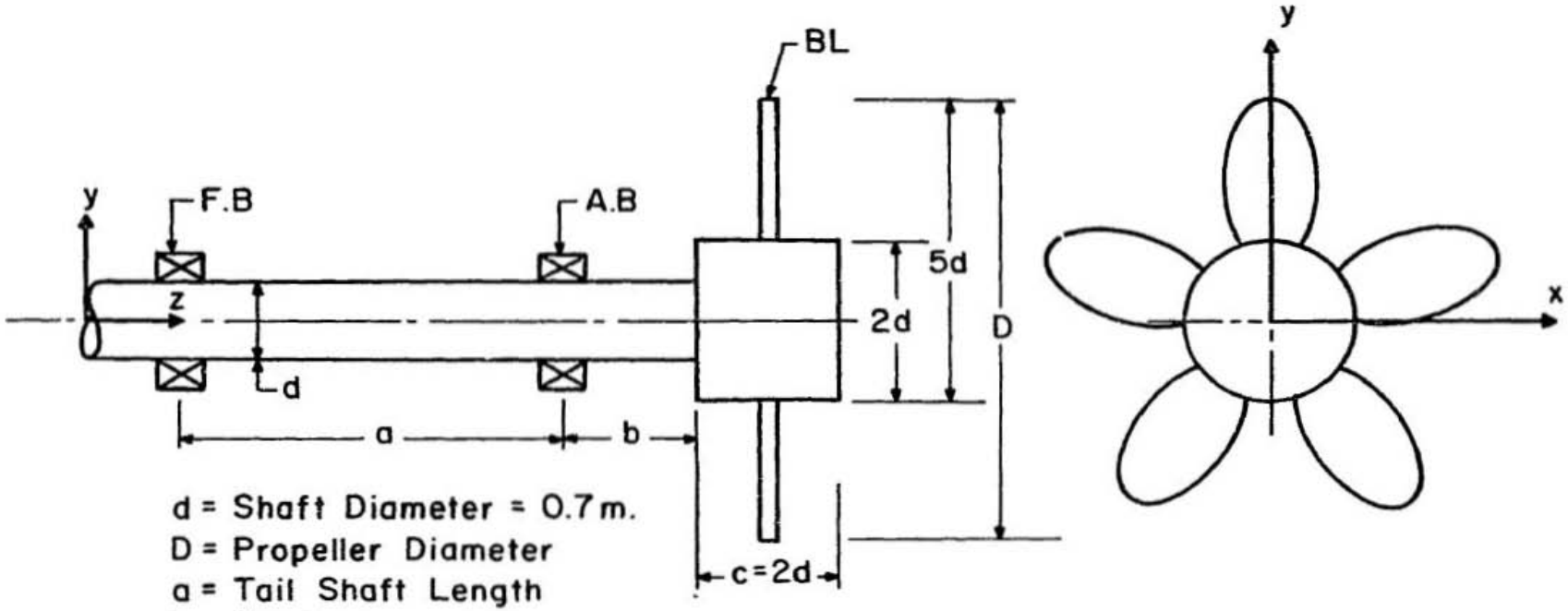

Figure 4.1: Propeller shaft schematic diagram

4.2 Formulation of the Rotor Equation

In this section the equation of motion of rotor in the complex plane in a non-rotating coordinate system has been derived. Since rotary inertia has been taken into consideration, we first find the angular momentum of the rotor.

4.2.1 Angular Momentum of the Rotor

As found in chapter 2 the angular velocity $\vec{\Omega}_1$ of the coordinate system xyz, with reference to XYZ, coordinate frame is:

$$\begin{aligned} \vec{\Omega}_1 &= \dot{\phi} I + \dot{\theta} \hat{j}_1 \\ &= \dot{\phi} \hat{i} + \dot{\theta} \hat{j} \end{aligned} \tag{4.1}$$

The angular momentum of the rotor in its local coordinates is given as :

$$\begin{aligned} \vec{H} &= I_{mx}\Omega_{1x}\hat{i} + I_{my}\Omega_{1y}\hat{j} + I_{mz}\Omega_{1z}\hat{k} \\ &= \frac{J}{2}\dot{\phi}\hat{i} + \frac{J}{2}\dot{\theta}\hat{j} + J\Omega\hat{k} \end{aligned} \tag{4.2}$$

where:

$I_{mx} = \dfrac{J}{2}$ = x component of total virtual mass moment of inertia of the rotor

$I_{my} = \dfrac{J}{2}$ = y component of total virtual mass moment of inertia of the rotor

$I_{mz} = J$ = z component of total virtual mass moment of inertia of the rotor

$\Omega_{1x} = \dot{\phi}$ = x component of the angular velocity of the rotor

$\Omega_{1y} = \dot{\theta}$ = y component of the angular velocity of the rotor

$\Omega_{1z} = \Omega$ = z component of the angular velocity of the rotor

θ = slope due to bending moment in xz plane

ϕ = slope due to bending moment in yz plane

Moment exerted by the rotor on the shaft, as given in Dimarogonas (1983) is given by :

$$\vec{M} = \frac{J}{2}\ddot{\phi}\hat{i} + \frac{J}{2}\ddot{\theta}\hat{j} + \vec{\Omega}_1 \times \vec{H}$$

$$\vec{\Omega}_1 \times \vec{H} = \begin{vmatrix} \vec{i} & \vec{j} & \vec{k} \\ \dot{\phi} & \dot{\theta} & 0 \\ \frac{J}{2}\dot{\phi} & \frac{J}{2}\dot{\theta} & J\Omega \end{vmatrix} \approx \dot{\theta}\Omega J\vec{i} - \dot{\phi}\Omega J\vec{j}$$

$$\begin{aligned} \vec{M} &= \frac{J}{2}(\ddot{\phi} + 2\Omega\dot{\theta})\vec{i} + \frac{J}{2}(\ddot{\theta} - 2\Omega\dot{\phi})\vec{j} \\ &= \rho I(\ddot{\phi} + 2\Omega\dot{\theta})\vec{i} + \rho I(\ddot{\theta} - 2\Omega\dot{\phi})\vec{j} = \vec{M}_x\vec{i} + \vec{M}_y\vec{j} \end{aligned} \tag{4.3}$$

where :

ρ = density of material

I = area moment of inertia about a diameter

4.2.2 Equation of Motion in xz and yz Planes

The free body diagrams of an element in the xz and yz planes are shown in Fig. 4.2.

where:

V_x = shear force along x axis

M_x = moment about x axis

V_y = shear force along y axis

M_y = moment about y axis

u_s = displacement along x axis.

v_s = displacement along y axis.

Equilibrium of forces in the vertical direction for the two planes yields :

$$V_x - (V_x + \frac{\partial V_x}{\partial z}dz) = m\ddot{u}_s dz$$

$$V_y - (V_y + \frac{\partial V_y}{\partial z}dz) = m\ddot{v}_s dz$$

or

$$-\frac{\partial V_x}{\partial z} = m\ddot{u}_s \tag{4.4}$$

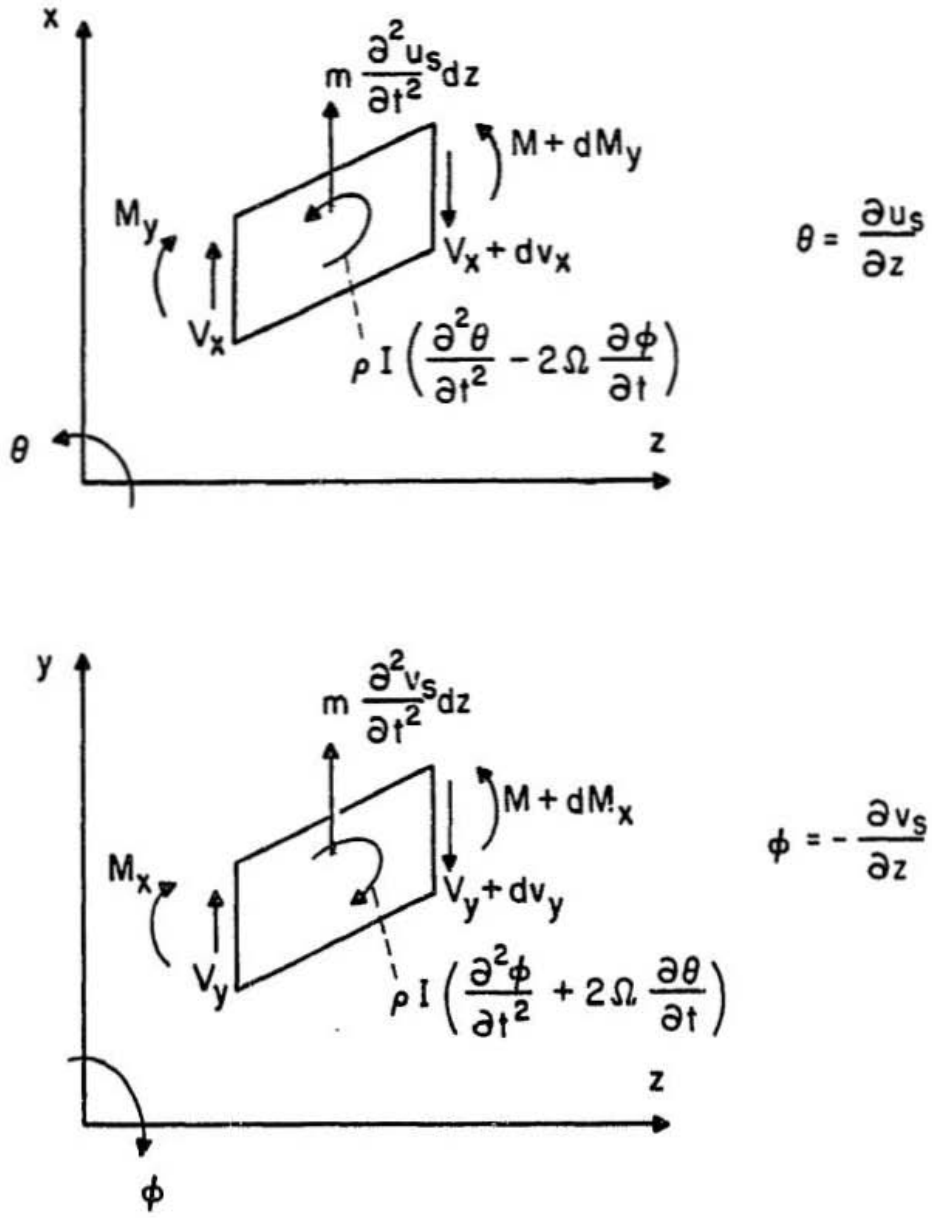

Figure 4.2: Free body diagram of the rotor element

$$-\frac{\partial V_y}{\partial z} = m\ddot{v}_s \tag{4.5}$$

using equation (4.3) equilibrium of moments in the two planes yields :

$$\begin{aligned} -(M_y + V_x dz) + M_y + dM_y &= \bar{M}_y dz \\ &= \rho I(\ddot{\theta} - 2\Omega\dot{\phi})dz \end{aligned}$$

$$\begin{aligned} (M_x + V_y dz) - (M_x + dM_x) &= \bar{M}_x dz \\ &= \rho I(\ddot{\phi} + 2\Omega\dot{\phi})dz \end{aligned}$$

or

$$V_x - \frac{\partial M_y}{\partial z} = -\rho I(\ddot{\theta} - 2\Omega\dot{\phi}) \tag{4.6}$$

$$V_y - \frac{\partial M_x}{\partial z} = \rho I(\ddot{\phi} + 2\Omega\dot{\theta}) \tag{4.7}$$

The expressions for the shear force and the bending moment in the two planes are given as :

$$M_x = -EI\frac{\partial \phi}{\partial z}$$

$$V_y = -KAG\left(\phi + \frac{\partial v_s}{\partial z}\right) \tag{4.8}$$

and

$$M_y = EI\frac{\partial \theta}{\partial z}$$

$$V_x = KAG\left(\theta + \frac{\partial u_s}{\partial z}\right) \tag{4.9}$$

where:

E = modulus of elasticity

G = modulus of elasticity in shear

A = cross-section area of the element

K = shape factor constant of the beam

Differentiating equations (4.8) and (4.9) and using (4.4), (4.5) we have:

$$\begin{aligned}\frac{\partial \phi}{\partial z} &= -\frac{1}{KAG}\frac{\partial V_y}{\partial z} - \frac{\partial^2 v_s}{\partial z^2} \\ &= -\frac{\partial^2 v_s}{\partial z^2} + \frac{m}{KAG}\frac{\partial^2 v_s}{\partial t^2} \qquad (4.10)\end{aligned}$$

$$\begin{aligned}\frac{\partial \theta}{\partial z} &= \frac{1}{KAG}\frac{\partial V_x}{\partial z} + \frac{\partial^2 u_s}{\partial z^2} \\ &= \frac{\partial^2 u_s}{\partial z^2} - \frac{m}{KAG}\frac{\partial^2 u_s}{\partial t^2} \qquad (4.11)\end{aligned}$$

equations (4.6) and (4.7) yield:

$$\frac{\partial V_x}{\partial z} - EI\frac{\partial^3 \theta}{\partial z^3} = -\rho I\left(\frac{\partial^3 \theta}{\partial z \partial t^2} - 2\Omega\frac{\partial^2 \phi}{\partial z \partial t}\right)$$

$$\frac{\partial V_y}{\partial z} - EI\frac{\partial^3 \phi}{\partial z^3} = \rho I\left(\frac{\partial^3 \phi}{\partial z \partial t^2} + 2\Omega\frac{\partial^2 \theta}{\partial z \partial t}\right)$$

using equations (4.4), (4.5), (4.10) and (4.11) in the above equations we get :

$$\begin{aligned}-m\frac{\partial^2 u_s}{\partial t^2} - EI\left[\frac{\partial^4 u_s}{\partial z^4} - \frac{m}{KAG}\frac{\partial^4 u_s}{\partial z^2 \partial t^2}\right] &= -\rho I\left[\frac{\partial^4 u_s}{\partial z^2 \partial t^2} - \frac{m}{KAG}\frac{\partial^4 u_s}{\partial t^4}\right] \\ &\quad +2\rho\Omega I\left[-\frac{\partial^3 v_s}{\partial z^2 \partial t} + \frac{m}{KAG}\frac{\partial^3 v_s}{\partial t^3}\right] \qquad (4.12)\end{aligned}$$

$$\begin{aligned}-m\frac{\partial^2 v_s}{\partial t^2} + EI\left[-\frac{\partial^4 v_s}{\partial z^4} - \frac{m}{KAG}\frac{\partial^4 v_s}{\partial z^2 \partial t^2}\right] &= \rho I\left[-\frac{\partial^4 v_s}{\partial z^2 \partial t^2} + \frac{m}{KAG}\frac{\partial^4 v_s}{\partial t^4}\right] \\ &\quad +2\rho I\Omega\left[\frac{\partial^3 u_s}{\partial z^2 \partial t} - \frac{m}{KAG}\frac{\partial^3 u_s}{\partial t^3}\right] \qquad (4.13)\end{aligned}$$

combining equations (4.12) and (4.13) and defining $w_r = u_s + iv_s$, we have :

$$\begin{aligned}m\frac{\partial^2 w_r}{\partial t^2} + EI\frac{\partial^4 w_r}{\partial z^4} - \frac{EIm}{KAG}\frac{\partial^4 w_r}{\partial z^2 \partial t^2} &= \rho I\frac{\partial^4 w_r}{\partial z^2 \partial t^2} - \frac{\rho I m}{KAG}\frac{\partial^4 w_r}{\partial t^4} \\ &\quad -2i\rho I\Omega\frac{\partial^3 w_r}{\partial z^2 \partial t} + 2i\frac{\rho I\Omega m}{KAG}\frac{\partial^3 w_r}{\partial t^3}\end{aligned}$$

$$\begin{aligned}m\frac{\partial^2 w_r}{\partial t^2} + EI\frac{\partial^4 w_r}{\partial t^4} - \rho I\left(1 + \frac{E}{KG}\right)\frac{\partial^4 w_r}{\partial z^2 \partial t^2} + \frac{\rho^2 I}{KG}\frac{\partial^4 w_r}{\partial t^4} \\ +2i\rho I\Omega\left(\frac{\partial^3 w_r}{\partial z^2 \partial t} - \frac{\rho}{KG}\frac{\partial^3 w_r}{\partial t^3}\right) = 0\end{aligned}$$

4.3 Equations for the Tail Shaft and the Overhang Portion

As was mentioned before, in the case of the tail shaft and the overhang portion, effects of shear deflection and rotary inertia, being small, have been ignored, hence the equations of motion for these segments are the conventional Euler-Bernoulli equation, given as :

$$m_s \frac{\partial^2 w_s}{\partial t^2} + EI_s \frac{\partial^4 w_s}{\partial z_s^4} = 0$$

$$m_s \frac{\partial^2 w_t}{\partial t^2} + EI_s \frac{\partial^4 w_t}{\partial z_t^4} = 0$$

where :

m_s = mass per unit length of shaft

I_s = area moment of inertia of shaft

w_r = transverse displacement for the rotor

w_s = transverse displacement for the overhang portion

w_t = transverse displacement for the tail shaft

z_s = axial coordinate for the overhang

z_t = axial coordinate for the tail shaft

The equations of motion for the propeller shaft assembly are thus given as :

$$m\frac{\partial^2 w_r}{\partial t^2} + EI\frac{\partial^4 w_r}{\partial t^4} - \rho I\left(1 + \frac{E}{KG}\right)\frac{\partial^4 w_r}{\partial z^2 \partial t^2} + \frac{\rho^2 I}{KG}\frac{\partial^4 w_r}{\partial t^4} + 2i\rho I\Omega\left(\frac{\partial^3 w_r}{\partial z^2 \partial t} - \frac{\rho}{KG}\frac{\partial^3 w_r}{\partial t^3}\right) = 0 \qquad (4.14)$$

$$m_s \frac{\partial^2 w_s}{\partial t^2} + EI_s \frac{\partial^4 w_s}{\partial z_s^4} = 0 \qquad (4.15)$$

$$m_s \frac{\partial^2 w_t}{\partial t^2} + EI_s \frac{\partial^4 w_t}{\partial z_t^4} = 0 \qquad (4.16)$$

with the boundary conditions :

1. $w_t(0) = 0$

2. $w_t''(0) - k w_t'(0) = 0$

3. $w_s(0) = 0$

4. $w_s'(0) = w_t'(a)$

5. $w_s''(0) = w_t''(a)$

6. $w_t(a) = 0$

7. $w_r(0) = w_s(b)$

8. $w_r'(0) = w_s'(b)$

9. $w_r''(0) = \mu w_s''(b)$

10. $w_r'''(0) = \mu w_s'''(b)$

11. $w_r''(c) = 0$

12. $w_r'''(c) = 0$

where:

a = rotor length

b = tail shaft length

c = overhang length

μ = ratio of the shaft and rotor moment of inertias.

4.4 Nondimensionalization

To put the equations of motion in the nondimensional form w.r.t. space and time variables, we define nondimensional variables:

$$y_r = \frac{w_r}{l}$$

$$y_s = \frac{w_s}{l}$$

$$y_t = \frac{w_t}{l}$$

$$x_r = \frac{z}{l}$$

$$x_s = \frac{z_s}{l}$$

$$x_t = \frac{z_t}{l}$$

$$\tau = \Omega t$$

where l is the total length of the propeller shaft.

Using the above relations equations (4.14), (4.15) and (4.16) take the following form :

$$m\Omega^2 l\frac{\partial^2 y_r}{\partial \tau^2} + \frac{EI}{l^3}\frac{\partial^4 y_r}{\partial x^4} - \rho I\left(1+\frac{E}{KG}\right)\frac{\Omega^2}{l}\frac{\partial^4 y_r}{\partial x^2 \partial \tau^2} + \frac{\rho^2 I}{KG}\Omega^4 l\frac{\partial^4 y_r}{\partial \tau^4} + 2i\rho I\Omega\left[\frac{\Omega}{l}\frac{\partial^3 y_r}{\partial x^2 \partial \tau} - \frac{\rho}{KG}\Omega^3 l\frac{\partial^3 y_r}{\partial \tau^3}\right] = 0 \qquad (4.17)$$

$$m_s\Omega^2 l\frac{\partial^2 y_s}{\partial \tau^2} + \frac{EI_s}{l^3}\frac{\partial^4 y_s}{\partial x_s^4} = 0 \qquad (4.18)$$

$$m_s\Omega^2 l\frac{\partial^2 y_t}{\partial \tau^2} + \frac{EI_s}{l^3}\frac{\partial^4 y_t}{\partial x_t^4} = 0 \qquad (4.19)$$

The equations of motion in the non-dimensional form for the system are thus given as :

$$\frac{\partial^2 y_r}{\partial \tau^2} + \xi_r\frac{\partial^4 y_r}{\partial x^4} - \frac{\xi_1}{l^2}\left(1+\frac{E}{KG}\right)\frac{\partial^4 y_r}{\partial x^2 \partial \tau^2} + \frac{\xi_1\rho\Omega^2}{KG}\frac{\partial^4 y_r}{\partial \tau^4} + 2i\xi_1\left[\frac{1}{l^2}\frac{\partial^3 y_r}{\partial x^2 \partial \tau} - \frac{\rho\Omega^2}{KG}\frac{\partial^3 y_r}{\partial \tau^3}\right] = 0 \qquad (4.20)$$

$$\frac{\partial^2 y_s}{\partial \tau^2} + \xi_s\frac{\partial^4 y_s}{\partial x_s^4} = 0 \qquad (4.21)$$

$$\frac{\partial^2 y_t}{\partial \tau^2} + \xi_s \frac{\partial^4 y_t}{\partial x_t^4} = 0 \tag{4.22}$$

where :

$$\xi_1 = \frac{\rho I}{m} \tag{4.23}$$

$$\xi_r = \frac{EI}{m\Omega^2 l^4} \tag{4.24}$$

$$\xi_s = \frac{EI_s}{m_s\Omega^2 l^4} \tag{4.25}$$

with the boundary conditions :

1. $y_t(0) = 0$
2. $y_t''(0) - k y_t'(0) = 0$
3. $y_s(0) = 0$
4. $y_s'(0) = y_t'(a)$
5. $y_s''(0) = y_t''(a)$
6. $y_t(a) = 0$
7. $y_r(0) = y_s(b)$
8. $y_r'(0) = y_s'(b)$
9. $y_r''(0) = \mu y_s''(b)$
10. $y_r'''(0) = \mu y_s'''(b)$
11. $y_r''(c) = 0$
12. $y_r'''(c) = 0$

4.5 Solution of the Equation

We assume a solution for y_r, y_s, y_t in terms of space and time functions as :

$$\begin{aligned} y_r &= e^{\eta x_r} e^{i\overset{*}{\omega}\tau} \\ y_s &= e^{\lambda x_s} e^{i\overset{*}{\omega}\tau} \\ y_t &= e^{\lambda x_t} e^{i\overset{*}{\omega}\tau} \end{aligned} \tag{4.26}$$

where :

$\overset{*}{\omega} = \dfrac{w}{\Omega}$

η = root of the spatial function for the rotor

λ= root of the spatial function for the shaft

$\overset{*}{\omega}$ = non-dimensional eigen value

ω = dimensional eigen value

substituting y_r, y_s, y_t in the equations (4.20), (4.21) and (4.22) we have :

$$\begin{aligned} -\omega^2 + \xi_r\eta^4 + \frac{\xi_1}{l^2}\left(1+\frac{E}{KG}\right)\overset{*}{\omega}^2\eta^2 + \frac{\rho\Omega^2}{KG}\xi_1\overset{*}{\omega}^4 \\ +2i\Omega\xi_1\left[\frac{1}{\Omega l^2}\eta^2(i\overset{*}{\omega}) + \frac{\rho\Omega}{KG}(i\overset{*}{\omega}^3)\right] = 0 \end{aligned} \tag{4.27}$$

and

$$-\overset{*}{\omega}^2 + \xi_s\lambda^4 = 0 \tag{4.28}$$

equation (4.27) and (4.28) on simplification take the form :

$$\eta^4 + \left[\frac{\xi_1}{\xi_r l^2}\left(1+\frac{E}{KG}\right)\overset{*}{\omega}^2 - \frac{2\xi_1\overset{*}{\omega}}{\xi_r l^2}\right]\eta^2 + \frac{\xi_1}{\xi_r}\frac{\rho\Omega^2\overset{*}{\omega}^3}{KG}\left(\overset{*}{\omega}-2\right) - \frac{\overset{*}{\omega}^2}{\xi_r} = 0 \tag{4.29}$$

$$\lambda^4 = \frac{\overset{*}{\omega}^2}{\xi_s} \tag{4.30}$$

equation (4.29) can be represented as :

$$\eta^4 + c_1\eta^2 + c_2 = 0$$

where :

$$c_1 = \frac{\xi_1}{\xi_r l^2}\overset{*}{\omega}^2\left[\epsilon + \frac{E}{KG}\right]$$

$$c_2 = \frac{\overset{*}{\omega}^2}{\xi_r}\left[\frac{\xi_1 \rho \Omega^2 \overset{*}{\omega}^2}{KG}\epsilon - 1\right]$$

$$\epsilon = 1 \pm \frac{2}{\overset{*}{\omega}}$$

where - and + sign for ϵ correspond to the forward and the reverse whirl of the shaft respectively.

The roots of the equation (4.29) are given as:

$$\eta^2 = \frac{-c_1 \pm \sqrt{c_1^2 - 4c_2}}{2} = \left(-\frac{c_1}{2}\right) \pm \sqrt{\left(\frac{c_1}{2}\right)^2 - c_2}$$

$$\eta = \pm \left[\left(-\frac{c_1}{2}\right) \pm \sqrt{\left(\frac{c_1}{2}\right)^2 - c_2}\right]^{\frac{1}{2}}$$

we have four values of η, defined as α_1, α_2, α_3 and α_4 where:

$$\alpha_1 = i\eta_2 \qquad \alpha_3 = \eta_1$$

and

$$\alpha_2 = -i\eta_2 \qquad \alpha_4 = -\eta_1$$

$$\eta_1 = \left[-\frac{c_1}{2} + \sqrt{\left(\frac{c_1}{2}\right)^2 - c_2}\right]^{\frac{1}{2}}$$

$$\eta_2 = \left[-\frac{c_1}{2} + \sqrt{\left(\frac{c_1}{2}\right)^2 - c_2}\right]^{\frac{1}{2}}$$

from equation (4.26), the solution for y_r can be given as :

$$\begin{aligned} y_r &= \left(Ae^{\eta_1 x} + Be^{-\eta_1 x} + Ce^{i\eta_2 x} + De^{-i\eta_2 x}\right) e^{i\overset{*}{\omega}\tau} \\ &= R(x_r)e^{i\overset{*}{\omega}\tau} \end{aligned}$$

similarly the solutions for the overhang and tail shaft portions of the shaft are given respectively as :

$$y_s = S(x_s)e^{i\overset{*}{\omega}\tau}$$

$$y_t = T(x_t)e^{i\bar{\omega}\tau}$$

where :

$$R(x_1) = A_1 \sin\beta_2 + A_2 \cos\beta_2 + A_3 \sinh\beta_1 + A_4 \cosh\beta_1$$

$$S(x_2) = P_1 \sin\gamma_2 + P_2 \cos\gamma_2 + p_3 \sinh\gamma_2 + P_4 \cosh\gamma_2$$

$$T(x_3) = Q_1 \sin\gamma_3 + Q_2 \cos\gamma_3 + Q_3 \sinh\gamma_3 + Q_4 \cosh\gamma_3$$

where :

$$\beta_i = \eta_i x_1 \quad i = 1,2$$

$$\gamma_k = \lambda x_k \quad k = 2,3$$

$A_i, P_i, Q_i (i = 1,...4)$ = arbitrary constants to be determined from the boundary conditions.

4.5.1 Application of the Boundary Conditions

To solve the shaft-rotor system equations (4.20), (4.21) and (4.22) we need to have twelve boundary conditions, so that we have twelve equations in twelve arbitrary constants and the eigen value $\bar{\omega}$. For a consistent solution of the system of equations we need to solve the characteristic equation of the system which becomes the eigen value equation for our system.

Boundary Conditions at A :

1) $T(0) = 0$

2) $T''(0) - KT'(0) = 0$

Boundary Conditions at B :

3) $S(0) = 0$

4) $S'(0) = T'(a)$

5) $S''(0) = T''(a)$

6) $T(a) = 0$

Boundary Conditions at C :

7) $R(0) = S(b)$

8) $R'(0) = S'(b)$

9) $R''(0) = \mu S''(b)$

10) $R'''(0) = \mu S'''(b)$

Boundary Conditions at D :

11) $R''(c) = 0$

12) $R'''(c) = 0$

where:

A = forward end bearing of the tail shaft

B = aft end bearing of the tail shaft

C = shaft rotor junction

D = free end of the rotor

Dash over the variable denotes differentiation w.r.t. the spatial variable.

The boundary condition (1) states that the deflection is zero at forward end bearing, the boundary condition (2) is written in a general form so that one can deal with a simple support, a clamped support or a general degree of fixity at this end. The difference in the natural frequencies for different fixities is evident from fig. 4.3.

Conditions (3), (6) state that the deflection is zero at the simple support B, while (4) and (5) are the continuity conditions at this support.

Boundary conditions (7) through (10) represent the continuity conditions at the shaft-rotor junction.

Conditions (11) and (12) state that the bending moment and shear force are zero at the free end of the rotor.

Using all the boundary conditions we can derive the following characteristic

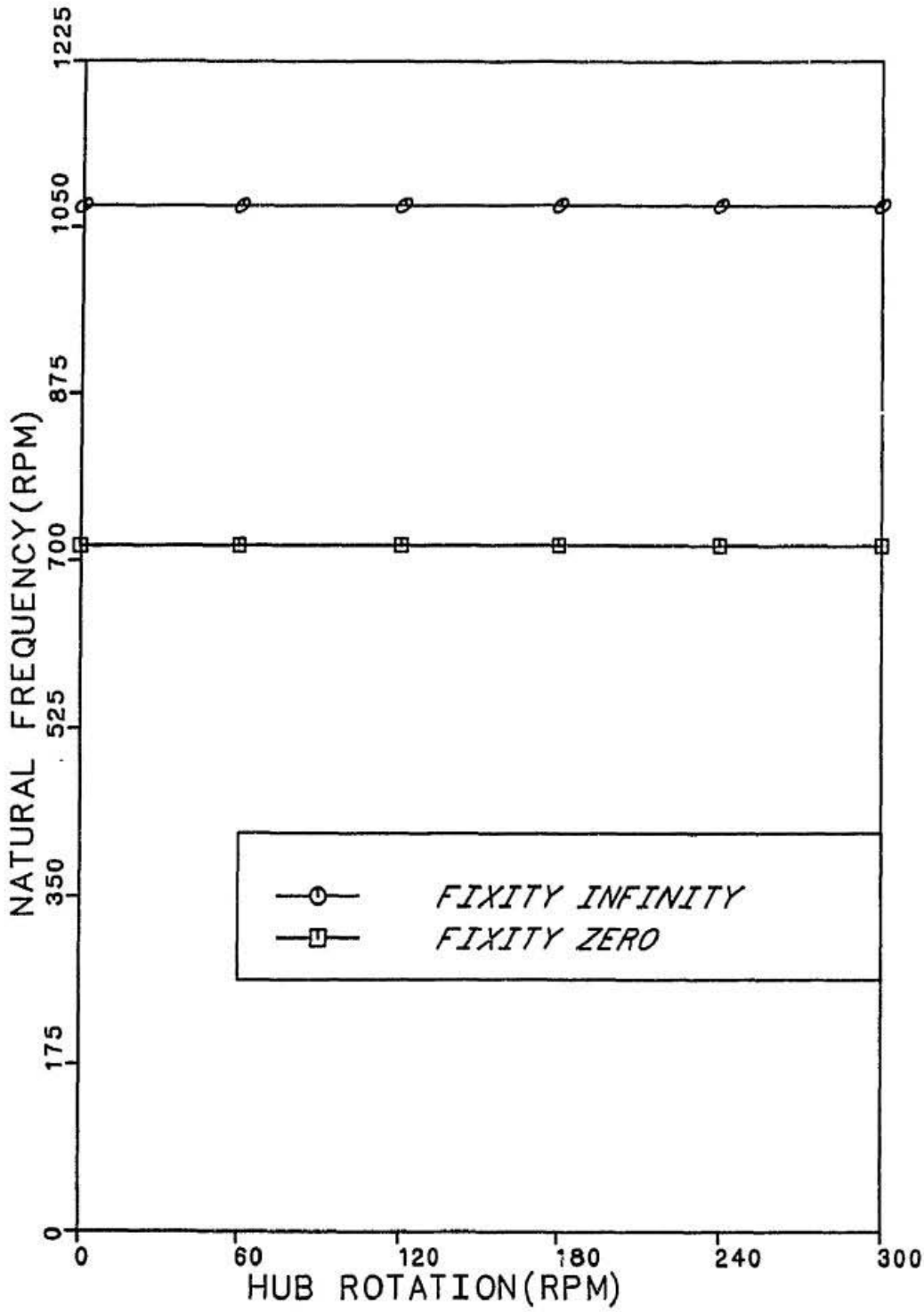

Figure 4.3: Variation of natural frequency with respect to the change in the shaft fixity.

equation in the variable ω.

$$(X_1 + X_3)W_1 - 2X_2W_2 = 0$$

where the expressions for X_1, X_2, X_3, W_1 and W_2 can be found in the appendix M.

Fig. 4.4 shows the difference in the natural freqencies corresponding to the forward and reverse whirl of the shaft, the difference is distinguishable at shorter tail shaft lengths where the rotor mass has an overriding effect over that of tail shaft.

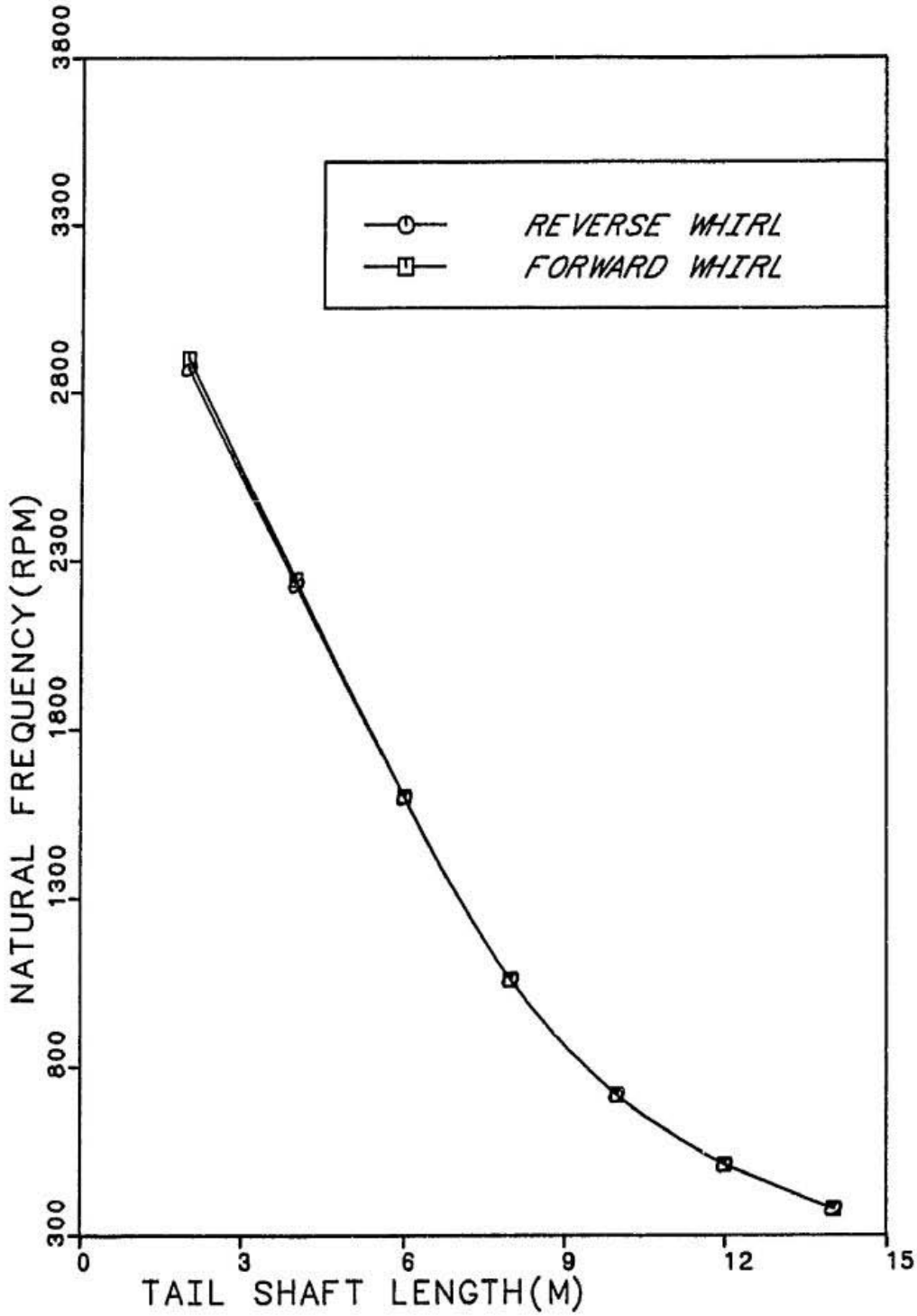

Figure 4.4: Natural frequency variation due to the varying tail shaft length.

Chapter 5

COUPLING OF BLADE AND ROTOR-SHAFT FREQUENCIES

5.1 Introduction

This chapter gives the formulation for finding the natural frequency of the propeller shaft system. The assembly was analysed in two independent parts, namely the blades and the rotor-shaft system. The resultant frequency, for the whole system was found by coupling the frequencies of these two parts. The method adopted is based on an extension of Southwell-Dunkerley methods for synthesizing isolated frequencies as given in Endo and Taniguchi, part I (1976).

5.2 Formulation of the Series Synthetic Method

Southwell-Dunkerley methods for the synthesis of the so-called inertia elements and the so-called restoring elements (shown in Fig. 5.1a and Fig. 5.1b respectively) give the following expressions for the frequencies.

$$\frac{1}{P^2} = \frac{1}{P_1^2} + \frac{1}{P_2^2} + \cdots \frac{1}{P_n^2} \qquad (5.1)$$

and

$$P^2 = P_1^2 + P_2^2 + \ldots P_n^2 \qquad (5.2)$$

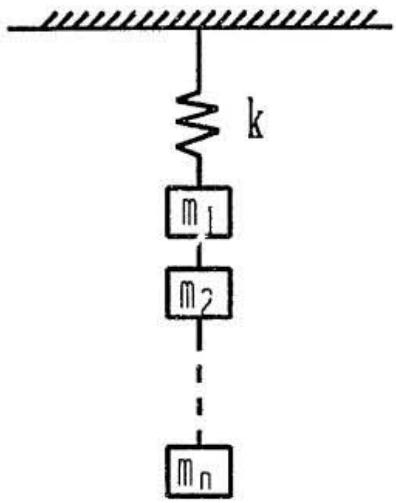

Fig. 5.1.a

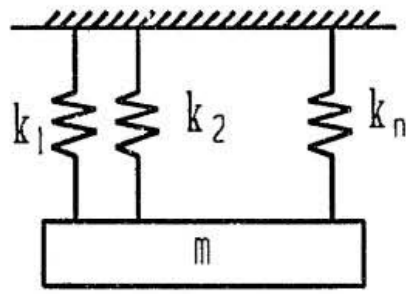

Fig. 5.1.b

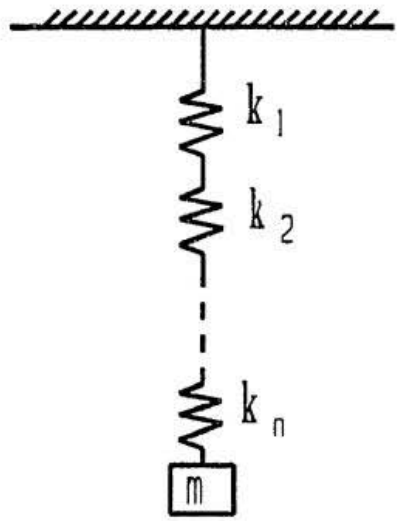

Fig. 5.1.c

Figure 5.1: Synthesis of inertia and restoring elements

where:

P_i = angular frequency of the respective isolated system composed of the mass and one of the restoring elements.

The series type synthetic method as presented in Endo and Taniguchi (1976) deals with another pattern of combining restoring elements (Fig. 5.1c). The method like Southwell-Dunkerley methods is based on Rayleigh's principle and gives the frequency of the system as

$$\frac{1}{P^2} = \frac{1}{P_1^2} + \frac{1}{P_2^2} + \cdots \frac{1}{P_n^2} \tag{5.3}$$

Although equation (5.3) is formally similar to equation (5.1), the structure of the present model is different from that used in the so-called inertia synthetic method. The advantages in this technique are that with the addition of each spring, the frequency of the system decreases and that different deflection functions must be assigned to respective restoring elements so that the deflection of the inertia element is to be a direct sum of those functions. The fact that with the addition of restoring element, the total frequency of the system decreases allows us to consider the effects of shear deflection in the beams by just adding one restoring element (having the deflection function proportional to the shear deflection) in series with that corresponding to the bending deformation of the beam.

5.3 Criterion for the Application of Series Type Solution

The expression given in the equation(5.3), like the other two Southwell-Dunkerley formulations, predicts a lower limit of the true frequency of the system. In order that this lower limit be expected to be very close to the true frequency of the composite system, another condition is demanded in addition to Rayleigh's principle on which the previous two methods are based. It is possible to obtain a better approximate frequency than the lower limit P_a by formally expanding the correct frequency in a power - series in terms of the perturbation parameters $\delta_{ij} < 1$.

As a mathematical model of the most general continuous system whose restoring elements are coupled mainly in series, one may consider a composite system which can be relaxed into n isolated systems. From Rayleigh's principle the true frequency P of this system is given as:

$$P^2 = \frac{\sum_{i=1}^{n} v_i}{\left[\sum_{i=1}^{n} t_i + \sum_{\substack{i=1 \\ i \neq j}}^{n} \sum_{j=1}^{n} t_{ij}\right]} \tag{5.4}$$

$$v_i = \int_0^L f_i(y_i)dx$$

$$t_i = m_i \int_0^L y_i^2 dx$$

$$t_{ij} = m_{ij} \int_0^L y_i y_j dx$$

m_{ij} = mass associated with the ith and jth restoring element.

y_i = deflection curve for the ith restoring element.

In the equation (5.4) v_i of the numerator denotes the potential energy term related to the respective restoring element, while the denominator is associated with the kinetic energy where in t_{ij} shows the coupling effect between two deflection functions (explained in appendix N)

From Rayleigh's principle the following inequalities hold.

$$\frac{v_i}{t_i} \geq \frac{V_i}{T_i} = P_i^2 \quad (i = 1 \sim n)$$

where V_i and T_i denote the potential and kinetic energies of the respective isolated

systems, which can be obtained by substituting the true deflection function Y_i of an isolated system into v_i and t_i, respectively, in place of y_i for the combined state. Hence P_i defines the true frequency of each isolated system.

From Schawarz's inequalities we have

$$\int_0^L y_i^2 dx \int_0^L y_j^2 dx \geq \left(\int_0^L y_i y_j dx \right)^2 \tag{5.5}$$

also we have

$$m_i m_j \geq m_{ij} \tag{5.6}$$

combining equations (5.5) and (5.6) we arrive at

$$t_i t_j \geq (t_{ij})^2$$

we define P_a given in equation (5.3) as :

$$\frac{1}{P_a^2} = \sum_{i=1}^{n} \frac{1}{P_i^2} \tag{5.7}$$

From equation (5.4) and (5.7) we have:

$$\frac{P^2}{P_a^2} = \frac{\sum_{i=1}^{n} v_i}{\sum_{i=1}^{n} t_i + \sum_{\substack{i=1 \\ i \neq j}}^{n} \sum_{j=1}^{n} t_{ij}} \sum_{i=1}^{n} \frac{T_i}{V_i}$$

$$\geq \frac{\sum_{i=1}^{n} v_i}{\sum_{i=1}^{n} t_i + \sum_{\substack{i=1 \\ i \neq j}}^{n} \sum_{j=1}^{n} \sqrt{t_i t_j}} \sum_{i=1}^{n} \frac{t_i}{v_i}$$

$$= 1 + \frac{\sum_{i=1}^{n}\sum_{j>i}^{n}\left[\sqrt{\frac{v_i}{v_j}}t_j - \sqrt{\frac{v_j}{v_i}}t_i\right]^2}{\left(\sum_{i=1}^{n}\sqrt{t_i}\right)^2} \geq 1 \qquad (5.8)$$

which yields:

$$P \geq P_a \qquad (5.9)$$

indicating conclusively that the value P_a gives a lower limit of the true frequency for the system.

Our aim now is to minimize the R.H.S. expression of equation (5.4) so that we can find an approximate value of the frequency which lies somewhere in between P and P_a which give upper and lower bound solutions respectively.

We define the following quantities

$$\lambda = \frac{1}{P^2}$$

$$\lambda_i = \frac{t_i}{v_i}$$

$$\lambda_s = \sum_{i=1}^{n}\lambda_i$$

$$x_i = \sqrt{t_i}$$

$$\delta_{ij} = \frac{2\lambda_i\lambda_j}{\lambda_s^2}\left(1 - \frac{t_{ij}}{\sqrt{t_i t_j}}\right) \quad (i,j = 1 \sim n, i \neq j)$$

using in the equation (5.4) we have:

$$\frac{1}{\lambda} = \frac{\sum_{i=1}^{n} \frac{x_i^2}{\lambda_i}}{\left[\left(\sum_{i=1}^{n} x_i\right)^2 - \sum_{\substack{i=1 \\ (i \neq j)}}^{n} \sum_{j=1}^{n} \frac{\lambda_s^2}{2\lambda_i \lambda_j} \delta_{ij} x_i x_j\right]} \tag{5.10}$$

we define the functional ϕ as

$$\phi = \frac{1}{\lambda}\left\{\left(\sum_{i=1}^{n} x_i\right)^2 - \sum_{\substack{i=1 \\ (i \neq j)}}^{n} \sum_{j=1}^{n} \frac{\lambda_s^2}{2\lambda_i \lambda_j} \delta_{ij} x_i x_j\right\} - \sum_{i=1}^{n} \frac{x_i^2}{\lambda_i} \tag{5.11}$$

To get the condition of stationarity we take the variation of the functional ϕ and set it to zero

$$\delta\phi = 0 \tag{5.12}$$

which after certain approximations yields (refer Endo and Taniguchi, 1976)

$$P^2 \cong P_a^2(1 + \delta_s) \tag{5.13}$$

under the condition that $\delta_s < 1$

where:

δ_s = perturbation parameter of the power series expansion of P_a

$$= \sum_{i=1}^{n} \sum_{j>i}^{n} \delta_{ij}$$

from equations (5.9) and (5.13) we can safely say that the true frequency P under consideration lies in the range

$$[P_a, P_a(1 + .5\delta_s)] \tag{5.14}$$

where:

P_a is called the zeroth order approximate solution for P and $P_a(1 + .5\delta_s)$ is called the first order approximate solution.

5.4 Modelling of the System

The sample propeller shaft considered in this work, consists of five blades. The propeller shaft assembly can be modelled as shown in Fig. 5.2a, wherein the system has been relaxed into single degree of freedom isolated sub-systems. The springs and masses used have the following meaning :

K_s = restoring element associated with transverse shear deformation of shaft

K_b = restoring element associated with bending deformation of shaft

k_s = restoring element associated with transverse shear deformation of blade

k_b = restoring element associated with bending deformation of blade

k_f = restoring element associated with axial force in the blade due to the rotation

M = inertia element of the shaft

m = inertia element of the blade

At the normal operating speeds of propeller shafts (upto 300 R.P.M.) the effects due to axial force and shear deformation are negligibly small, hence the model can be put in a simplified form as shown in Fig. 5.2b.

Looking at Fig. 5.2a and the three methods given in section 5.2 we can clearly see that the series type synthetic method of analysis is applicable to our system, since one mass unit is connected to a series of springs. Fig. 5.2b being a simplified case of Fig. 5.2a can also be solved by series type synthesis. In order to distinguish all the isolated systems in the model, we consider all the combinations of the restoring elements and inertia ones as given in Fig. 5.3.

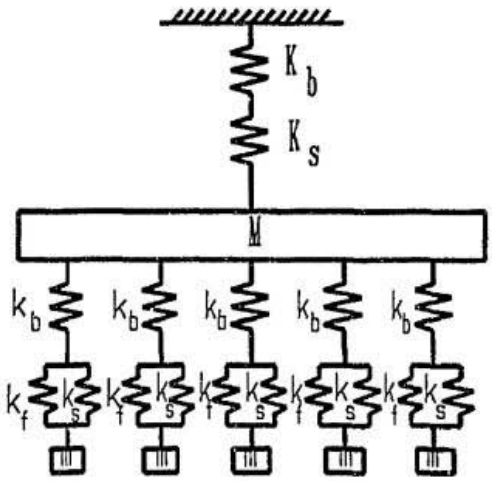

Fig. 5.2.a

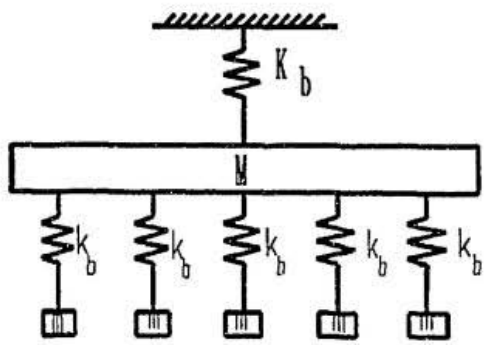

Fig. 5.2.b

Figure 5.2: Modelling of the propeller shaft assembly

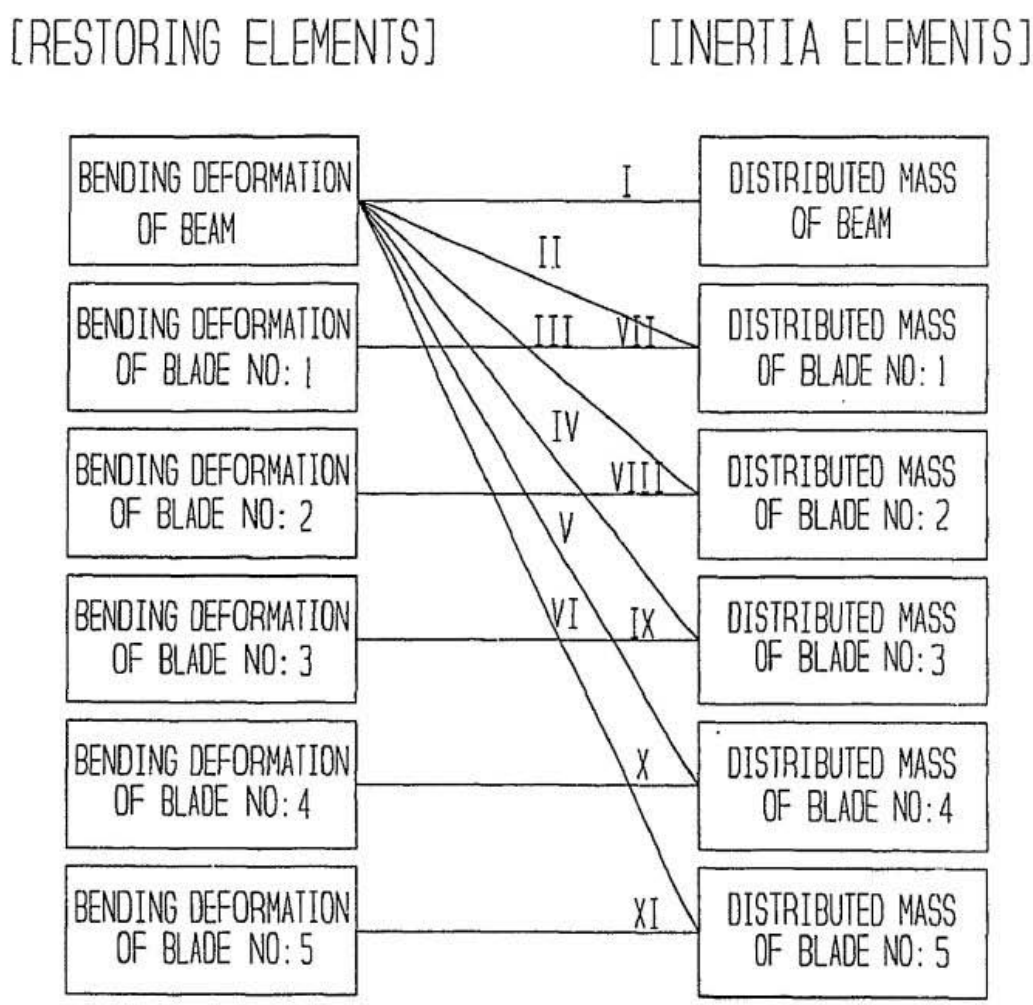

Figure 5.3: All combinations of inertia and restoring elements

The natural frequency of these eleven types of isolated systems, given by $P_i(i \sim 11)$, as given in Endo and Taniguchi, part II (1976), is given as :

1. For an isolated system subjected to bending effect of the beam and having the distributed mass of the beam. The frequency ω_I for this case has already been obtained in chapter 4.

2. For an isolated system subjected to bending effect of the beam and having the distributed mass of the blade. The frequecy ω_{II} for this case is given as :

$$\omega_{II}^2 = \frac{\int_0^1 \left(\frac{d^2y}{dz^2}\right)^2 dz}{M \int_0^1 \delta(z-1) y^2 dz} \tag{5.15}$$

where:

y = nondimensional displacement function of the rotor-shaft system, which can be well approximated by that of the tail shaft portion given as $Q_1 \sin \lambda z + Q_2 \cos \lambda z + Q_3 \sinh \lambda z + Q_4 \cosh \lambda z$ (derived in chapter 4).

$Q_i(i = 1, \cdots 4)$ = constants depending on the rotational speed of the shaft.

$\lambda^4 = \frac{M_s \omega_I^2}{EI_s}$

M_s = mass per unit length of the tailshaft.

I_s = area moment of inertia of the tailshaft.

E = modulus of elasticity.

L = length of the tailshaft.

M = total virtual mass of the blade.

The Dirac-Delta function indicates that the blade is a concentrated mass at the end of the tail shaft.

Equation (5.15) represents the frequencies $\omega_{II}, \omega_{III} \cdots \omega_{VI}$ since all the five blades are identically attached to the shaft.

3. For an isolated system subjected to the bending effect of the blade and having the distributed mass of the blade. The frequency ω_{VII} for this case has already been obtained in chapter 2. Frequencies ω_{VII} to ω_{XI} have the same magnitude as all the blades are identical.

Referring to expression (5.14) the zeroth order approximate solution for the frequency is given by P_a where :

$$\frac{1}{P_a^2} = \frac{1}{\omega^2} = \frac{1}{\omega_I^2} + \frac{1}{\omega_{II}^2} + \cdots \frac{1}{\omega_{XI}^2}$$

The first order approximation is given by $P_a(1 + .5\delta_s)$ where:

$$\delta_s = \sum_{i=1}^{n} \sum_{j>i}^{n} \delta_{ij}$$

For the case of our study only the perturbation parameters $\delta_{12}, \delta_{13} \cdots \delta_{16}$ exist, the rest all vanish as five identical blades have same deflection functions for their restoring elements.

5.5 Determination of the Critical Speed

The curve shown in fig. 5.4 gives the values of the resultant natural frequency of the propeller shaft assembly for various values of shaft rotational speeds. The critical speed of the system is the intersection of this curve with the line whose slope equals the number of blades of the propeller shaft. Equation (5.14) was used to give the limits of the natural frequency for the system considered in the present work, for different blade numbers. The true value of the natural frequency is supposed to lie between these limits, as can be seen from fig. 5.5

The formulation was verified by checking the results obtained for the case studied in Toms and Martin (1972), as can be seen in fig. 5.6.

Woytowich (1979), calculates the natural frequencies of a propeller shaft having a tail shaft of 228 inches and diameter 11 inches. The results obtained with the approximate method, presented in the reference, were checked against those computed using ABS coputer program.

The comparisons for the forward whirl and simply supported forward bearing end conditions are given in table 5.1, where in it is evident that our approach gives better results.

As mentioned before the dimensions of the propeller blades and the hub have not been given in the references and the following approximate relations were used to get their approximate values.

$$W = .26D^3(\mathrm{MWR})(\mathrm{BTF})$$

where:

W = weight of the blades

$$MWR = \frac{\text{developed area per blade}}{\text{D(propeller radius-hub radius)}}$$

D = propeller diameter in inches.

BTF = .004

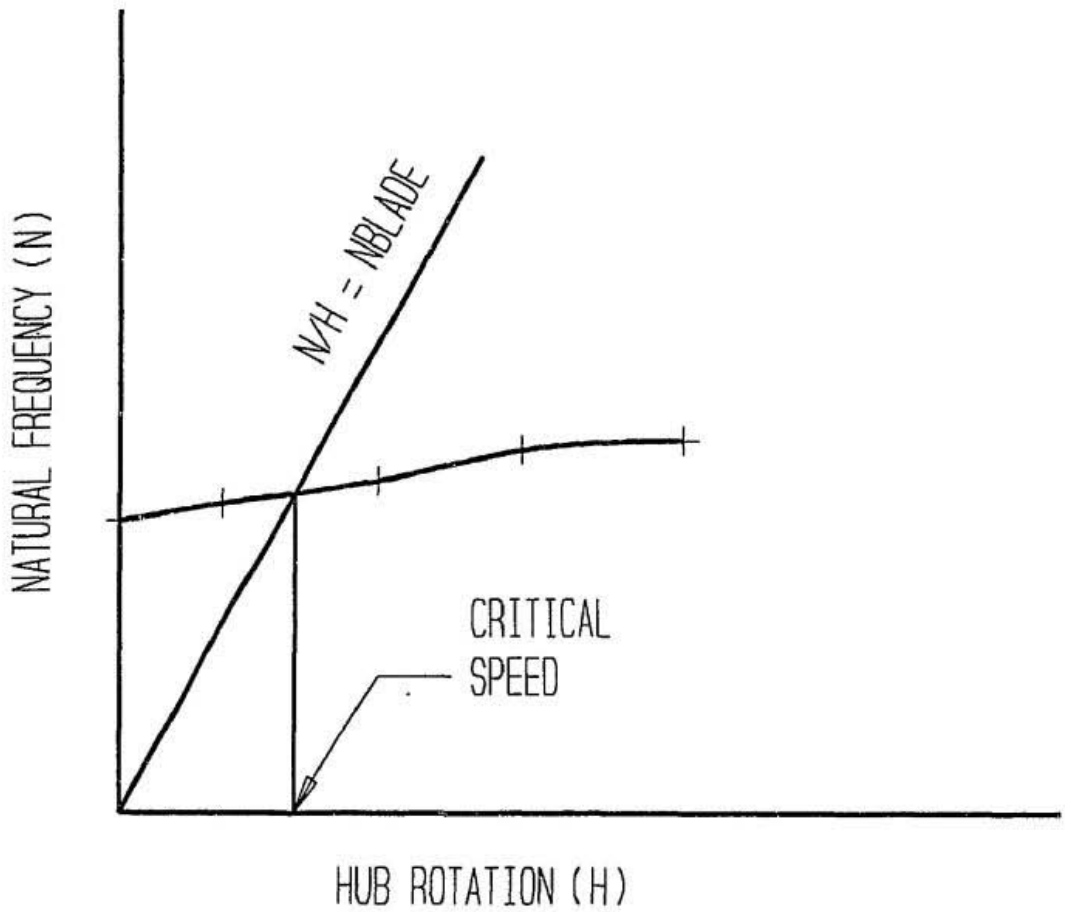

Figure 5.4: Determination of critical speed

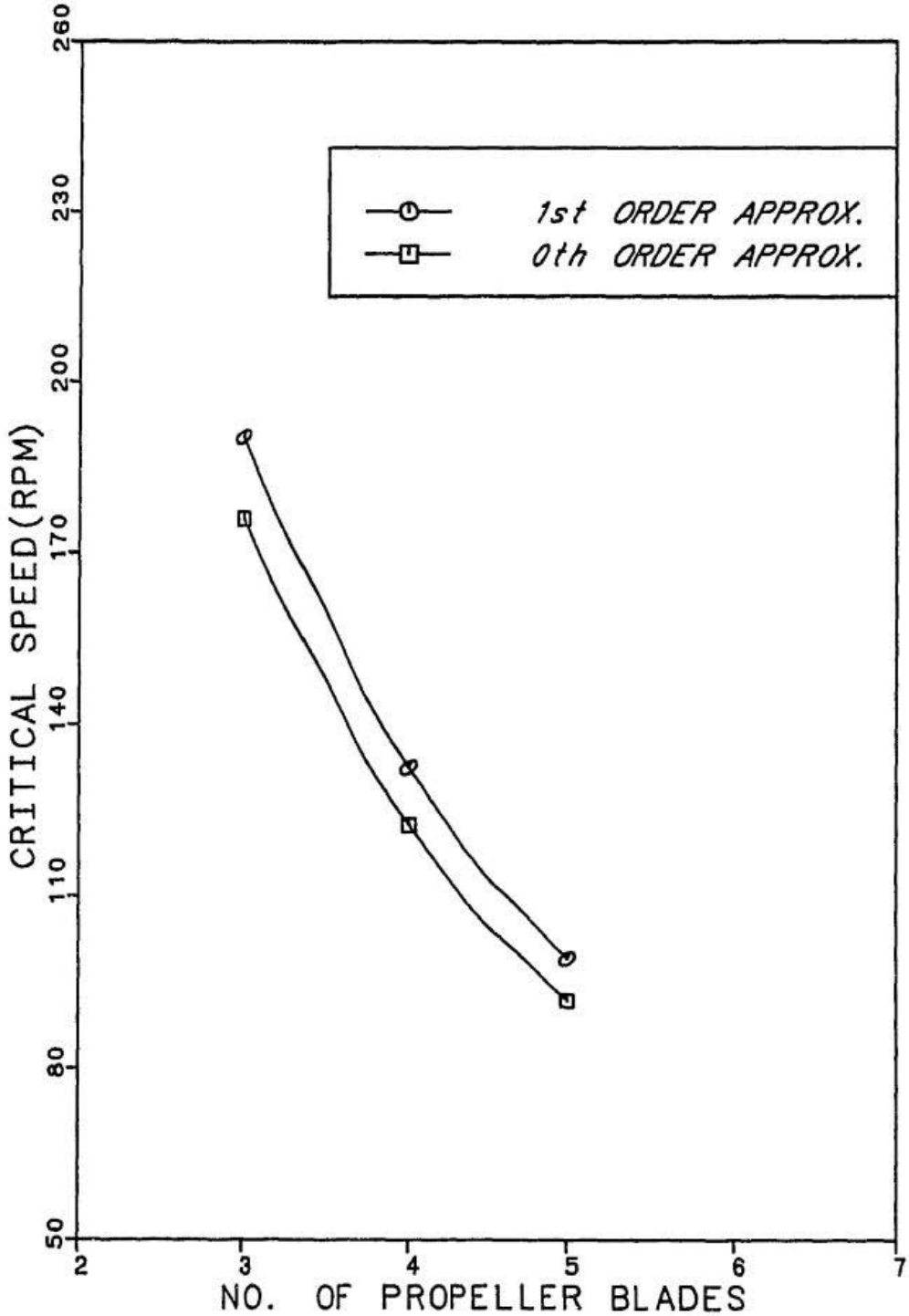

Figure 5.5: Effect of blade number on the natural frequency of the propeller shaft

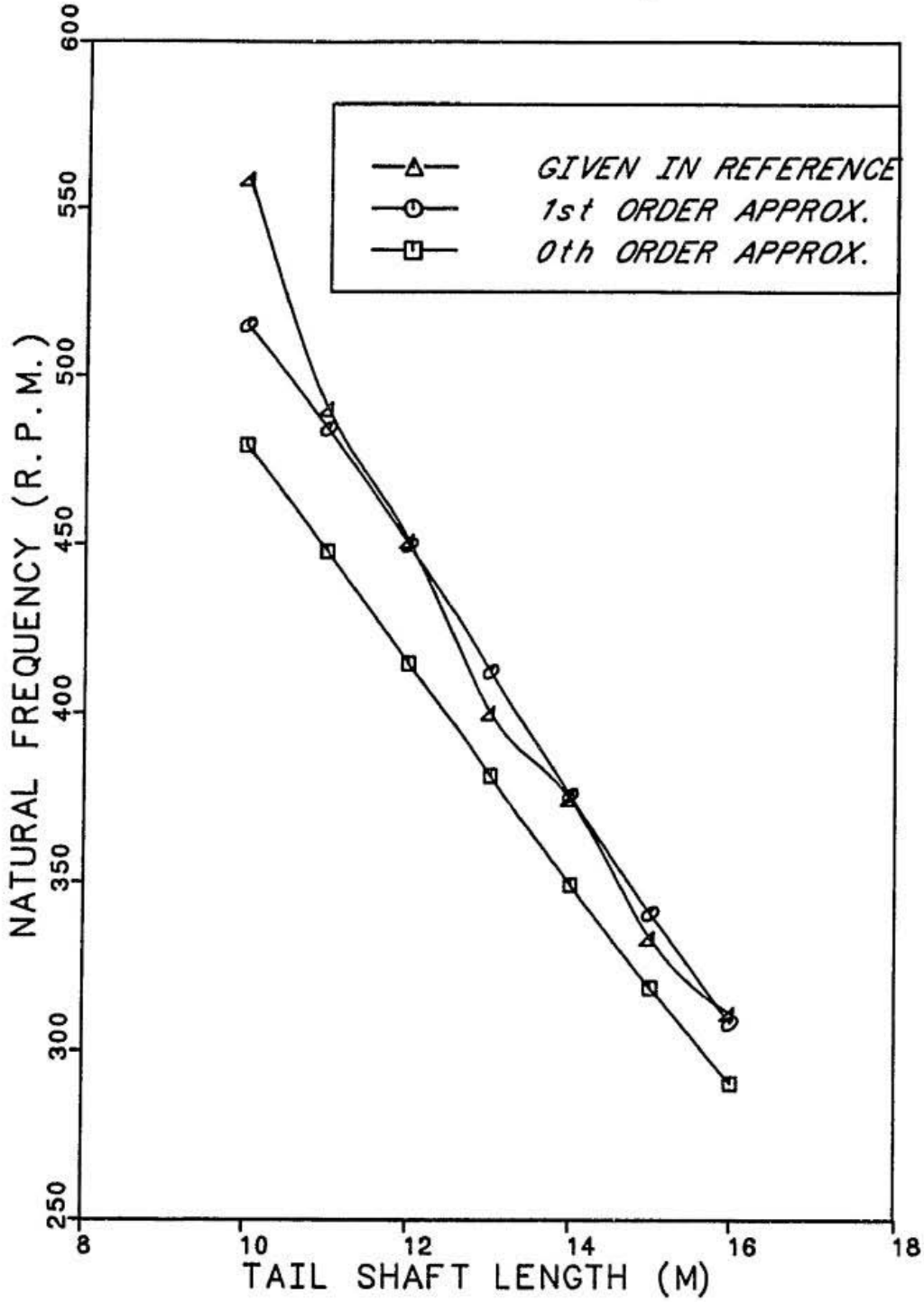

Figure 5.6: Comparisons of natural frequency with the case studied in Toms and Martin 1972.

Table 5.1: Comparisons of critical speeds (RPM) with the case studied in Woytowich, 1979.

Reference	*ABS program*	*Present work*	
		zeroth order approx.	first order approx.
157.6	170.2	174.2	188.4

Chapter 6

CONCLUSIONS

6.1 Summary of the Present Work

The purpose of this project was to find a method, which can prove to be a handy and effective tool for determining the natural frequencies of a propeller shaft system. There are methods which can do the same job and may be more accurate, but need a lot of initial data for giving a solution. Moreover, the solution proves costly because of the time consumed in lengthy numerical calculations. It can be stated safely that at the beginning of design we just need to have an idea of the shaft critical speeds and the approximate and inexpensive methods should prove fairly reliable. This fact depicts the importance of the class of approximate methods, to which the present work is an important contribution.

The work accomplished in this investigation takes into consideration some of the characteristics of the propeller shaft, the importance of which may be felt in certain conditions of propeller operation or intricate geometry. The modelling of the propeller as a thin rigid disc, as available in the existing literature, was improved upon by taking the propeller in its exact form, that is, a flexible hub mounted with blades. The work was carried out in different stages, first the propeller blades were analysed and later the shaft-rotor system. The isolated frequencies of the two systems of the propeller shaft assembly were then coupled using a technique given by Endo and Taniguchi (1976), for the application of which our system met the

requirements.

The method developed for getting the eigenvalues and eigenvectors for the propeller blade transverse vibrations takes into consideration the airfoil section of the blade, which was not to be found in the literature. The software developed was applied to several blade profiles for estimating their natural frequencies and the results were quite convincing. To obtain the equation of motion for the transverse vibrations the blade was assumed to be a cantilever, which proved to be quite valid after the analysis was cross checked against the results obtained from 3-D isoparametric finite element formulation.

In the case of the shaft-rotor assembly the frequencies were obtained by considering the transverse vibration of the three segments: Tail shaft, Overhang and the Rotor linked by the boundary conditions.

As is clear from the preceeding sections the method formulated minimizes the approximations to be made for the solution of natural frequencies of a propeller shaft system and was seen to give fairly accurate results.

6.2 Conclusions

Based on the investigation carried out, some important conclusions can be drawn.

1. For finding the fundamental frequency of transverse vibrations of a propeller blade, the approximation that it can be assumed to be a cantilever is fairly accurate.
2. For the range of speeds of interest in case of marine propellers, shaft rotation has a small effect on the natural frequencies.
3. Increase in the stagger angle decreases the natural frequency of the blade and so do the shear deflection and rotary inertia. The effects due to shear deflection are more pre-dominant at higher modes.

4. Obtaining the natural frequencies of a propeller shaft by coupling the frequencies of the blades and that of the shaft-rotor system seems to be a satisfactory method since it involves less approximations.
5. The natural frequency of a propeller shaft decreases with the increase in the tail shaft length. The difference between the forward and reverse whirling frequencies of a propeller shaft is distinguishable at shorter tail shaft lengths, since in such a situation the rotor mass has an appreciable effect.
6. Increase in the number of blades decreases the natural frequency of the propeller shaft assembly.
7. Natural frequency is appreciably affected by the varying fixity of the forward end bearing of the propeller shaft.

6.3 Limitations and Recommendations

The coupling of the natural frequencies for the two isolated systems still needs some improvement, since the method is based on approximations. The displacement function for the shaft-rotor system was taken to be the same as that obtained for the tail shaft, which gave very close results for the cases where the tail shaft was of relatively large dimensions. The cases where the tail shaft length is comparable with that of the rotor and the overhang could not be solved with accuracy. The coupling method used seems to be very sensitive to the displacement function assumed, because of its influence over the frequencies for the cross terms. In addition, the dimensions of the propeller for a given propeller shaft were obtained by approximations since the existing work assumes the propeller to be a disc and hence does not provide the actual dimensions for the complete propeller shaft assembly.

The propeller blade is of intricate geometry, factors like the blade rake angle, angle of twist and the torsional coupling arising in the cases where the center of mass does not pass through the neutral axis remain to be incorporated in the work.

References

Bahree, Rajeeve 1987. *Analysis and Design of Rotor Blades Due to the Transient Thermal and Vibratory Loads.* M.Eng. Thesis, Memorial University of Newfoundland, 1987.

Beek, G.H.M. 1976. *A Contribution to Tailshaft Dynamics.* Int. Shipbldg Prog. 23, (261), 131-137.

Brooks, J.E. and Taylor, D.W. 1980. *Vibrations of a marine propellcr operating in a nonuniform flow.* Naval Ship Research and Development Center, Report no. 801056.

Chivens, D.R. and Nelson, H.D. 1975. *The Natural Frequencies and Critical Speeds of a Rotating, Flexible Shaft-Disc System.* Journal of Engineering for Industry, vol.107, 881-886.

Conolly, J.E. 1960. *Strength of Propellers.*Trans. The Royal Institute of Naval Architects, vol.103, 139-160.

Cook, R.D. 1987. *Concepts and Applications of Finite Element Analysis.* John Wiley & Sons.

Dimarogonas, A.D. and Paipetis, S.A. 1983. *Analytic Methods in Rotor Dynamics.* Applied Science Publishers.

Endo, M. and Taniguchi, O. 1976. *An Extension of Southwell-Dunkreley Methods for Synthesizing Frequencies, Part I: Principles.* Journal of Sound and Vibration, 49(4), 501-516.

Endo, M. and Taniguchi, O., 1976. *An Extension of Southwell-Dunkreley Methods for Synthesizing Frequencies, Part II: Applications.* Journal of Sound and Vibration, 49(4), 517-533.

Fox, C.H.J. 1985. *The Free Vibration of Compact Rotating Radial Cantilevers.* Journal of Sound and Vibration, 98(3), 325-336.

Guyan, R.J. 1965. *Reduction of Stiffness and Mass matrices.* AIAA Journal, Vol. 3, No. 2., 380.

Haddara, M.R. 1988. *On The Transverse Vibration Of a Propellcr Tail Shaft System.* Ocean Engng. Vol. 15, No. 2, 119-126.

Jasper, N.H. 1956. *A Design Approach to the Problem of Critical Whirling Speeds of Shaft-Disk Systems.* I.S.P. Vol. 3, No. 17, 314-381.

Kuo, J.F. and Vorus, W. 1985. *Propeller Blade Dynamic Stresses.* The Society of Naval Architects and Marine Engineers, STAR Symposium, Norfolk, Va. 39-69.

Hartog, D. 1956. *Mechanical Vibrations,*McGraw-Hill Book Company.

Meirovitch, L. 1967. *Analytical Methods in Vibrations,* The Macmillan Company.

O'Brien, T.P. 1962. *The Design of Marine Screw Propellers.* Hutchinson Scientific & Technical, London.

Panagopulos, E. 1950. *Design Stage Calculation of Torsional, Axial and Lateral Vibrations of Marine Shafting.* Trans. Soc. Nav. Archit. Mar. Engrs 58, 329-384.

Rao, S.S. 1982. *The Finite Element Methods in Engineering.* Pergamon Press.

Rao, S.S. 1986. *Mechanical Vibrations.* Addison-Wesley Publishing Company.

Scarborough, J.B. 1966. *Numerical Mathematical Analysis.* Oxford & IBH Publishing Co.

Storti, D. and Aboelnaga, Y. 1987. *Bending Vibration of a Class of Rotating Beams with Hypergeometric Solutions.* Journal of Applied Mechanics, Vol. 54, 54/311.

Subrahmanyam, K.B., Kulkarni, S.V. and Rao, J.S. 1982. *Analysis of Lateral Vibrations of Rotating Cantilever Blades Allowing For Shear Deflection and Rotary Inertia by Reissner and Potential Energy Methods.* Mechanism and Machine Theory, Vol. 17, No.4, 235-241.

Thomson, W.T. 1988. *Theory of Vibration with Applications.* Prentice Hall.

Toms, A.E. and Martyn, D.K. 1972. *Whirling of Line Shafting.* Trans. Inst. Mar. Engrs. Vol. 84, 176-191.

Torby, B.J. 1984. *Advanced Dynamic for Engineers.*CBS College Publishing.

Warikoo, R. and Haddara, M.R. *On the Free Response of Propeller Blades.* To be Published in International Ship Building Progress.

Warikoo, R. and Haddara, M.R. 1989. *On the natural Frequency of Propeller Blades.*Proceedings of Canadian Applied Mechanics Congress(CANCAM 89), 432-433.

Woytowich, R. 1979. *Calculation of Propeller excited Whirling critical speeds.* J. Ship Res. 23(4), 235-241.

Yagoda, H.P. and Ketchman, J. 1982. *Design Charts for Self-Excited Whirling Critical Speeds.* Journal of Ship Research, Vol. 26, No. 3, 190-208.

APPENDICES

Appendix A

ARRANGEMENT OF COORDINATE AXES (FLOW CHART)

Details given on nextpage

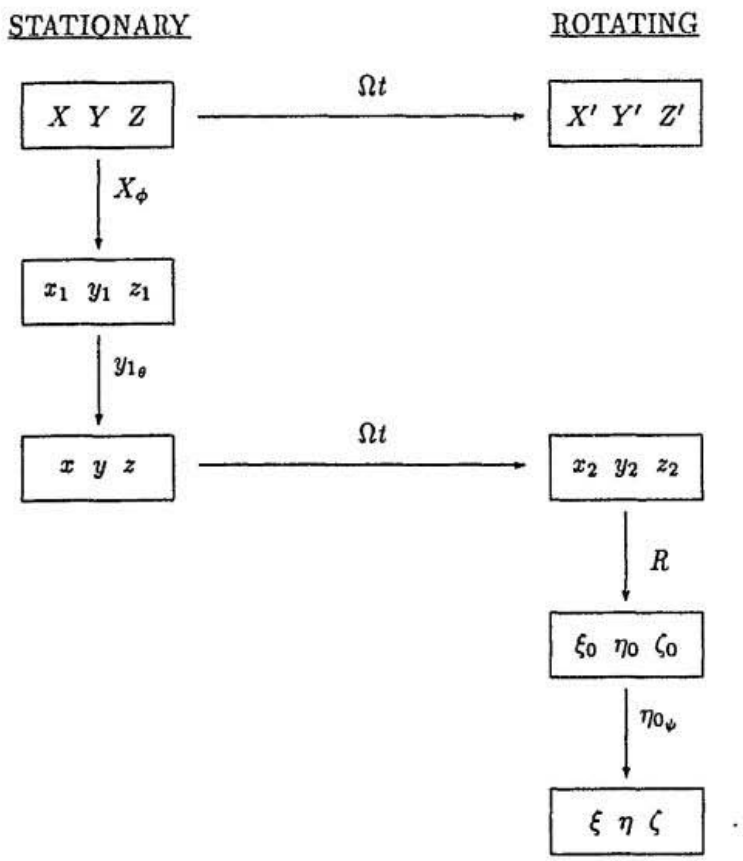

	Coordinate Systems	Description	Unit Vectors
1.	$X\ Y\ Z$	fixed to the undeflected shaft center line	$I\ J\ K$
2.	$x_1\ y_1\ z_1$	$X\ Y\ Z$ rotated about X by an angle ϕ	$i_1\ j_1\ k_1$
3.	$x\ y\ z$	$x_1\ y_1\ z_1$ rotated about y_1 by an angle θ	$i\ j\ k$
4.	$x_2\ y_2\ z_2$	rotating at Ω about z_2, coinciding z	$i_2\ j_2\ k_2$
5.	$\xi_0\ \eta_0\ \zeta_0$	$x_2\ y_2\ z_2$, translated by R along y_2	$e_1^0\ e_2^0\ e_3^0$
6.	$\xi\ \eta\ \zeta$	$\xi_0\ \eta_0\ \zeta_0$, rotated about η_0 by an angle ψ	$e_1\ e_2\ e_3$
7.	$X'\ Y'\ Z'$	rotating at Ω about Z', coinciding Z	$I'\ J'\ K'$

Appendix B

TRANSFORMATION OF COORDINATE AXES

Transformation between xyz and $x_1y_1z_1$:

$$\begin{Bmatrix} I \\ J \\ K \end{Bmatrix} = \begin{bmatrix} 1 & 0 & 1 \\ 0 & \cos\phi & -\sin\phi \\ 0 & \sin\phi & \cos\phi \end{bmatrix} \begin{Bmatrix} \hat{i}_1 \\ \hat{j}_1 \\ \hat{k}_1 \end{Bmatrix}$$

Transformation between $x_1y_1z_1$ and xyz :

$$\begin{Bmatrix} \hat{i}_1 \\ \hat{j}_1 \\ \hat{k}_1 \end{Bmatrix} = \begin{bmatrix} \cos\theta & 0 & \sin\theta \\ 0 & 1 & 0 \\ -\sin\theta & 0 & \cos\theta \end{bmatrix} \begin{Bmatrix} \hat{i} \\ \hat{j} \\ \hat{k} \end{Bmatrix}$$

$$\begin{Bmatrix} I \\ J \\ K \end{Bmatrix} = \begin{bmatrix} 1 & 0 & 0 \\ 0 & \cos\phi & -\sin\phi \\ 0 & \sin\phi & \cos\phi \end{bmatrix} \begin{bmatrix} \cos\theta & 0 & \sin\theta \\ 0 & 1 & 0 \\ -\sin\theta & 0 & \cos\theta \end{bmatrix} \begin{Bmatrix} \hat{i} \\ \hat{j} \\ \hat{k} \end{Bmatrix}$$

$$= \begin{bmatrix} \cos\theta & 0 & \sin\theta \\ 0 & \cos\phi & -\sin\phi\cos\theta \\ -\cos\phi\sin\theta & \sin\phi & \cos\phi\cos\theta \end{bmatrix} \begin{Bmatrix} \hat{i} \\ \hat{j} \\ \hat{k} \end{Bmatrix}$$

$$= \begin{bmatrix} 1 & 0 & 0 \\ 0 & 1 & -\phi \\ -\theta & \phi & 1 \end{bmatrix} \begin{Bmatrix} \hat{i} \\ \hat{j} \\ \hat{k} \end{Bmatrix}$$

TRANSFORMATION OF BLADE LOCAL COORDINATE AXES

$$\begin{Bmatrix} \hat{e}_1^0 \\ \hat{e}_2^0 \\ \hat{e}_3^0 \end{Bmatrix} = \begin{bmatrix} \cos\psi & 0 & \sin\psi \\ 0 & 1 & 0 \\ -\sin\psi & 0 & \cos\psi \end{bmatrix} \begin{Bmatrix} e_1 \\ e_2 \\ e_3 \end{Bmatrix}$$

$$\begin{aligned} \hat{\imath}_2 &= \hat{e}_1^0 = \hat{e}_1 \cos\psi + \hat{e}_3 \sin\psi \\ \hat{\jmath}_2 &= \hat{e}_2^0 \end{aligned}$$

$$\begin{aligned} \vec{r}_p &= u_s' \hat{\imath}_2 + (v_s' + R)\hat{\jmath}_2 + u_b \hat{e}_1 + \eta \hat{e}_2 + w_b \hat{e}_3 \\ &= u_s'(\hat{e}_1 \cos\psi + \hat{e}_3 \sin\psi) + (v_s' + R)\hat{e}_2 + u_b \hat{e}_1 + \eta \hat{e}_2 + w_b \hat{e}_3 \\ &= (u_s' \cos\psi + u_b)\hat{e}_1 + (v_s' + R + \eta)\hat{e}_2 + (u_s' \sin\psi + w_b)\hat{e}_3 \end{aligned}$$

$$\begin{aligned} \vec{\Omega}_3 &= \dot{\phi}\hat{\imath} + \dot{\theta}\hat{\jmath} + \Omega\hat{k} \\ &= \dot{\phi}(\hat{\imath}_2 \cos\Omega t - \hat{\jmath}_2 \sin\Omega t) + \dot{\theta}(\hat{\imath}_2 \sin\Omega t + \hat{\jmath}_2 \cos\Omega t) + \Omega\hat{k}_2 \\ &= \dot{\phi}[\cos\Omega t(\hat{e}_1 \cos\psi + \hat{e}_3 \sin\psi) - \hat{e}_2 \sin\Omega t] \\ &\quad + \dot{\theta}[\sin\Omega t(\hat{e}_1 \cos\psi + e_3 \sin\psi) + \hat{e}_2 \cos\Omega t] \\ &\quad + \Omega[-\hat{e}_1 \sin\psi + \hat{e}_3 \cos\psi] \\ &= e_1\left[\dot{\phi}\cos\Omega t \cos\psi + \dot{\theta}\sin\Omega t \cos\psi - \Omega\sin\psi\right] \\ &\quad + e_2\left[-\dot{\phi}\sin\Omega t + \dot{\theta}\cos\omega t\right] \\ &\quad + e_3\left[\dot{\phi}\cos\Omega t \sin\psi + \dot{\theta}\sin\Omega t \sin\psi + \Omega\cos\psi\right] \end{aligned}$$

Appendix C

VELOCITY OF A POINT ON THE BLADE

$$\begin{aligned}\vec{\dot{r}}_p &= (\dot{u}'_s \cos\psi + \dot{u}_b)\hat{e}_1 + \dot{v}'_s\hat{e}_2 + (\dot{u}'_s \sin\psi + \dot{w}_b)\hat{e}_3 \\ &\quad + \vec{\Omega}_3 \times \vec{r}_p \end{aligned} \tag{C.1}$$

$$\vec{\Omega}_3 \times \vec{r}_p = \begin{vmatrix} \hat{e}_1 & \hat{e}_2 & \hat{e}_3 \\ \Omega_{31} & \Omega_{32} & \Omega_{33} \\ r_1 & r_2 & r_3 \end{vmatrix}$$

where:

$\Omega_{31}, \Omega_{32}, \Omega_{33} = x, y, z$ components of $\vec{\Omega}_3$

$r_1, r_2, r_3 = x, y, z$ components of $\vec{r}_p$

$$\begin{aligned}\vec{\Omega}_3 \times \vec{r}_p &= \hat{e}_1(\Omega_{32}r_3 - \Omega_{33}r_2) - \hat{e}_2(\Omega_{31}r_3 - \Omega_{33}r_1) + \hat{e}_3(\Omega_{31}r_2 - \Omega_{32}r_1) \\ &= \hat{e}_1\Big[(-\dot{\phi}\sin\Omega t + \dot{\theta}\cos\Omega t)(u'_s\sin\psi + w_b) \\ &\quad -(\dot{\phi}\cos\Omega t\sin\psi + \dot{\theta}\sin\Omega t\sin\psi + \Omega\cos\psi)(v'_s + R + \eta)\Big] \\ &\quad -\hat{e}_2\Big[(\dot{\phi}\cos\Omega t\cos\psi + \dot{\theta}\sin\Omega t\cos\psi - \Omega\sin\psi)(u'_s\sin\psi + w_b) \\ &\quad -(\dot{\phi}\cos\Omega + \sin\psi + \dot{\theta}\sin\Omega t\sin\psi + \Omega\cos\psi)(u'_s\cos\psi + u_b)\Big] \\ &\quad +\hat{e}_3\Big[(\dot{\phi}\cos\Omega t\cos\psi + \dot{\theta}\sin\Omega t\cos\psi - \Omega\sin\psi)(v'_s + R + \eta) \\ &\quad -(-\dot{\phi}\sin\Omega t + \dot{\theta}\cos\Omega t)(u'_s\cos\psi + u_b)\Big]\end{aligned}$$

ignoring the magnitude of smaller terms, we have:

$$\begin{aligned}\vec{\Omega}_3 \times \vec{r}_p &= \hat{e}_1[-(R+\eta)(\dot{\phi}\cos\Omega t\sin\psi + \dot{\theta}\sin\Omega t\sin\psi + \Omega\cos\psi) - v_s'\Omega\cos\psi] \\ &\quad -\hat{e}_2[-\Omega\sin\psi(u_s'\sin\psi + w_b) - \Omega\cos\psi(u_s'\cos\psi + u_b)] \\ &\quad +\hat{e}_3[(R+\eta)(\dot{\phi}\cos\Omega t\cos\psi + \dot{\theta}\sin\Omega t\cos\psi - \Omega\sin\psi) - v_s'\Omega\sin\psi]\end{aligned}$$

using the above expression in equation C.1 we get :

$$\begin{aligned}\ddot{\vec{r}}_p &= \hat{e}_1[(\dot{u}_s'\cos\psi + \dot{u}_b) - (R+\eta)(\dot{\phi}\cos\Omega t + \dot{\theta}\sin\Omega t)\sin\psi - \Omega(v_s' + R + \eta)\cos\psi] \\ &\quad \hat{e}_2[\dot{v}_s' + \Omega(u_s'\sin\psi + w_b)\sin\psi + \Omega(u_s'\cos\psi + u_b)\cos\psi] \\ &\quad \hat{e}_3[(\dot{u}_s'\sin\psi + \dot{w}_b) + (R+\eta)(\dot{\phi}\cos\Omega t + \dot{\theta}\sin\Omega t)\cos\psi - \Omega(v_s' + R + \eta)\sin\psi]\end{aligned}$$

$$
\begin{aligned}
\vec{\Omega}_3 \times \vec{r}_p \;=\; & e_1 \Big[\{-\dot{\phi}\sin\Omega t + \dot{\theta}\cos\Omega t\}\{(\dot{u}'_s \sin\psi + \dot{w}_b) \\
& +(R+\eta)(\dot{\phi}\cos\Omega t + \dot{\theta}\sin\Omega t)\cos\psi \\
& -\Omega(v'_s + R + \eta)\sin\psi\} - \{\dot{\phi}\cos\Omega t\sin\psi + \dot{\theta}\sin\Omega t\sin\psi + \Omega\cos\psi\}+ \\
& \{\dot{v}'_s + \Omega(u'_s\sin\psi + w_b)\sin\psi + \Omega(u'_s\cos\psi + u_b)\cos\psi\}] \\
& -e_2\Big[\{\dot{\phi}\cos\Omega t\cos\psi + \dot{\theta}\sin\Omega t\cos\psi - \Omega\sin\psi\}\{(\dot{u}'_s\sin\psi + \dot{w}_b) \\
& +(R+\eta)(\dot{\phi}\cos\Omega t + \dot{\theta}\sin\Omega t)\cos\psi - \Omega(v'_s + R + \eta)\sin\psi\} \\
& -\{\dot{\phi}\cos\Omega t\sin\psi + \dot{\theta}\sin\Omega t\sin\psi + \Omega\cos\psi\}\{(\dot{u}'_s\cos\psi + \dot{u}_b) \\
& -(R+\eta)(\dot{\phi}\cos\Omega t + \dot{\theta}\sin\Omega t)\sin\psi - \Omega(v'_s + R + \eta)\cos\psi\}\Big] \\
& +\hat{e}_3\Big[\{\dot{\phi}\cos\Omega t\cos\psi + \dot{\theta}\sin\Omega t\cos\psi - \Omega\sin\psi\} \\
& \{\dot{v}'_s + \Omega(u'_s\sin\psi + w_b)\sin\psi \\
& +\Omega(u'_s\cos\psi + u_b)\cos\psi\} - \{-\dot{\phi}\sin\Omega t + \dot{\theta}\cos\Omega t\}\{(\dot{u}'_s\cos\psi + \dot{u}_b) \\
& -(R+\eta)(\dot{\phi}\sin\Omega t + \dot{\theta}\sin\Omega t)\sin\psi - \Omega(v'_s + R + \eta)\cos\psi\}\Big] \\
=\; & -\hat{e}_1\Big[(R+\eta)(\dot{\phi}\sin\Omega t - \dot{\theta}\cos\Omega t)\sin\psi \\
& -\{\dot{v}'_s + \Omega(u'_s + w_b\sin\psi + u_b\cos\psi)\}\cos\psi]\Omega \\
& -\hat{e}_2[-\Omega(v'_s + R + \eta) - \dot{u}'_s - \dot{w}_b\sin\psi - \dot{u}_b\cos\psi]\Omega \\
& +\hat{e}_3[-\Omega\{\dot{v}'_s + \Omega(u'_s + w_b\sin\psi + u_b\cos\psi)\}\sin\psi \\
& -\Omega(R+\eta)(\dot{\phi}\sin\Omega t - \dot{\theta}\cos\Omega t)\cos\psi\Big]
\end{aligned}
$$

now

$$
\begin{aligned}
\ddot{\vec{r}}_p &= [(\ddot{u}'_s\cos\psi + \ddot{u}_b) - (R+\eta)(\ddot{\phi}\cos\Omega t + \ddot{\theta}\sin\Omega t)\sin\psi \\
&\quad -(R+\eta)(-\dot{\phi}\sin\Omega t + \dot{\theta}\cos\Omega t)\Omega\sin\psi - \Omega\dot{v}'_s\cos\psi]\hat{e}_1 \\
&\quad +[\ddot{v}'_s + \Omega(\dot{u}'_s\sin\psi + \dot{w}_b)\sin\psi + \Omega(\dot{u}'_s\cos\psi + \dot{u}_b)\cos\psi]\hat{e}_2 \\
&\quad +[(\ddot{u}'_s\sin\psi + \ddot{w}_b) + (R+\eta)(\ddot{\phi}\cos\Omega t + \ddot{\theta}\sin\Omega t)\cos\psi \\
&\quad +(R+\eta)(-\dot{\phi}\sin\Omega t + \dot{\theta}\cos\Omega t)\Omega\cos\psi - \Omega\dot{v}'_s\sin\psi]\hat{e}_3 \\
&\quad +\vec{\Omega}_3 \times \ddot{\vec{r}}_p \\
&= \hat{e}_1[(\ddot{u}'_s\cos\psi + \ddot{u}_b) \\
&\quad +(R+\eta)\sin\psi(2\Omega\dot{\phi}\sin\Omega t - 2\Omega\dot{\theta}\cos\Omega t - \ddot{\phi}\cos\Omega t - \ddot{\theta}\sin\Omega t) \\
&\quad -\Omega\{2\dot{v}'_s + \Omega(u'_s + w_b\sin\psi + u_b\cos\psi)\}\cos\psi] \\
&\quad +\hat{e}_2[\ddot{v}'_s + (1+\Omega)\dot{u}'_s + 2\Omega(\dot{w}_b\sin\psi + \dot{u}_b\cos\psi) - \Omega(v'_s + R + \eta)] \\
&\quad +\hat{e}_3[(\ddot{u}'_s\sin\psi + \ddot{w}_b) \\
&\quad +(R+\eta)\cos\psi(-2\Omega\dot{\phi}\sin\Omega t + 2\Omega\dot{\theta}\cos\Omega t + \ddot{\phi}\cos\Omega t + \ddot{\theta}\sin\Omega t) \\
&\quad -\Omega\{2\dot{v}'_s + \Omega(u'_s + w_b\sin\psi + u_b\cos\psi)\}\sin\psi] \\
&= \hat{e}_1\left[\ddot{u}_b - \Omega^2(w_b\sin\psi\cos\psi + u_b\cos^2\psi) + (\ddot{u}'_s - 2\Omega\dot{v}'_s - \Omega^2u'_s)\cos\psi\right. \\
&\quad \left.-(R+\eta)(\ddot{\phi}\cos\Omega t + \ddot{\theta}\sin\Omega t)\sin\psi + 2\Omega(R+\eta)(\dot{\phi}\sin\Omega t - \dot{\theta}\cos\Omega t)\sin\psi\right] \\
&\quad \hat{e}_2[\ddot{v}'_s + \dot{u}'_s + \Omega(2\dot{w}_b\sin\psi + 2\dot{u}_b\cos\psi + \dot{u}'_s - v'_s - R - \eta)] \\
&\quad \hat{e}_3\left[\ddot{w}_b - \Omega^2(u_b\sin\psi\cos\psi + w_b\sin^2\psi) + (\ddot{u}'_s - 2\Omega\dot{v}'_s - \Omega^2u'_s)\sin\psi\right. \\
&\quad \left.+(R+\eta)(\ddot{\phi}\cos\Omega t + \ddot{\theta}\sin\Omega t)\cos\psi - 2\Omega(R+\eta)(\dot{\phi}\sin\Omega t - \dot{\theta}\cos\Omega t)\cos\psi\right]
\end{aligned}
$$

Appendix D

APPLICATION OF BOUNDARY CONDITIONS TO THE BLADE

$$\begin{aligned}
\epsilon_1 \int_0^1 [\dot{\bar{A}}\,(p_k - q_k')]' q_r dy &= \epsilon_1 [\{\dot{\bar{A}}\,(p_k - q_k') q_r\}_0^1 - \int_0^1 \dot{\bar{A}}\,(p_k - q_k') q_r' dy] \\
&= -\epsilon_1 \int_0^1 \dot{\bar{A}}\, q_r' (p_k - q_k') dy \\
\int q_r (k_N q_k')' dy &= [\{q_r (k_N q_k')\}_0^1 - \int_0^1 q_r' k_N q_k' dy] \\
&= -\int_0^1 k_N q_r' q_k' dy \\
\epsilon_2 \int (\dot{\bar{I}}\, p_k')' p_r dy &= \epsilon_2 [\{\dot{\bar{I}}\, p_k' p_r\}_0^1 - \int_0^1 \dot{\bar{I}}\, p_k' p_r' dy] \\
&= -\epsilon_2 \int_0^1 \dot{\bar{I}}\, p_k' p_r' dy
\end{aligned}$$

Appendix E

EXPLICIT EXPRESSION FOR $\sum_{k=1}^{n} p_k$

From equation (2.35), we have :

$$\sum_{k=1}^{n}[\dot{A}\,(p_k - q_k')]' = \frac{1}{\epsilon_1}\sum_{k=1}^{n}[k_N q_k']' + \frac{\sin^2\psi}{\epsilon_1}\sum_{k=1}^{n}\dot{A}\,q_k + \frac{\omega_k^2}{\epsilon_1}\sum_{k=1}^{n}\dot{A}\,q_k$$

Integrating :

$$\sum_{k=1}^{n}[\dot{A}\,(p_k - q_k')] = \frac{1}{\epsilon_1}\sum_{k=1}^{n}[k_N q_k'] + \frac{\sin^2\psi}{\epsilon_1}\sum_{k=1}^{n}\int_0^1 \dot{A}\,q_k dy + \frac{\omega_k^2}{\epsilon_1}\sum_{k=1}^{n}\int_0^1 \dot{A}\,q_k dy$$

$$\begin{aligned}\sum_{k=1}^{n} p_k &= \frac{1}{\dot{A}\,\epsilon_1}\sum_{k=1}^{n}[k_N q_k'] + \frac{\sin^2\psi}{\dot{A}\,\epsilon_1}\sum_{k=1}^{n}\int_0^1 \dot{A}\,q_k dy + \frac{\omega_k^2}{\epsilon_1\,\dot{A}}\sum\int_0^1 \dot{A}\,q_k dy + \sum_{k=1}^{n} q_k' \\ &= \frac{\lambda}{\epsilon_1\,\dot{A}}\sum_{k=1}^{n}\int_0^1 \dot{A}\,q_k dy + \frac{\sin^2\psi}{\dot{A}\,\epsilon_1}\sum_{k=1}^{n}\int_0^1 \dot{A}\,q_k dy + \sum_{k=1}^{n} q_k' + \frac{1}{\dot{A}\,\epsilon_1}\sum_{k=1}^{n}[k_N q_k']\end{aligned}$$

EXPLICIT EXPRESSION FOR $\sum_{k=1}^{n} p_k'$

$$(\dot{A}\,p_k)' = \dot{A}'p_k + \dot{A}\,p_k'$$

$$p_k' = \frac{(\dot{A}\,p_k)' - \dot{A}'p_k}{\dot{A}} = \frac{(\dot{A}\,p_k)'}{\dot{A}} - \frac{\dot{A}'p_k}{\dot{A}} = \frac{1}{\dot{A}}[(\dot{A}\,p_k)' - \dot{A}'p_k]$$

$$\sum_{k=1}^{n} p'_k = \frac{1}{\overset{*}{A}} \sum_{k=1}^{n} [(\overset{*}{A}\, p_k)' - \overset{*}{A}'\, p_k] \tag{E.1}$$

from equation (2.35), we have :

$$\sum_{k=1}^{n} [-\lambda\, \overset{*}{A}\, q_k - \overset{*}{A}\, q_k \sin^2 \psi] = -\epsilon_1 \sum_{k=1}^{n} [\overset{*}{A}\, (p_k - q'_k)]' + \sum_{k=1}^{n} [k_N q'_k]'$$

or

$$\epsilon_1 \sum_{k=1}^{n} (\overset{*}{A}\, p_k)' = \lambda\, \overset{*}{A} \sum_{k=1}^{n} q_k + \overset{*}{A} \sin^2 \psi \sum_{k=1}^{n} q_k + \epsilon_1 \sum_{k=1}^{n} (\overset{*}{A}\, q'_k)' + \sum_{k=1}^{n} [k_N q'_k]'$$

using the expression in (E.1), we have :

$$\begin{aligned} \sum_{k=1}^{n} p'_k &= \frac{1}{\overset{*}{A}} \left[\frac{\lambda\, \overset{*}{A}}{\epsilon_1} \sum_{k=1}^{n} q_k + \frac{\overset{*}{A} \sin^2 \psi}{\epsilon_1} \sum_{k=1}^{n} q_k + \sum_{k=1}^{n} (\overset{*}{A}\, q'_k)' \right. \\ &\qquad \left. \frac{1}{\epsilon_1} \sum_{k=1}^{n} (k_N q''_k + k'_K q'_k) - \overset{*}{A}' \sum_{k=1}^{n} p_k \right] \\ &= \frac{\lambda}{\epsilon_1} \sum_{k=1}^{n} q_k + \left[\frac{\sin^2 \psi}{\epsilon_1} \sum_{k=1}^{n} q_k + \sum_{k=1}^{n} \frac{(\overset{*}{A}\, q'_k)'}{\overset{*}{A}} + \right. \\ &\qquad \left. \frac{1}{\overset{*}{A}\, \epsilon_1} \sum_{k=1}^{n} (k_N q''_k + k'_N q'_k) - \frac{\overset{*}{A}'}{\overset{*}{A}} \sum_{k=1}^{n} p_k \right] \end{aligned}$$

using equation (2.48), we have :

$$\begin{aligned} \sum_{k=1}^{n} p'_k &= \frac{\lambda}{\epsilon_1} \sum_{k=1}^{n} q_k + \left[\frac{\sin^2 \psi}{\epsilon_1} \sum_{k=1}^{n} q_k + \sum_{k=1}^{n} \frac{(\overset{*}{A}\, q'_k)'}{\overset{*}{A}} + \right. \\ &\qquad \left. \frac{1}{\overset{*}{A}\, \epsilon_1} \sum_{k=1}^{n} (k_N q''_k + k'_N q'_k) \right] - \frac{\overset{*}{A}'}{\overset{*}{A}} \sum_{k=1}^{n} (\lambda P_{KA} + P_{KB}) \\ &= \lambda \left[\frac{\sum_{k=1}^{n} q_k}{\epsilon_1} - \frac{\overset{*}{A}'}{\overset{*}{A}} \sum_{k=1}^{n} P_{KA} \right] + \left[\frac{\sin^2 \psi}{\epsilon_1} \sum_{k=1}^{n} q_k + \sum_{k=1}^{n} \frac{(\overset{*}{A}\, q'_k)'}{\overset{*}{A}} \right. \\ &\qquad \left. + \frac{1}{\overset{*}{A}\, \epsilon_1} \sum_{k=1}^{n} (k_N q''_k + k'_N q'_k) - \frac{\overset{*}{A}'}{\overset{*}{A}} \sum_{k=1}^{n} P_{KB} \right] \\ &= \lambda \sum_{k=1}^{n} P_{K1A} + \sum_{k=1}^{n} P_{K1B} \end{aligned}$$

Appendix F

SIMPLIFIED EIGENVALUE EQUATION

Equation (2.52) can be written as :

$$M_1 + M_2 + M_3 = S_1 + S_2 + S_3$$

Expansion of M_2 :

$$\lambda \sum_{r=1}^{n}\sum_{k=1}^{n} \int_0^1 \dot{I}\, p_r p_k dy = \lambda \sum_{r=1}^{n}\sum_{k=1}^{n} \int_0^1 \dot{I}\, (\lambda P_{RA} + P_{RB})(\lambda P_{KA} + P_{KB})$$

$$= \lambda \sum_{r=1}^{n}\sum_{k=1}^{n} \int_0^1 \dot{I}\, [\lambda(P_{KA}P_{RB} + P_{KB}P_{RA}) + P_{KB}P_{RB} + \lambda^2 P_{KA}P_{RA}]$$

$$= \lambda \sum_{r=1}^{n}\sum_{k=1}^{n} \int_0^1 \dot{I}\, P_{KB}P_{RB}$$

[Ignoring λ^2 and λ^3 terms, because of their small magnitude]

Expansion of S_1 :

$$\epsilon_2 \sum_{r=1}^{n}\sum_{k=1}^{n} \int_0^1 \dot{I}\, p'_r p'_k dy = \epsilon_2 \sum_{r=1}^{n}\sum_{k=1}^{n} \int_0^1 \dot{I}\, (\lambda P_{R1A} + P_{R1B})(\lambda P_{K1A} + P_{K1B})$$

$$= \epsilon_2 \sum_{r=1}^{n}\sum_{k=1}^{n} \int_0^1 \dot{I}\, [\lambda(P_{R1A}P_{K1B} + P_{R1B}P_{K1A}) + P_{R1B}P_{K1B}]$$

[neglecting λ^2 term]

Expansion of S_3 :

$$\epsilon_1 \sum_{r=1}^{n}\sum_{k=1}^{n}\int_0^1 \dot{A}\,[p_r p_k - (p_r q'_k + q'_r p_k) + q'_r q'_k]dy$$

$$= \epsilon_1 \sum_{r=1}^{n}\sum_{k=1}^{n}\int_0^1 \dot{A}\,[(\lambda P_{RA} + P_{RB})(\lambda P_{KA} + P_{KB})$$

$$-\{(\lambda P_{RA} + P_{RB})q'_k + q'_r(\lambda P_{KA} + P_{KB})\} + q'_r q'_k]$$

$$= \epsilon_1 \sum_{r=1}^{n}\sum_{k=1}^{n}\int_0^1 \dot{A}\,[\lambda(P_{KA}P_{RB} + P_{KB}P_{RA}) + P_{KB}P_{RB}$$

$$-\lambda(P_{RA}q'_k + q'_r P_{KA} - (P_{RB}q'_k + q'_r P_{KB}) + q'_r q'_k]$$

[ignoring λ^2 term]

Substituting in equation (2.52), we get :

$$\lambda\left[\int_0^1 \dot{A}\sum_{r=1}^{n}\sum_{k=1}^{n} q_r q_k dy + \int_0^1 \dot{I}\sum_{r=1}^{n}\sum_{k=1}^{n} P_{RB}P_{KB}dy\right.$$

$$\left. + \sin^2\psi \int_0^1 \dot{A}\sum_{r=1}^{n}\sum_{k=1}^{n} q_r q_k dy\right.$$

$$= \epsilon_2 \int_0^1 \dot{I}\sum_{r=1}^{n}\sum_{k=1}^{n}[\lambda(P_{R1A}P_{K1B} + P_{R1B}P_{K1A}) + P_{R1B}P_{K1B}]$$

$$+ \int_0^1 k_N \sum_{r=1}^{n}\sum_{k=1}^{n} q'_r q'_k dy$$

$$+\epsilon_1 \int_0^1 \dot{A}\left[\lambda\sum_{r=1}^{n}\sum_{k=1}^{n}(P_{RB}P_{KA} + P_{RA}P_{KB}) + \sum_{r=1}^{n}\sum_{k=1}^{n} P_{RB}P_{KB}\right.$$

$$-\lambda\sum_{r=1}^{n}\sum_{k=1}^{n}(P_{RA}q'_k + q'_r P_{KA}) - \sum_{r=1}^{n}\sum_{k=1}^{n}(P_{RB}q'_k + q'_r P_{KB})$$

$$\left. + \sum_{r=1}^{n}\sum_{k=1}^{n} q'_r q'_k\right]$$

Rearranging the terms, we have :

$$\lambda \left[\int_0^1 \dot{A} \sum_{r=1}^{n} \sum_{k=1}^{n} q_r q_k dy + \int_0^1 \dot{I} \sum_{r=1}^{n} \sum_{k=1}^{n} P_{RB} P_{KB} dy \right.$$

$$-\epsilon_2 \int_0^1 \dot{\gamma} \sum_{r=1}^{n} \sum_{k=1}^{n} (P_{R1A} P_{K1B} + P_{R1B} P_{K1A}) dy$$

$$-\epsilon_1 \int_0^1 \dot{A} \sum_{r=1}^{n} \sum_{k=1}^{n} (P_{RB} P_{KA} + P_{RA} P_{KB}) dy +$$

$$\left. \epsilon_1 \int_0^1 \dot{A} \left(\sum_{r=1}^{n} \sum_{k=1}^{n} P_{RA} q'_k + \sum_{r=1}^{n} \sum_{k=1}^{n} q'_r P_{KA} \right) dy \right]$$

$$= -\sin^2 \psi \int_0^1 \dot{A} \sum_{r=1}^{n} \sum_{k=1}^{n} q_r q_k dy + \epsilon_2 \int_0^1 \dot{I} \sum_{r=1}^{n} \sum_{k=1}^{n} P_{R1B} P_{K1B} dy +$$

$$+ \int_0^1 k_N \sum_{r=1}^{n} \sum_{k=1}^{n} q'_r q'_k dy$$

$$+\epsilon_1 \int_0^1 \dot{A} \sum_{r=1}^{n} \sum_{k=1}^{n} (P_{RB} P_{KB} - P_{RB} q'_k - q'_r P_{KB} + q'_r q'_k) dy$$

Appendix G

EXPRESSION FOR $\int_0^1 Aq_k dy$

$$\int_0^1 Aq_k dy = \int_0^1 (A_1 + A_2 y + A_3 y^2 + A_4 y^3)$$
$$(\cosh b_j y - \cos b_j y + \sigma_j \sin b_j y - \sigma_j \sinh b_j y)$$

$$= \int_0^1 A_1(\cosh b_j y - \cos b_j y + \sigma_j \sin b_j y - \sigma_j \sinh b_j y)$$
$$+ \int_0^1 A_2 y(\cosh b_j y - \cos b_j y + \sigma_j \sin b_j y - \sigma_j \sinh b_j y)$$
$$+ \int_0^1 A_3 y^2(\cosh b_j y - \cos b_j y + \sigma_j \sin b_j y - \sigma_j \sinh b_j y)$$
$$+ \int_0^1 A_4 y^3(\cosh b_j y - \cos b_j y + \sigma_j \sin b_j y - \sigma_j \sinh b_j y)$$

$$= \frac{A_1}{b_j}(\sinh b_j y - \sin b_j y - \sigma_j \cos b_j y - \sigma_j \sinh b_j y$$
$$+A_2\left[\left(\frac{y \sinh b_j y}{b_j} - \frac{\cosh b_j y}{b_j^2}\right) - \left(\frac{\cos b_j y}{b_j^2} + \frac{y \sin b_j y}{b_j}\right)\right.$$
$$\left.+\sigma_j\left(\frac{\sin b_j y}{b_j^2} - \frac{y \cos b_j y}{b_j}\right) - \sigma_j\left(\frac{y \cosh b_j y}{b_j} - \frac{\sinh b_j y}{b_j^2}\right)\right]$$

$$+A_3\left[\left\{\frac{-2y \cosh b_j y}{b_j^2} + \left(\frac{y^2}{b} + \frac{2}{b^3}\right)\sinh b_j y\right\}\right.$$
$$-\left\{\tfrac{2y}{b_j^2}\cos b_j y + \left(\tfrac{y^2}{b_j} - \tfrac{2}{b_j^3}\right)\sin b_j y\right\}$$
$$+\sigma_j\left\{\frac{2y}{b_j^2}\sin b_j y + \left(\frac{2}{b_j^3} - \frac{y^2}{b_j}\right)\cos b_j y\right\}$$
$$\left.-\sigma_j\left\{\left(\tfrac{y^2}{b_j} + \tfrac{2}{b_j^3}\right)\cosh b_j y - \tfrac{2y}{b_j^2}\sinh b_j y\right\}\right]$$
$$+A_4\left[\frac{y^3 \sinh b_j y}{b_j} - \int_0^1 \frac{3y^2 \sinh b_j y}{b_j} - \left(\frac{y^3 \sin b_j y}{b_j} - \int_0^1 \frac{3y^2 \sin b_j y}{b_j}\right)\right.$$
$$+\sigma_j\left(\frac{-y^3 \cos b_j y}{b_j} + \int_0^1 \frac{3y^2}{b_j}\cos b_j y\right)$$
$$\left.-\sigma_j\left(\frac{y^3 \cosh b_j y}{b_j} - \int_0^1 \frac{3y^2}{b_j}\cosh b_j y\right)\right]$$

$$
\begin{aligned}
= \quad & \frac{A_1}{b_j}(\sinh b_j y - \sin b_j y - \sigma_j \cos b_j y - \sigma_j \sinh b_j y) \\
& + A_2 \left[\left(\frac{y \sinh b_j y}{b_j} - \frac{\cosh b_j y}{b_j^2} \right) - \left(\frac{\cos b_j y}{b_j^2} + \frac{y \sin b_j y}{b_j} \right) \right. \\
& \left. + \sigma_j \left(\frac{\sin b_j y}{b_j^2} - \frac{y \cos b_j y}{b_j} \right) - \sigma_j \left(\frac{y \cosh b_j y}{b_j} - \frac{\sinh b_j y}{b_j^2} \right) \right] \\
& + A_3 \left[\left\{ \frac{-2y \cosh b_j y}{b_j^2} + \left(\frac{y^2}{b_j} + \frac{2}{b_j^3} \right) \sinh b_j y \right\} \right. \\
& - \left\{ \frac{2y}{b_j^2} \cos b_j y + \left(\frac{y^2}{b_j} - \frac{2}{b_j^3} \right) \sin b_j y \right\} \\
& + \sigma_j \left\{ \frac{2y}{b_j^2} \sin b_j y + \left(\frac{2}{b_j^3} - \frac{y^2}{b_j} \right) \cos b_j y \right\} \\
& \left. - \sigma_j \left\{ \left(\frac{y^2}{b_j} + \frac{2}{b_j^3} \right) \cosh b_j y - \frac{2y}{b_j^2} \sinh b_j y \right\} \right] \\
& + A_4 \left[\frac{y^3 \sinh b_j y}{b_j} - \frac{3}{b_j} \left\{ \left(\frac{y^2}{b_j} + \frac{2}{b_j^3} \right) \cosh b_j y - \frac{2y}{b_j^2} \sinh by \right\} \right. \\
& - \frac{y^3 \sin b_j y}{b_j} + \frac{3}{b_j} \left\{ \frac{2y}{b_j^2} \sin b_j y + \left(\frac{2}{b_j^3} - \frac{y^2}{b_j} \right) \cos b_j y \right\} \\
& - \frac{\sigma_j}{b_j} y^3 \cos b_j y + \frac{3\sigma_j}{b_j} \left\{ \frac{2y}{b_j^2} \cos b_j y + \left(\frac{y^2}{b_j} - \frac{2}{b_j^3} \right) \sin b_j y \right\} \\
& \left. - \frac{\sigma_j}{b_j} x^3 \cosh b_j y + \frac{3\sigma_j}{b_j} \left\{ \frac{-2y \cosh b_j y}{b_j^2} + \left(\frac{y^2}{b_j} + \frac{2}{b_j^3} \right) \sinh b_j y \right\} \right]
\end{aligned}
$$

$$\int_0^1 Aq_k dy = \frac{A_1}{b_j}(\sinh b_j y - \sin b_j y - \sigma_j \cos b_j y - \sigma_j \cosh b_j y$$
$$+A_2\left[\left(\frac{y\sinh b_j y}{b_j} - \frac{\cosh b_j y}{b_j^2}\right) - \left(\frac{\cos b_j y}{b_j^2} + \frac{y\sin b_j y}{b_j}\right)\right.$$
$$\left.+\sigma_j\left(\frac{\sin b_j y}{b_j^2} - \frac{y\cos b_j y}{b_j}\right) - \sigma_j\left(\frac{y\cosh b_j y}{b_j} - \frac{\sinh b_j y}{b_j^2}\right)\right]$$
$$+\left[A_3 + \frac{3\sigma_j A_4}{b_j}\right]\left[\frac{-2y\cosh b_j y}{b_j^2} + \left(\frac{y^2}{b_j} + \frac{2}{b_j^3}\right)\sinh b_j y\right] +$$
$$+\frac{A_4 y^3}{b_j}\sinh b_j y$$
$$+\left[-A_3 + \frac{3\sigma_j A_4}{b_j}\right]\left[\frac{2y}{b_j^2}\cos b_j y + \left(\frac{y^2}{b_j} - \frac{2}{b_j^3}\right)\sin b_j y\right] + A_4 y^3\frac{\sin b_j y}{b_j}$$
$$+\left[A_3\sigma_j + \frac{3A_4}{b_j}\right]\left[\frac{2y}{b_j^2}\sin b_j y + \left(\frac{2}{b_j^3} - \frac{y^2}{b_j}\right)\cos b_j y\right] - \frac{A_4\sigma_j}{b}y^3\cos b_j y$$
$$+\left[-A_3\sigma_j - \frac{3A_4}{b_j}\right]\left[\left(\frac{y^2}{b_j} + \frac{2}{b_j^3}\right)\cosh b_j y - \frac{2y}{b_j^2}\sinh b_j y\right]$$
$$-\frac{A_4\sigma_j}{b_j}y^3\cosh b_j y$$

$$\int_0^1 \dot{A}\, q_k dy = \frac{1}{l^2}\int_0^1 Aq_k dy$$

Appendix H

BOUNDARY CONDITIONS APPLIED TO THE THIRD TERM ON THE MASS SIDE

$$\epsilon_2 \int_0^1 \overset{*}{I} (P_{R1A}P_{K1B} + P_{R1B}P_{K1A})dy$$

$$P_{R1A}P_{K1B} = (\frac{q_r}{\epsilon_1} - \frac{A'}{A}P_{RA})(P_{K1B}) = \frac{q_r}{\epsilon_1}P_{K1B} - \frac{A'}{A}P_{RA}P_{K1B}$$

$$\frac{q_r}{\epsilon_1}P_{K1B} = \frac{q_r}{\epsilon_1}\left[\frac{\sin^2\psi}{\epsilon_1}q_k + \frac{Aq_k'' + A'q_k'}{A} + \frac{l^2}{A\epsilon_1}k_N q_k'' + \frac{l^2}{A\epsilon_1}k_N' q_k' - \frac{A'}{A}P_{KB}\right]$$

Boundary conditions will be applied to the terms appearing with q_k''

$$\epsilon_2 \int_0^1 \frac{\overset{*}{I}}{\epsilon_1} q_r q_k'' = \frac{\epsilon_2}{\epsilon_1}\left[\{\overset{*}{I}\, q_r q_k'\}_0^1 - \int_0^1 \overset{*}{I}\, q_r' q_k' dy\right]$$

$$= -\frac{\epsilon_2}{\epsilon_1}\int_0^1 \overset{*}{I}\, q_r' q_k' dy$$

[Since $\overset{*}{I}$ vanishes at $y = 1$ and q_r is zero at $y = 0$]

also

$$\epsilon_2 \int_0^1 \frac{\overset{*}{I}}{\epsilon_1}\frac{l^2 k_N}{A\epsilon_1} q_r q_k'' = \frac{\epsilon_2 l^2}{\epsilon_1^2}\int_0^1 \frac{\overset{*}{I}\, k_N}{A} q_r q_k''$$

$$= -\frac{\epsilon_2 l^2}{\epsilon_1^2}\int_0^1 \frac{\overset{*}{I}\, k_N}{A} q_r' q_k'$$

Similarily for $P_{R1B}\ P_{K1A}$ we will get two terms where q_k and q_r'' appear together and after the application of boundary conditions, their form reduces to $q_r'\ q_k'$ with a change in the sign.

$$\epsilon_2 \int \overset{*}{I}\, P_{R1A} P_{K1B} = \int \overset{*}{I} \left[\frac{\epsilon_2}{\epsilon_1^2} \sin^2\psi q_r q_k + \frac{\epsilon_2}{\overset{*}{A}\,\epsilon_1}\, \overset{*}{A}{}'\, q_r q_k' - \frac{\epsilon_2}{\epsilon_1} q_r' q_k' \right.$$
$$\left. - \frac{\epsilon_2}{\epsilon_1^2} \frac{k_N}{\overset{*}{A}} q_r' q_k' + \frac{\epsilon_2 k_N'}{\overset{*}{A}\,\epsilon_1^2} q_r q_k' - \frac{\epsilon_2\, \overset{*}{A}{}'}{\overset{*}{A}\,\epsilon_1} P_{KB} q_r \right] dy$$

Similar expression can be obtained for $P_{R1A}\ P_{K1B}$ with k and r interchanged in the above expression.

Appendix I

EXPRESSION FOR CENTRIFUGAL FORCE EXERTED ON A ROTATING CANTILEVER

Consider a cantilever of length l rotating about an axis, at a distance of R from its root, with an angular velocity Ω, give in fig. I.1

Centrifugal force exerted on an element $d\eta$, at a distance of η from the root of the cantilever can be given as :

$$dN = (\rho A d\eta)\Omega^2(R+\eta)$$

Total centrifugal force on the whole cantilever is :

$$N = \int_\eta^l dN = \int_\eta^l \rho A d\eta \Omega^2 (R+\eta) = \Omega^2 \int_\eta^l \rho A(\eta + R) d\eta$$

Since the cantilever is a blade of airfoil cross section, we write A as

$$A(\eta) = A_1 + A_2\eta + A_3\eta^2 + A_4\eta^3$$

$$N = \Omega^2 \rho \int_\eta^l (A_1 + A_2\eta + A_3\eta^2 + A_4\eta^3)(\eta + R) d\eta$$

we define a dimensionless parameter k_N as

$$k_N = \frac{1}{l^4} \int_\eta^l A(\eta)(\eta + R) d\eta$$

so that

$$N = \Omega^2 \rho k_N l^4$$

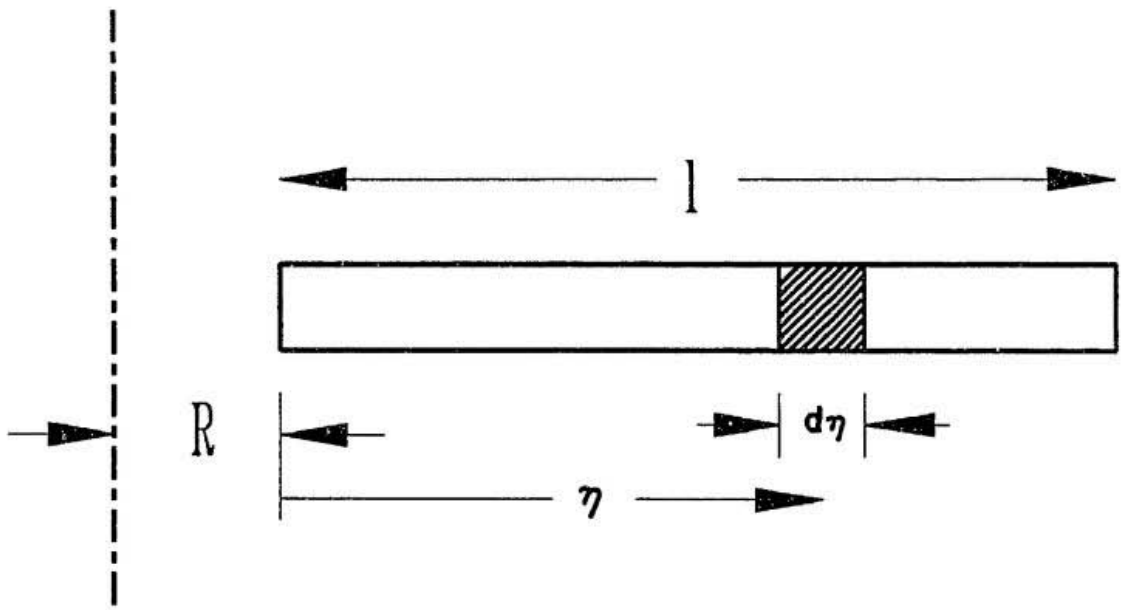

Figure I.1: Rotating cantilever

$$
\begin{aligned}
k_N &= \frac{1}{l^4}\int_{\eta}^{l}(A_1 + A_2\eta + A_3\,\eta^2 + A_4\eta^3)(\eta + R)d\eta \\
&= \frac{1}{l^4}\int_{\eta}^{l} A_1R + {}'A_1 + A_2R)\eta + (A_3R_2 + A_2)\eta^2 + (A_3 + A_4R)\eta^3 + A_4\eta^4\}d\eta \\
&= \frac{1}{l^4}\left[A_1R(l-\eta) + (A_1 + A_2R)\frac{(l^2-\eta^2)}{2} + \frac{A_2 + A_3R}{3}(l^3-\eta^3)\right. \\
&\quad \left. + \frac{A_3 + A_4R}{4}(l^4-\eta^4) + \frac{A_4}{5}(l^5-\eta^5)\right] \\
&= \frac{A_1}{l^2}\frac{R}{l}\frac{l}{l}(1-y) + \left(\frac{A_1}{l^2} + \frac{A_2R}{l^2}\right)\frac{l^2}{2l^2}(1-y^2) \\
&\quad + \left(\frac{A_2}{l} + \frac{A_3R}{l}\right)\frac{l^3}{3l^3}(1-y^3) + (A_3 + A_4R)\frac{l^4}{4l^4}(1-y^4) \\
&\quad + \frac{A_4}{5}\frac{l^5}{l^4}(1-y^5)
\end{aligned}
$$

we define non-dimensional constants :

$$
\begin{aligned}
R_{ND} &= \frac{R}{l} \\
A_{11} &= \frac{A_1}{l^2} \\
A_{12} &= \frac{A_2}{l} \\
A_{13} &= A_3 \\
A_{14} &= A_4 l
\end{aligned}
$$

$$
\begin{aligned}
k_N &= A_{11}R_{ND}(1-y) + (A_{11} + A_{12}R_{ND})\frac{(1-y^2)}{2} + (A_{12} + A_{13}R_{ND})\frac{(1-y^3)}{3} \\
&\quad + (A_{13} + A_{14}R_{ND})\frac{(1-y^4)}{4} + A_{14}\frac{(1-y^5)}{5}
\end{aligned}
$$

Appendix J

GAUSS QUADRATURE INTEGRATION SCHEME

$$
\begin{aligned}
[k_e] &= \int_{-1}^{1}\int_{-1}^{1}\int_{-1}^{1}[B]^T[D][B]Jd\xi d\eta d\zeta \\
&= \int_{-1}^{1}\int_{-1}^{1}\int_{-1}^{1}\phi(\xi,\eta,\zeta)d\xi d\eta d\zeta \\
&= \int_{-1}^{1}\int_{-1}^{1}[\phi(\xi,\eta,\zeta_1)W_1+\phi(\xi,\eta,\zeta_2)W_2]d\xi d\eta \\
&= \int_{-1}^{1}[\{\phi(\xi,\eta_1,\zeta_1)W_1+\phi(\xi,\eta_1,\zeta_2)W_2\}W_1 \\
&\quad +\{\phi(\xi,\eta_2,\zeta_1)W_1+\phi(\xi,\eta_2,\zeta_2)W_2\}W_2] \\
&= [\{\phi(\xi_1,\eta_1,\zeta_1)W_1+\phi(\xi_1,\eta_1,\zeta_2)W_2\}W_1 \\
&\quad +\{\phi(\xi_1,\eta_2,\zeta_1)W_1+\phi(\xi_1,\eta_2,\zeta_2)W_2\}W_2]W_1 \\
&\quad +[\{\phi(\xi_2,\eta_1,\zeta_1)W_1+\phi(\xi_2,\eta_2,\zeta_2)W_2\}W_1 \\
&\quad +\{\phi(\xi_2,\eta_2,\zeta_1)W_1+\phi(\xi_2,\eta_2,\zeta_2)W_2\}W_2]W_2 \\
&= W_1W_1W_1\phi(\xi_1,\eta_1,\zeta_1)+W_1W_1W_2\phi(\xi_1,\eta_1,\zeta_2)+W_1W_2W_1\phi(\xi_1,\eta_2,\zeta_1) \\
&\quad +W_1W_2W_2\phi(\xi_2,\eta_2,\zeta_2)+W_2W_1W_1\phi(\xi_2,\eta_1,\zeta_1)+W_2W_1W_2\phi(\xi_2,\eta_1,\zeta_2) \\
&+ \quad W_2W_2W_1\phi(\xi_2,\eta_2,\zeta_1)+W_2W_2W_2\phi(\xi_2,\eta_2,\zeta_2) \\
&= \sum_{i=1}^{2}\sum_{j=1}^{2}\sum_{k=1}^{2}W_iW_jW_k\phi_s(\xi_i,\eta_j,\zeta_k)
\end{aligned}
$$

Appendix K

RELATION OF $[k_\sigma]$ WITH NON-LINEAR STRAINS

Consider a rigid bar of length l, fixed to a spring k_s as shown in the Fig. K.1. Spring k_s is constrained to remain horizontal and is initially stretched an amount y to produce a force F. Load R is applied externally to the rod, so that it gets deflected by an angle θ.

Assuming the bar to be infinitely stiff in bending, the axial strain for small displacements is :

$$\epsilon_x = \epsilon_u + \epsilon_v$$

where :

$$\epsilon_u = \frac{u_2 - u_1}{l}$$

$$\epsilon_v = \frac{\Delta l}{l} = \frac{\frac{l}{\cos\theta} - l}{l} = \frac{1}{2}\left(\frac{v_2 - v_1}{l}\right)^2$$

Strain energy stored in the bar is given as :

$$U = \frac{AEl\epsilon_x^2}{2} = \frac{AEl}{2}\left(\epsilon_u^2 + \epsilon_v^2\right) + Fl\epsilon_v$$

The terms ϵ_u^2 and ϵ_v are quadratic in nodal d.o.f. but ϵ_v^2 is quartic, so ϵ_v^2 can be considered neglegible as compared to the first two terms.

$$U = \frac{AEl}{2}\epsilon_u^2 + Fl\epsilon_v$$

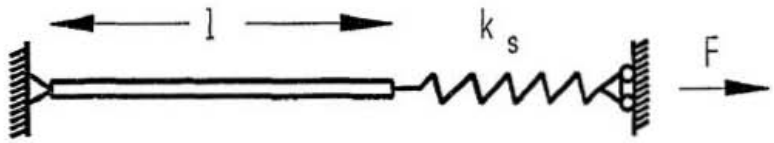

(a) Initial Position

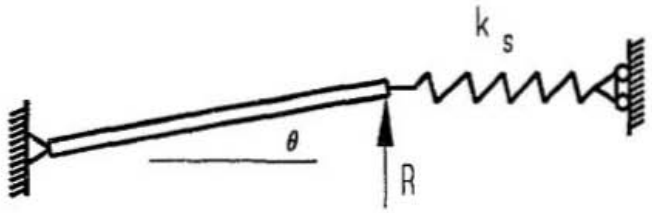

(b) Final Position

Figure K.1: Transverse force on an axially loaded truss member

In the matrix notation

$$\epsilon_u = \frac{1}{l}\begin{bmatrix} -1 & 1 \end{bmatrix}\begin{bmatrix} u_1 & u_2 \end{bmatrix}^T$$

$$\epsilon_v = \frac{1}{2l^2}\begin{Bmatrix} v_1 \\ v_2 \end{Bmatrix}^T\begin{bmatrix} -1 & 1 \end{bmatrix}^T\begin{bmatrix} -1 & 1 \end{bmatrix}\begin{Bmatrix} v_1 \\ v_2 \end{Bmatrix}$$

$$\{d\} = \begin{bmatrix} u_1 & v_1 & u_2 & v_2 \end{bmatrix}^T$$

$$U = \frac{1}{2}\{d\}^T\left(\frac{AE}{L}\begin{bmatrix} 1 & 0 & -1 & 0 \\ 0 & 0 & 0 & 0 \\ -1 & 0 & 1 & 0 \\ 0 & 0 & 0 & 0 \end{bmatrix} + \frac{F}{L}\begin{bmatrix} 0 & 0 & 0 & 0 \\ 0 & 1 & 0 & -1 \\ 0 & 0 & 0 & 0 \\ 0 & -1 & 0 & 1 \end{bmatrix}\right)\{d\}$$

from the above expression it is clear that the two matricies in the brackets are the stiffness matricies for the system. The first 4×4 matrix with coefficient $\frac{AE}{L}$ is the conventional stiffness matrix $[k]$ for a truss element, the other one associated with the axial force F and non-linear strain ϵ_v is termed as the stress stiffness matrix $[k_\sigma]$.

Appendix L

STRESS MATRIX $[s]$

$$
\begin{aligned}
[s] &= \begin{bmatrix} E\epsilon_{xx} & (u_{,y}+v_{,x})G & (u_{,z}+w_{,x})G \\ (u_{,y}+v_{,x})G & E\epsilon_{yy} & (v_{,z}+w_{,y})G \\ (u_{,y}+w_{,x})G & (v_{,z}+w_{,y})G & E\epsilon_{zz} \end{bmatrix} \\
&= \begin{bmatrix} Eu_{,x} & (u_{,y}+v_{,x})G & (u_{,z}+w_{,x})G \\ (u_{,y}+v_{,x})G & Ev_{,y} & (v_{,z}+w_{,y})G \\ (u_{,z}+w_{,x})G & (v_{,z}+w_{,y})G & Ew_{,z} \end{bmatrix} \\
&= \begin{bmatrix} Eu_{,x} & 0 & 0 \\ (u_{,y}+v_{,x})G & 0 & 0 \\ (u_{,z}+w_{,x})G & 0 & 0 \end{bmatrix} + \begin{bmatrix} 0 & (u_{,y}+v_{,x})G & 0 \\ 0 & Ev_{,y} & 0 \\ 0 & (v_{,z}+w_{,y})G & 0 \end{bmatrix} \\
&\quad + \begin{bmatrix} 0 & 0 & (u_{,z}+w_{,x})G \\ 0 & 0 & (v_{,z}+w_{,y})G \\ 0 & 0 & Ew_{,z} \end{bmatrix} \\
&= [EG_1]\{\delta\}[C_A] + [EG_2]\{\delta\}[C_B] + [EG_3]\{\delta\}[C_C]
\end{aligned}
$$

where :

$$[EG_1] = \begin{bmatrix} E & 0 & 0 & 0 & 0 & 0 & 0 & 0 & 0 \\ 0 & G & 0 & G & 0 & 0 & 0 & 0 & 0 \\ 0 & 0 & G & 0 & 0 & 0 & G & 0 & 0 \end{bmatrix}$$

$$[EG_2] = \begin{bmatrix} 0 & G & 0 & G & 0 & 0 & 0 & 0 & 0 \\ 0 & 0 & 0 & 0 & E & 0 & 0 & 0 & 0 \\ 0 & 0 & 0 & 0 & 0 & G & 0 & G & 0 \end{bmatrix}$$

$$[EG_3] = \begin{bmatrix} 0 & 0 & G & 0 & 0 & 0 & G & 0 & 0 \\ 0 & 0 & 0 & 0 & 0 & G & 0 & G & 0 \\ 0 & 0 & 0 & 0 & 0 & 0 & 0 & 0 & E \end{bmatrix}$$

$$[C_A] = \begin{bmatrix} 1 & 0 & 0 \end{bmatrix}$$

$$[C_B] = \begin{bmatrix} 0 & 1 & 0 \end{bmatrix}$$

$$[C_C] = \begin{bmatrix} 0 & 0 & 1 \end{bmatrix}$$

The expression of $\{\delta\}$ can be obtained from equation (3.12).

$$\{\delta\} = [AJ][DS]\{d\}$$

the displacement vector $\{d\}$ is obtained from the relation:

$$\{F\} = [K]\{d\}$$

where:

$[K]$ = structural stiffness matrix of the system.

$[F]$ = force vector for the system obtained after assembling $\{f\}$.

$\{f\}$ = force vector for an element given by $\int_v N^T f' dv$.

f' = cetrifugal force acting on the element.

Appendix M

CHARACTERISTIC EQUATION FOR THE SHAFT-ROTOR SYSTEM

From the boundary conditions (11) and (12) in section 4.5 we have

$$R''(c) = 0$$
$$R'''(c) = 0$$

The above two equations lead to the following expression

$$A_1 = \psi_1 A_3 + \psi_2 A_4$$
$$A_2 = \psi_3 A_3 + \psi_4 A_4$$

where :

$$\begin{aligned}
\psi_1 &= \gamma^3 \cosh \eta_1 c \cos \eta_2 c + \gamma^2 \sin \eta_2 c \sinh \eta_1 c \\
\psi_2 &= \gamma^3 \cos \eta_2 c \sinh \eta_1 c + \gamma^2 \cosh \eta_1 c \sin \eta_2 c \\
\psi_3 &= \gamma^2 \cos \eta_2 c \sinh \eta_1 c - \gamma^3 \cosh \eta_1 c \sin \eta_2 c \\
\psi_4 &= \gamma^2 \cosh \eta_1 c \cos \eta_2 c - \gamma^3 \sinh \eta_1 c \sin \eta_2 c \\
\gamma &= \frac{\eta_1}{\eta_2}
\end{aligned}$$

from the boundary conditions (3), (7), (8), (9) and (10) in section 4.5 we have :

$$
\begin{aligned}
X_1 &= \frac{1}{2}\left[(1+\nu^2)\psi_3\phi_3 + \left\{(1+\nu^2)\psi_4 + (1-\nu^2\gamma^2)\right\}\right]\sin\lambda b \\
&\quad + \frac{\nu}{2}\left[\left\{(1+\nu^2)\psi_1 + \gamma(1-\nu^2\gamma^2)\right\}\phi_3 + (1+\nu^2)\psi_2\right]\cos\lambda b
\end{aligned}
$$

$$
\begin{aligned}
X_2 &= \frac{1}{2}\left[(1+\nu^2)\psi_2\phi_3 + \left\{(1+\nu^2)\psi_4 + (1-\nu^2\gamma^2)\right\}\right]\cos\lambda b \\
&\quad - \frac{\nu}{2}\left[\left\{(1+\nu^2)\psi_1 + \gamma(1-\nu^2\gamma^2)\right\}\phi_3 + (1+\nu^2)\psi_2\right]\sin\lambda b
\end{aligned}
$$

$$
\begin{aligned}
X_3 &= -\frac{1}{2}\left[(1-\nu^2)\psi_3\phi_3 + \left\{(1-\nu^2)\psi_4 + (1+\nu^2\gamma^2)\right\}\right]\sinh\lambda b \\
&\quad + \frac{\nu}{2}\left[\left\{(1-\nu^2)\psi_1 + \gamma(1+\nu^2\gamma^2)\right\}\phi_3 + (1-\nu^2)\psi_2\right]\cosh\lambda b
\end{aligned}
$$

where :

$$\nu = \frac{\eta_2}{\lambda}$$

$$
\begin{aligned}
\phi_1 &= (1+\nu^2)\psi_3\cos\lambda b - \nu\left\{(1+\nu^2)\psi_1 + \gamma(1-\nu^2\gamma^2)\right\}\sin\lambda b + (1-\nu^2)\psi_3\cosh\lambda b \\
&\quad - \nu\left\{(1-\nu^2)\psi_1 + \gamma(1+\nu^2\gamma^2)\right\}\sinh\lambda b
\end{aligned}
$$

$$
\begin{aligned}
\phi_2 &= -\left[\left\{(1+\nu^2)\psi_4 + (1-\nu^2\gamma^2)\right\}\cos\lambda b - \nu(1+\nu^2)\psi_2\sin\lambda b\right. \\
&\quad \left. + \left\{(1-\nu^2)\psi_4 + (1+\gamma^2\nu^2)\right\}\cosh\lambda b - \nu(1-\nu^2)\psi_2\sinh\lambda b\right]
\end{aligned}
$$

$$\phi_3 = \frac{\phi_2}{\phi_1}$$

From the boundary conditions (1), (2), (4) and (5) in section 4.5 we have :

$$Q_1 = \theta_1 Q_3$$

$$Q_2 = \theta_2 Q_3$$

$$2P_2 = Q_3 W_1$$

After further algebraic simplifications we get the characteristic equation of the form :

$$(X_1 + X_3)W_1 - 2X_2 W_2 = 0$$

where :

$$\theta_1 = -\left[\frac{2\lambda \sinh \lambda a + k(\cosh \lambda a - \cos \lambda a)}{2\lambda \sin \lambda a + k(\cosh \lambda a - \cos \lambda a)}\right]$$

$$\theta_2 = \frac{k \sinh \lambda a - k \sin \lambda a}{2\lambda \sin \lambda a + k(\cosh \lambda a - \cos \lambda a)}$$

$$W_1 = \theta_1 \sin \lambda a + \theta_2(\cos \lambda a + \cosh \lambda a) - \sinh \lambda a$$

$$W_2 = \theta_1 \cos \lambda a - \theta_2(\sin \lambda a + \sinh \lambda a) + \cosh \lambda a$$

SPECIAL CASES :

(a) Simply supported forward end bearing :

$$k = 0$$
$$\theta_1 = -\frac{\sinh \lambda a}{\sin \lambda a}$$
$$\theta_2 = 0$$

(b) Clamped forward end bearing :

$$k = \infty$$
$$\theta_1 = -1$$
$$\theta_2 = \frac{\sinh \lambda a - \sin \lambda a}{\cosh \lambda a - \cos \lambda a}$$

Appendix N

COUPLING OF DEFLECTION FUNCTIONS

Referring to Fig (5.3), if we consider a mass m attached to three springs having deflection functions y_1, y_2, y_3, the expression for the kinetic energy of the system can be given as :

$$\begin{aligned} K.E. &= m(y_1 + y_2 + y_3)^2 \\ &= m(y_1^2 + y_2^2 + y_3^2) + 2m(y_1y_2 + y_1y_3 + y_2y_3) \\ &= m_i \sum_{i=1}^{3} y_i^2 + m_{ij} \sum_{\substack{i=1 \\ i \neq j}}^{3} \sum_{j=1}^{3} y_i y_j \\ &= \sum_{i=1}^{3} t_i + \sum_{\substack{i=1 \\ i \neq j}}^{3} \sum_{j=1}^{3} t_{ij} \end{aligned}$$

where :

t_{ij} represents the coupling effect between two deflection functions y_i and y_j.

Appendix O

COMPUTER PROGRAM FOR FINDING THE NATURAL FREQUENCIES AND MODE SHAPES OF A ROTATING PROPELLER BLADE

```
c ***************************************************************************
c ***************************************************************************
C ******** THE PROGRAM FINDS THE NATURAL FREQ. OF A ROTATING BLADE ****
C ******** HAVING AIRFOIL SECTION, EFFECTS OF STAGGER ANGLE SETTING,***
C ******** SHEAR DEFLECTION AND ROTARY INERTIA ARE CONSIDERED.     ****
C ***************************************************************************
C ***************************************************************************

C ***************************************************************************
C NOMENCLATURE:-
C ***************************************************************************
C BBI      = EIGEN VALUE INDEX FOR A CANTILEVER
C U        = GAUSS POINTS OF INTEGERATION
C R        = WEIGHTS AT GAUSS POINTS
C A        = AREA OF THE BLADE AT A SECTION
C S        = AREA MOMENT OF INERTIA OF THE BLADE AT A SECTION
C CA       = COEFFICIENTS OF THE CUBIC FIT FOR AREA
C CS       = COEFFICIENTS OF THE CUBIC FIT FOR AREA MOMENT OF INERTIA
C AVAR     = AVERAGE AREA OF THE BLADE
C AVIR     = AVERAGE INERTIA OF THE BLADE
C RPS      = HUB ROTATION IN R.P.S.
C PSI      = PITCH ANGLE SETTING OF THE BLADE ON THE HUB
C S1       = MASS MATRIX OF THE SYSTEM
C S2       = STIFFNESS MATRIX OF THE SYSTEM
C G1       = FUNCTION REPRESENTING MASS OF THE EIGEN VALUE EQUATION
C G2       = FUNCTION REPRESENTING STIFFNESS OF THE EIGEN VALUE EQUATION
C FREQN    = NATURAL FREQUENCY OF THE BLADE IN HZ.
C BL       = BLADE LENGTH
C R        = RADIUS OF THE HUB
C D        = DIAMETER OF THE PROPELLER SHAFT
C C        = CORD LENGTH OF THE BLADE
C CD       = CORD LENGTH TO DIAMETER RATIOS
C YC       = BLADE THICKNESS COORDINATE
C ZC       = BLADE WIDTH COORDINATE
C XR       = BLADE LENGTH COORDINATE
C AK       = SHAPE FACTOR OF THE BLADE PROFILE
C MM       = ITERATIVE INDEX OF THE PROGRAM
C ***************************************************************************

IMPLICIT REAL*8 (A-H,O-Z)
DIMENSION G1(10),G2(10),BB(4),S1(4,4),S2(4,4),BBETA(4),BETABL(4),
     1 PSI(3),RPS(6),OMEGAN(4),BBI(4),
     1 U(10),R(10),CA(4),CS(4)
DOUBLE COMPLEX EVAL(4),OMEGA

OPEN(UNIT=6,FILE='BLADEFREQ.ANS',TYPE='NEW')
PI=3.1415926
BL=2.8
ROE=7850.
c ROE=7850.*1.25

U(1)=.0744371695
U(2)=.2166976971
U(3)=.3397047841
U(4)=.4325316833
```

```
U(5)=.4869532643
R(1)=.1477621124
R(2)=.1346333597
R(3)=.1095431813
R(4)=.07472567458
R(5)=.03333567215

DO 11 I=1,5
U(5+I)=-U(I)
R(5+I)=R(I)
11 CONTINUE

CALL AERO(CA,CS,AVAR,AVIN)

DATA BBI/1.875,4.694,7.854,10.995/
c DATA RPS/1.E-05,5.,10.,15.,20.,25./
DATA RPS/1.E-05,2.,4.,6.,8.,10./
DATA PSI/0.,.5236,.78539/

DO 31 I=1,4
DO 31 J=1,4
S1(I,J)=0.
S2(I,J)=0.
31 CONTINUE

WRITE(6,*)' HUB ROT.(HZ)    STG. ANGLE       NAT. FREQ.(HZ) EIGEN
     1 INDEX  '

DO 100 II=1,3
NSTG=PSI(II)*180./PI
WRITE(6,*)'          STAGGER ANGLE =',NSTG
DO 100 JJ=1,6
WRITE(6,*)' '
DO 83 KK=1,4
BB(KK)=BBI(KK)
83 CONTINUE

WS=2.*PI*RPS(JJ)
THETA=PSI(II)
ALPHA=(SIN(THETA))**2

AALPHA=0.
ABETA=1.

C ***********************************************************************
C ITERATION INDEX MM, ITERATIONS NEEDED TO GENERATE REFINED EIGEN
C VALUES FROM THE ASSUMED VALUES FOR A CANTILEVER
C ***********************************************************************
DO 100 MM=1,4

DO 30 K=1,4
BI=BB(K)
DO 30 M=1,4
BJ=BB(M)
```

```
CALL QFUNCTION(U,BI,BJ,G1,G11,G12,G13,G14,G15,F2,F3,F4,F5,G2,
     1 G21,G22,G23,WS,ALPHA,CA,CS)
SUM1=0.
SUM2=0.

DO 13 J=1,10
SUM1=(ABETA-AALPHA)*(SUM1+R(J)*G1(J))
SUM2=(ABETA-AALPHA)*(SUM2+R(J)*G2(J))
13 CONTINUE

S1(K,M)=SUM1
S2(K,M)=SUM2
30 CONTINUE
C WRITE(6,*)'          MASS      MATRIX          '
C WRITE(6,1000)((S1(I,J),J=1,4),I=1,4)
C WRITE(6,*)'        STIFFNESS   MATRIX          '
C WRITE(6,1000)((S2(I,J),J=1,4),I=1,4)
1000 FORMAT(1X,4G16.8)
CALL EIGEN(S1,S2,EVAL)

DO 29 I=1,4
OMEGAN(I)=WS*EVAL(I)**.5
FREQN=OMEGAN(I)/(2.*PI)
C ****************************************************************
C ADDED MASS EFFECT DUE TO WATER TAKEN CARE BY THE DENSITY
c ADJUSTMENT
C ****************************************************************
AVM=ROE*AVAR
BBETA(I)=(AVM*OMEGAN(I)**2/(20.6E10*AVIN))**.25
BETABL(I)=BBETA(I)*BL
IF(MM.EQ.4) WRITE(6,222)RPS(JJ),PSI(II),freqn,BETABL(I)
BB(I)=BETABL(I)
29 CONTINUE

BB(1)=1.875
100 CONTINUE
222  FORMAT(F11.4,5X,F11.4,5X,F11.4,4X,F11.4)
STOP
END


C ********************************************************************
C  SUBROUTINE FOR FINDING THE EIGEN VALUES AND EIGEN VECTORS
C OF THE SYSTEM
C ********************************************************************
       SUBROUTINE EIGEN(B,A,EVAL)
PARAMETER (N=4,LDA=N,LDB=N)
INTEGER I
DOUBLE PRECISION A(LDA,N),AMACH,B(LDB,N),BETA(N)
DOUBLE COMPLEX ALPHA(N),EVAL(N),EVEC(N,N)
EXTERNAL AMACH,DGPIRG,DGVCRG,UMACH,DWRCRN
CALL DGVCRG(N,A,LDA,B,LDB,ALPHA,BETA,EVEC,N)

DO 10 I=1,N
  IF (BETA(I).NE.0.)THEN
```

```
    EVAL(I)=ALPHA(I)/BETA(I)
  ELSE
    EVAL(I)= AMACH(2)
  END IF
10 CONTINUE

C CALL DWRCRN('EVAL',1,N,EVAL,1,0)
C CALL DWRCRN('EVEC',N,N,EVEC,N,0)
RETURN
END

C ***************************************************************************
C  SUBROUTINE FOR FINDING THE MASS AND STIFFNESS OF THE SYSTEM
C ***************************************************************************
SUBROUTINE QFUNCTION(U,BI,BJ,G1,G11,G12,G13,G14,G15,F2,F3,F4,F5,
     1 G2,G21,G22,G23,WS,ALPHA,CA,CS)
IMPLICIT REAL*8 (A-H,O-Z)
Dimension G1(10),G11(10),G12(10),G13(10),G14(10),G15(10),F2(10),
     1 F3(10),F4(10),F5(10),G2(10),G21(10),G22(10),G23(10),U(10),
     1 CA(4),CS(4)

c ROE=7850.*1.25
ROE=7850.
ELAS=20.6E+10
ANUE=.3
PI=3.1415926
BL=2.8
R=.7
RND=R/BL
SHEAR=ELAS/((1.+ANUE)*2.)
AK=1.2

C ***************************************************************************
C NON DIMENSIONAL COEFFICIENTS OF AREA AND MOMENT OF INERTIA
C ***************************************************************************

A11=CA(1)/BL**2
A12=CA(2)/BL
A13=CA(3)
A14=CA(4)*BL

S11=CS(1)/BL**4
S12=CS(2)/BL**3
S13=CS(3)/BL**2
S14=CS(4)/BL

C1=CA(1)
C2=CA(2)*BL
C3=CA(3)*BL**2
C4=CA(4)*BL**3

C ***************************************************************************
C GAUSSIAN INTEGERATION, NO. OF GAUSS POINTS=10
C ***************************************************************************
```

```
DO 200 I=1,10
X=U(I)+.5
EE=X*BL
BIX=BI*X
BJX=BJ*X
A=COS(BIX)
B=SIN(BIX)
C=COSH(BIX)
D=SINH(BIX)
E=COS(BJX)
F=SIN(BJX)
Y=COSH(BJX)
H=SINH(BJX)
SI=(COS(BI)+COSH(BI))/(SIN(BI)+SINH(BI))
SJ=(COS(BJ)+COSH(BJ))/(SIN(BJ)+SINH(BJ))

CN1=A11*RND*(1.-X)
CN2=(A11+A12*RND)*(1.-X**2)/2.
CN3=(A12+A13*RND)*(1.-X**3)/3.
CN4=(A13+A14*RND)*(1.-X**4)/4.
CN5=A14*(1.-X**5)/5.
CN=CN1+CN2+CN3+CN4+CN5

ACN1=-A11*RND
ACN2=-X*(A11+A12*RND)
ACN3=-X**2*(A12+A13*RND)
ACN4=-X**3*(A13+A14*RND)
ACN5=-X**4*A14
ACN=ACN1+ACN2+ACN3+ACN4+ACN5

G3=(C-A-SI*D+SI*B)*(Y-E-SJ*H+SJ*F)
G4=BI*BJ*(D+B-SI*C+SI*A)*(H+F-SJ*Y+SJ*E)
G5=(BI*BJ)**2*(C+A-SI*D-SI*B)*(Y+E-SJ*H-SJ*F)

QR=C-A-SI*D+SI*B
QR1=BI*(D+B-SI*C+SI*A)
QR2=BI**2*(C+A-SI*D-SI*B)
QR3=BI**3*(D-B-SI*C-SI*A)
QK=Y-E-SJ*H+SJ*F
QK1=BJ*(H+F-SJ*Y+SJ*E)
QK2=BJ**2*(Y+E-SJ*H-SJ*F)
QK3=BJ**3*(H-F-SJ*Y-SJ*E)
QK4=BJ**4*(Y-E-SJ*H+SJ*F)

AXX=C1+C2*X+C3*X**2+C4*X**3
AAXX=C2+2.*C3*X+3.*C4*X**2

AND=A11+A12*X+A13*X**2+A14*X**3
SND=S11+S12*X+S13*X**2+S14*X**3

EN=WS**2*ROE*CN*BL**4
AEN=WS**2*ROE*ACN*BL**4

CON1=X**2/BJ+2./BJ**3
CON2=X**2/BJ-2./BJ**3
```

```
CON3=2.*X/BJ**2

AQ1=C1*(H-F-SJ*E-SJ*Y)/BJ
AQ21=X*H/BJ-Y/BJ**2
AQ22=-(E/BJ**2+X*F/BJ)
AQ23=SJ*(F/BJ**2-X*E/BJ)
AQ24=-SJ*(X*Y/BJ-H/BJ**2)
AQ2=C2*(AQ21+AQ22+AQ23+AQ24)
AQ31=C3+3.*SJ*C4/BJ
AQ32=-CON3*Y+CON1*H
AQ3=AQ31*AQ32
AQ41=-C3+3.*SJ*C4/BJ
AQ42=CON3*E+CON2*F
AQ4=AQ41*AQ42
AQ51=C3*SJ+3.*C4/BJ
AQ52=CON3*F-CON2*E
AQ5=AQ51*AQ52
AQ61=-C3*SJ-3.*C4/BJ
AQ62=CON1*Y-CON3*H
AQ6=AQ61*AQ62
AQ7=C4*X**3*H/BJ
AQ8=-C4*X**3*F/BJ
AQ9=-C4*SJ*X**3*E/BJ
AQ10=-C4*SJ*X**3*Y/BJ
AQ=AQ1+AQ2+AQ3+AQ4+AQ5+AQ6+AQ7+AQ8+AQ9+AQ10

ACON1=X**2/BI+2./BI**3
ACON2=X**2/BI-2./BI**3
ACON3=2.*X/BI**2

AR1=C1*(D-B-SI*A-SI*C)/BI
AR21=X*D/BI-C/BI**2
AR22=-(A/BI**2+X*B/BI)
AR23=SI*(B/BI**2-X*A/BI)
AR24=-SI*(X*C/BI-D/BI**2)
AR2=C2*(AR21+AR22+AR23+AR24)
AR31=C3+3.*SI*C4/BI
AR32=-ACON3*C+ACON1*D
AR3=AR31*AR32
AR41=-C3+3.*SI*C4/BI
AR42=ACON3*A+ACON2*B
AR4=AR41*AR42
AR51=C3*SI+3.*C4/BI
AR52=ACON3*B-ACON2*A
AR5=AR51*AR52
AR61=-C3*SI-3.*C4/BI
AR62=ACON1*C-ACON3*D
AR6=AR61*AR62
AR7=C4*X**3*D/BI
AR8=-C4*X**3*B/BI
AR9=-C4*SI*X**3*A/BI
AR10=-C4*SI*X**3*C/BI
AR=AR1+AR2+AR3+AR4+AR5+AR6+AR7+AR8+AR9+AR10

EFS1=SHEAR/(AK*ROE*WS**2*BL**2)
```

```
EFS2=ELAS/(ROE*WS**2*BL**2)

PKA=AQ/(AXX*EFS1)

PKB1=QK1
PKB2=BL**2*CN*QK1/(EFS1*AXX)
PKB3=ALPHA*AQ/(EFS1*AXX)
PKB=PKB1+PKB2+PKB3

PK1A1=QK/EFS1
PK1A2=-AAXX*PKA/AXX
PK1A=PK1A1+PK1A2

PK1B1=QK*ALPHA/EFS1
PK1B2=(AAXX*QK1+AXX*QK2)/AXX
PK1B3=BL**2*(CN*QK2+ACN*QK1)/(AXX*EFS1)
PK1B4=-AAXX*PKB/AXX
PK1B=PK1B1+PK1B2+PK1B3+PK1B4

PRA=AR/(AXX*EFS1)

PRB1=QR1
PRB2=BL**2*CN*QR1/(EFS1*AXX)
PRB3=ALPHA*AR/(EFS1*AXX)
PRB=PRB1+PRB2+PRB3

PR1A1=QR/EFS1
PR1A2=-AAXX*PRA/AXX
PR1A=PR1A1+PR1A2

PR1B1=QR*ALPHA/EFS1
PR1B2=(AAXX*QR1+AXX*QR2)/AXX
PR1B3=BL**2*(CN*QR2+ACN*QR1)/(AXX*EFS1)
PR1B4=-AAXX*PRB/AXX
PR1B=PR1B1+PR1B2+PR1B3+PR1B4

C ***********************************************************************
C THIRD TERM ON THE MASS SIDE(AM3) HAS BEEN SPLIT TO APPLY THE
C BOUNDARY CONDITIONS
C ***********************************************************************
AM31=QK*QR*ALPHA/(EFS1**2)
AM32=-QR1*QK1/(EFS1)
AM33=AAXX*QR*QK1/(AXX*EFS1)
AM34=-BL**2*CN*QR1*QK1/(AXX*EFS1**2)
AM35=BL**2*ACN*QR*QK1/(AXX*EFS1**2)
AM36=-AAXX*ALPHA*QR*AQ/(AXX*EFS1)**2
AM37=-AAXX*QR*QK1/(AXX*EFS1)
AM38=-AAXX*BL**2*CN*QR*QK1/(AXX*EFS1)**2

AM39A=-AAXX*PRA/AXX
AA1=ALPHA*QK/EFS1
AA2=QK2
AA3=AAXX*QK1/AXX
AA4=BL**2*CN*QK2/(EFS1*AXX)
AA5=BL**2*ACN*QK1/(EFS1*AXX)
```

```
AA6=-AAXX*ALPHA*AQ/(AXX**2*EFS1)
AA7=-AAXX*QK1/AXX
AA8=-AAXX*BL**2*CN*QK1/(AXX**2*EFS1)
AM39B=AA1+AA2+AA3+AA4+AA5+AA6+AA7+AA8
AM39=AM39A*AM39B

AM310=QK*QR*ALPHA/(EFS1**2)
AM311=-QR1*QK1/(EFS1)
AM312=AAXX*QK*QR1/(AXX*EFS1)
AM313=-BL**2*CN*QR1*QK1/(AXX*EFS1**2)
AM314=BL**2*ACN*QK*QR1/(AXX*EFS1**2)
AM315=-AAXX*ALPHA*QK*AR/(AXX*EFS1)**2
AM316=-AAXX*QK*QR1/(AXX*EFS1)
AM317=-AAXX*BL**2*CN*QK*QR1/(AXX*EFS1)**2

AM318A=-AAXX*PKA/AXX
AAA1=ALPHA*QR/EFS1
AAA2=QR2
AAA3=AAXX*QR1/AXX
AAA4=BL**2*CN*QR2/(EFS1*AXX)
AAA5=BL**2*ACN*QR1/(EFS1*AXX)
AAA6=-AAXX*ALPHA*AR/(AXX**2*EFS1)
AAA7=-AAXX*QR1/AXX
AAA8=-AAXX*BL**2*CN*QR1/(AXX**2*EFS1)
AM318B=AAA1+AAA2+AAA3+AAA4+AAA5+AAA6+AAA7+AAA8
AM318=AM318A*AM318B

AM3=-(EFS2*SND)*(AM31+AM32+AM33+AM34+AM35+AM36+AM37+AM38+
     1 AM39+AM310+AM311+AM312+AM313+AM314+AM315+AM316+AM317+AM318)

G1A=QK*QR*AND
G1B=SND*PKB*PRB
G1D=-EFS1*(PKA*PRB+PKB*PRA)*AND
G1E=EFS1*(QK1*PRA+QR1*PKA)*AND

G2A=EFS2*SND*PK1B*PR1B
G2B=-ALPHA*QK*QR*AND
G2C=CN*QK1*QR1
G2D1=PKB*PRB
G2D2=-(QK1*PRB+QR1*PKB)
G2D3=QK1*QR1
G2D=EFS1*(G2D1+G2D2+G2D3)*AND

C ***********************************************************************
C        WITHOUT SHEAR DEFLECTION AND ROT. INERT. EFFECTS
C ***********************************************************************
C G1(I)=G1A
C G2(I)=(G2A+G2B+G2C)

C ***********************************************************************
C        WITH SHEAR DEFLECTION AND ROT. INERT. EFFECTS
C ***********************************************************************
G1(I)=(G1A+G1B+AM3+G1D+G1E)
G2(I)=(G2A+G2B+G2C+G2D)
```

```
C ***********************************************************************
C        WITH SHEAR DEFLECTION ONLY
C G1(I)=(G1A+AM3+G1D+G1E)
C G2(I)=(G2A+G2B+G2C+G2D)

200 CONTINUE
RETURN
END

C ***********************************************************************
C SUBROUTINE FOR FINDING CUBIC FIT
C ***********************************************************************
SUBROUTINE AERO(CA,CS,AVAREA,AVINER)
IMPLICIT REAL*8 (A-H,O-Z)
DIMENSION CD(10),C(10),ZC(17),Z(170),YC(17),Y(170),A(10),S(10),
     1 X(10),XR(10),T(4,4),F(4),G(4),AINV(4,4),CA(4),CS(4),
     1 AT(4,4)
D=7.
DATA CD/.325,.35,.375,.387,.39,.375,.333,.275,.2,0./
DATA ZC/0.,1.25,2.5,5.,7.5,10.,15.,20.,30.,40.,50.,60.,
     1 70.,80.,90.,95.,100/
  DATA YC/0.,1.938,2.708,3.764,4.548,5.186,6.202,6.996,8.126,
     1 8.782,9.,8.752,7.904,6.298,3.776,2.122,.18/
        K=0

DO 15 I=1,10
C(I)=CD(I)*D
DO 15 J=1,17
        K=K+1
Z(K)=ZC(J)*C(I)/100.
Y(K)=(YC(J)/2.)*C(I)/100.
15 CONTINUE

K=0
DO 17 J=1,10
DO 17 I=1,17
K=K+1
L=11+(J-1)*17
17 CONTINUE

CALL AREASECT(Z,Y,A,S)

CALL MATRICIES(X,A,S,T,F,G)

WRITE(6,*)'RADIAL DIST.              AREAS          INERTIAS '

AVAREA=0.
AVINER=0.
DO 11 I=1,10
AVAREA=AVAREA+A(I)
AVINER=AVINER+S(I)
WRITE(6,*)X(I),A(I),S(I)
11 CONTINUE

AVAREA=AVAREA/10.
```

```
AVINER=AVINER/10.

CALL SOLUTION(T,F,G,CA,CS)

WRITE(6,*)'   AREA COEFF.                    INERTIA COEFF.'

DO 10 I=1,4
WRITE(6,*)CA(I),CS(I)
10 CONTINUE

WRITE(6,*)'  AVERAGE AREA                  AVERAGE INERTIA'
WRITE(6,*),AVAREA,AVINER

RETURN
END

C ********************************************************** ************
C  SUBROUTINE FOR FINDING AREA AND AREA MOMENT OF INERTIA
C AT VARIOUS SECTIONS OF THE BLADE
C ********************************************************************
SUBROUTINE AREASECT(Z,Y,A,S)
IMPLICIT REAL*8 (A-H,O-Z)
DIMENSION Z(170),Y(170),S(10),A(10)
DO 35 J=1,10
A(J)=0
S(J)=0
DO 35 I=1,16
KK2=17*(J-1)+I+1
KK1=17*(J-1)+I
A(J)=A(J)+2*.5*(Z(KK2)-Z(KK1))*
     1  (Y(KK2)+Y(KK1))
S(J)=S(J)+2*((Z(KK2)-Z(KK1))*
     1 (Y(KK2)+Y(KK1))**3/(3.*8.))
35 CONTINUE

RETURN
END

C ********************************************************************
C SUROUTINE FOR FINDING THE MATRICIES NEEDED FOR CURVE FITTING
C ********************************************************************

SUBROUTINE MATRICIES(X,A,S,T,F,G)
IMPLICIT REAL*8 (A-H,O-Z)
DIMENSION X(10),XR(10),A(10),S(10),T(4,4),F(4),G(4)
BL=2.8
DATA XR/1.E-15,.125,.25,.375,.5,.625,.75,.875,.937,1./

DO 11 I=1,10
X(I)=XR(I)*BL
11  CONTINUE

DO 39 I=1,4
DO 39 J=1,4
T(I,J)=0.
```

```
DO 39 K=1,10
T(I,J)=T(I,J)+X(K)**(I+J-2)
39  CONTINUE

C AREA AND MOMENT OF INER. MATRIX F AND G   **********************

DO 49 I=1,4
F(I)=0.
G(I)=0.
DO 49 J=1,10
F(I)=F(I)+A(J)*X(J)**(I-1)
G(I)=G(I)+S(J)*X(J)**(I-1)
49 CONTINUE
RETURN
END

C ***************************************************************************
C SUROUTINE FOR FINDING THE COEFFICIENTS OF AREA AND
C INERTIA POLYNOMIALS
C ***************************************************************************

SUBROUTINE SOLUTION(T,F,G,CA,CS)
IMPLICIT REAL*8 (A-H,0-Z)
PARAMETER (IPATH=1,LDA=4,N=4)
REAL T(LDA,LDA),F(N),G(N),CA(N),CS(N)

CALL DLSLRG(N,T,LDA,F,IPATH,CA)
CALL DLSLRG(N,T,LDA,G,IPATH,CS)

RETURN
END
```

Appendix P

COMPUTER PROGRAM FOR FINDING THE NATURAL FREQUENCIES OF A ROTATING PROPELLER BLADE USING FINITE ELEMENT ANALYSIS

```
c ***********************************************************************
c ***********************************************************************
C THE PROGRAMME COMPUTES THE EIGENVALUES OF A ROTATING CANTILEVER
C USING FINITE ELEMENT TECHNIQUE. 3-D  20-NODED ISOPARAMETRIC
C ELEMENTS WERE USED. THE EFFECT OF ROTATION IS EXPRESSED IN TERMS
C OF A SECONDARY STIFFNESS MATRIX CALLED STRESS STIFFENING MATRIX.
c TO DECREASE THE TIME CONSUMED IN EIGENVALUE EXTRACTION
C DYNAMIC CONDENSATION HAS BEEN PERFORMED WITH THE MASTER DEGREES
C OF FREEDOM AS w WHERE u,v,w ARE THE DEGREES OF FREEDOM AT A NODE.
C 42  ELEMENTS  WITH  362  NODES HAVE BEEN TAKEN.
c COORDINATES OF NODES ARE IN METERS
c ***********************************************************************
c ***********************************************************************

C ***********************************************************************
C NOMENCLATURE:-
C ***********************************************************************
C NFIX FIXED NODES
C COORD COORDINATES OF NODES OF AN ELEMENT
C GCOORD GLOBAL COORDINATES OF NODES
C SHP SHAPE FUNCTION MATRIX
C DSHP DERIVATIVE OF SHAPE FUNCTION MATRIX W.R.T. NATURAL COORD.
C EMASS  ELEMENT MASS MATRIX
C ESTIFF ELEMENT STIFFNESS MATRIX
C ESTSTIF ELEMENT STRESS STIFFENING MATRIX
C EFORCE ELEMENT FORCE MATRIX
C EDISP ELEMENT DISPLACEMENT MATRIX
C FVEC FORCE VECTOR FOR ALL 42 ELEMENTS
C FV ELEMENTAL FORCE VECTOR
C GFORCE GLOBAL FORCE MATRIX
C GSTIFF GLOBAL STIFFNESS MATRIX
C GMASS GLOBAL MASS MATRIX
C GSTR REDUCED STIFFNESS MATRIX
C GMASR REDUCED MASS MATRIX
C G 9x9  JACOBI MATRIX *9x60  DERIVATIVE SHAPE FUNCTION MATRIX
C GALL G FOR ALL 8 GAUSS POINTS
C DETALL DETERMINANT OF JACOBI3x3MATRIX AT 8 G.POINTS TO GET VOLUME
C VOL VOLUME OF AN ELEMENT
c GS21 2x1 PARTITION MATRIX OF GLOBAL STIFFNESS MATRIX
C GS22 2x2 PARTITION MATRIX OF GLOBAL STIFFNESS MATRIX
C T TRANSFORMATION MATRIX OF ORIG. DISP TO CONDENS. DISP
C TT TRANSPOSE OF TRANSFORMATION MATRIX
C ***********************************************************************
C ***********************************************************************


IMPLICIT REAL*8 (A-H,O-Z)
PARAMETER(NRA=1086,NC=724,NM=362)
DIMENSION NODE(20),X(20),Y(20),Z(20),NFIX(33),COORD(3,20),
     1 GCOORD(3,362),NDNUM(362),
     1 SHP(8,20),DSHP(3,8,20),
     1 ESTIFF(60,60),EMASS(60,60),ESTSTIF(60,60),
     1 EFORCE(60),EDISP(60,1),
     1 FVEC(3,42),FV(3),GDISP(1086),GFORCE(1086),
     1 GSTIFF(1086,1086),GMASS(1086,1086),GSTSTIF(1086,1086),
```

```
     1 G(9,60),GALL(9,60,8),DETALL(8),
     1 VOL(42),
     1 GS21(724,362),GS22(724,724),GS22INV(724,724),T21(724,362),
     1  T(1086,362),TT(362,1086),TTS(362,1086),TTM(362,1086),
     1 GSTR(362,362),GMASR(362,362)

COMPLEX*16 EVAL(362)
COMMON /WORKSP/ RWKSP
REAL RWKSP(6000000)
CALL IWKIN(6000000)
OPEN(UNIT=1,FILE='MESHBLADE42.INP',TYPE='OLD')
OPEN(UNIT=2,FILE='NODEBLADE42.INP',TYPE='OLD')
OPEN(UNIT=6,FILE='BLADEFIN.ANS',TYPE='NEW')
C fixed   nodes   ******************************************
DO 274 I=1,33
NFIX(I)=I
274 CONTINUE

C ***********************************************************************
C INITIALISATION OF GMASS GSTIFF GDISP GFORCE EDISP  matricies
c ***********************************************************************

DO 500 I=1,1086
GDISP(I)=0.
GFORCE(I)=0.
DO 500 J=1,1086
GMASS(I,J)=0.
GSTIFF(I,J)=0.
500 CONTINUE

DO 525 I=1,362
DO 525 J=1,1086
T(J,I)=0.
TT(I,J)=0.
525 CONTINUE

DO 550 I=1,60
EDISP(I,1)=0.
550 CONTINUE

DO 6 I=1,362
READ(1,*)NDNUM(I),GCOORD(1,I),GCOORD(2,I),GCOORD(3,I)
C WRITE(6,*)NDNUM(I),GCOORD(1,I),GCOORD(2,I),GCOORD(3,I)
6 CONTINUE

CALL SHAPE(SHP,DSHP)

DO 5 NE=1,42

READ(2,*)NELMT
READ(2,*)(NODE(I),I=1,20)

DO 7 I=1,20
K=NODE(I)
COORD(1,I)=GCOORD(1,K)
```

```
COORD(2,I)=GCOORD(2,K)
COORD(3,I)=GCOORD(3,K)
7 CONTINUE

CALL ELVOLUME(COORD,DSHP,VOLUME)
VOL(NE)=VOLUME

5 CONTINUE

CALL FORCE(VOL,FVEC)

REWIND(2)
DO 1500 NE=1,42

READ(2,*)NELMT
READ(2,*)(NODE(I),I=1,20)

DO 170 I=1,20
K=NODE(I)
COORD(1,I)=GCOORD(1,K)
COORD(2,I)=GCOORD(2,K)
COORD(3,I)=GCOORD(3,K)
170 CONTINUE

DO 80 I=1,3
FV(I)=FVEC(I,NE)
80 CONTINUE

CALL EMASTIF(COORD,SHP,DSHP,ESTIFF,EMASS,FV,EFORCE,GALL,DETALL)

C ***********************************************************************
C ASSEMBLY   IN THE CONDENSED  FORM
C ***********************************************************************


DO 23 I=1,20
DO 23 IDOF=1,3
IF(IDOF.EQ.1)IG=NM+NODE(I)*2-1
IF(IDOF.EQ.1)IE=I*3-2
IF(IDOF.EQ.2)IG=NM+NODE(I)*2
IF(IDOF.EQ.2)IE=I*3-1
IF(IDOF.EQ.3)IG=NODE(I)
IF(IDOF.EQ.3)IE=I*3

GFORCE(IG)=GFORCE(IG)+EFORCE(IE)

DO 23 J=1,20
DO 23 JDOF=1,3
IF(JDOF.EQ.1)JG=NM+NODE(J)*2-1
IF(JDOF.EQ.1)JE=J*3-2
IF(JDOF.EQ.2)JG=NM+NODE(J)*2
IF(JDOF.EQ.2)JE=J*3-1
IF(JDOF.EQ.3)JG=NODE(J)
IF(JDOF.EQ.3)JE=J*3
```

```
GSTIFF(IG,JG)=GSTIFF(IG,JG)+ESTIFF(IE,JE)
GMASS(IG,JG)=GMASS(IG,JG)+EMASS(IE,JE)
23 CONTINUE
1500 CONTINUE

C ***************************************************************************
C BOUNDARY CONDITIONS
C ***************************************************************************
DO 70  I=1,33

IG1=NFIX(I)
IG2=NM+NFIX(I)*2-1
IG3=NM+NFIX(I)*2

GFORCE(IG1)=0.
GFORCE(IG2)=0.
GFORCE(IG3)=0.

DO 70 NN=1,1086
GSTIFF(IG1,NN)=0.0
GSTIFF(IG2,NN)=0.0
GSTIFF(IG3,NN)=0.0
GSTIFF(NN,IG1)=0.0
GSTIFF(NN,IG2)=0.0
GSTIFF(NN,IG3)=0.0

GMASS(IG1,NN)=0.0
GMASS(IG2,NN)=0.0
GMASS(IG3,NN)=0.0
GMASS(NN,IG1)=0.0
GMASS(NN,IG2)=0.0
GMASS(NN,IG3)=0.0

70 CONTINUE

C ***************************************************************************
C POSITIVE  DEFINITE MATRIX
C ***************************************************************************
DO 800 I=1,1086
IF(GSTIFF(I,I).EQ.0.0) GSTIFF(I,I)=1E+20
800 CONTINUE

C IMSL SUBROUTINE FINDS THE GDISP FOR A SYMM. LINEAR SYSTEM  ****

CALL DLSASF(NRA,GSTIFF,NRA,GFORCE,GDISP)

c ***************************************************************************
c ELEMENT  DISP.  MATRIX
C ***************************************************************************

REWIND(2)
DO 1000 NE=1,42

READ(2,*)NELMT
READ(2,*)(NODE(I),I=1,20)
```

```
DO 17 I=1,20

MM1=NM+NODE(I)*2-1
MM2=NM+NODE(I)*2
MM3=NODE(I)

EDISP(3*I-2,1)=GDISP(MM1)
EDISP(3*I-1,1)=GDISP(MM2)
EDISP(3*I,1)=GDISP(MM3)

17 CONTINUE

CALL STRESS(EDISP,GALL,ESTSTIF,DETALL)

DO 231 II=1,20
DO 231 IDOF=1,3

IF(IDOF.EQ.1)IG=NM+NODE(II)*2-1
IF(IDOF.EQ.1)IE=II*3-2
IF(IDOF.EQ.2)IG=NM+NODE(II)*2
IF(IDOF.EQ.2)IE=II*3-1
IF(IDOF.EQ.3)IG=NODE(II)
IF(IDOF.EQ.3)IE=II*3

DO 231 JJ=1,20
DO 231 JDOF=1,3

IF(JDOF.EQ.1)JG=NM+NODE(JJ)*2-1
IF(JDOF.EQ.1)JE=JJ*3-2
IF(JDOF.EQ.2)JG=NM+NODE(JJ)*2
IF(JDOF.EQ.2)JE=JJ*3-1
IF(JDOF.EQ.3)JG=NODE(JJ)
IF(JDOF.EQ.3)JE=JJ*3

GSTSTIF(IG,JG)=GSTSTIF(IG,JG)+ESTSTIF(IE,JE)

231 CONTINUE

1000 CONTINUE

DO 600 I=1,1086
DO 600 J=1,1086
GSTIFF(I,J)=GSTIFF(I,J)+GSTSTIF(I,J)
600 CONTINUE

DO 700 I=1,1086
IF(GSTIFF(I,I).EQ.0.0) GSTIFF(I,I)=1E+20
700 CONTINUE

DO 52 I=1,724
DO 52 J=1,362
GS21(I,J)=GSTIFF(362+I,J)
52 CONTINUE
```

```
DO 54 I=1,724
DO 54 J=1,724
GS22(I,J)=GSTIFF(362+I,362+J)
54 CONTINUE

C ***********************************************************************
C   CONDENSED  MASS AND STIFFNESS MATRICIES
C ***********************************************************************
CALL DLINDS(NC,GS22,NC,GS22INV,NC)
CALL MATMUL(GS22INV,GS21,T21,724,724,362)

DO 270 I=1,362
T(I,I)=1.
270 CONTINUE

DO 280 I=1,724
DO 280 J=1,362
T(I+362,J)=-T21(I,J)
280 CONTINUE

DO 290 I=1,362
DO 290 J=1,1086
TT(I,J)=T(J,I)
290 CONTINUE

CALL MATMUL(TT,GSTIFF,TTS,362,1086,1086)
CALL MATMUL(TTS,T,GSTR,362,1086,362)

CALL MATMUL(TT,GMASS,TTM,362,1086,1086)
CALL MATMUL(TTM,T,GMASR,362,1086,362)

DO 350 I=1,362
DO 350 J=1,362
GSTR(I,J)=1.E-14*GSTR(I,J)
350 CONTINUE

DO 750 I=1,362
IF(GSTR(I,I).EQ.0.0) GSTR(I,I)=1E+20
IF(GMASR(I,I).EQ.0.0) GMASR(I,I)=1E-10
750 CONTINUE

CALL EIGEN(GMASR,GSTR,EVAL)

STOP
END

C ***********************************************************************

      SUBROUTINE EIGEN(B,A,EVAL)
C ***********************************************************************

PARAMETER (N=362)
DOUBLE PRECISION A(N,N),AMACH,B(N,N),BETA(N),GPIRG,PI
DOUBLE COMPLEX ALPHA(N),EVAL(N),EVEC(N,N)
EXTERNAL AMACH,GPIRG,GVCRG,UMACH,WRCRN
```

```
CALL DGVCRG(N,A,N,B,N,ALPHA,BETA,EVEC,N)
PI=3.1415926
DO 10 I=1,N
IF(BETA(I).NE.0.) THEN
EVAL(I)=ALPHA(I)/BETA(I)
ELSE
EVAL(I)=AMACH(2)
END IF
10 CONTINUE

DO 20 I=1,30
WRITE(6,*)'EVAL RPS ',I
WRITE(6,*)EVAL(I)**.5/(2.*PI)
20 CONTINUE

CALL DWRCRN('EVEC',N,N-347,EVEC,N,0)
RETURN
END

c ***********************************************************************
SUBROUTINE EMASTIF(COORD,SHP,DSHP,ESTIFF,EMASS,FV,EFORCE,
     1 GALL,DETALL)
C ***********************************************************  *******
IMPLICIT REAL*8 (A-H,O-Z)
PARAMETER(NJ=3)
DIMENSION C(6,9),AJ(9,9),DS(9,60),DSHP(3,8,20),SHP(8,20),
     1 D(6,6),CAJ(6,9),B(6,60),BT(60,6),BTD(60,6),ESTIFF(60,60),
     1 EMASS(60,60),COORD(3,20),AJINV(3,3),AN(3,60),ANT(60,3),
     1 BTDB(60,60),ANTN(60,60),ANTNR(60,60),WT(8),AJAC(3,3),
     1 FV(3),EFORCE(60),ANTF(60,1),ESTSTIF(60,60),
     1 GALL(9,60,8),DETALL(8),G(9,60)

DATA WT/8*1./
ROE=7850.
ANUE=.3
ELAS=20.6E10
COEF=ELAS*(1.-ANUE)/((1.+ANUE)*(1.-2.*ANUE))
CN1=ANUE/(1.-ANUE)
CN2=.5*(1.-2.*ANUE)/(1.-ANUE)
C ***********************************************************************
C                          INITIALIZATION
C ***********************************************************************
DO 112 I=1,60
EFORCE(I)=0.
ANTF(I,1)=0.
DO 112 J=1,60
EMASS(I,J)=0.
ESTIFF(I,J)=0.
BTDB(I,J)=0.
ANTNR(I,J)=0.
ANTN(I,J)=0.
112 CONTINUE

DO 116 I=1,9
DO 116 J=1,9
```

```
AJ(I,J)=0.
116 CONTINUE
DO 118 I=1,9
DO 118 J=1,60
DS(I,J)=0.
118 CONTINUE
DO 122 I=1,6
DO 122 J=1,60
B(I,J)=0.
BT(J,I)=0.
BTD(J,I)=0.
122 CONTINUE

DO 111 I=1,6
DO 111 J=1,9
C(I,J)=0.
111 CONTINUE
DO 36 I=1,3
DO 36 J=1,60
AN(I,J)=0.
ANT(J,I)=0.
36 CONTINUE
DO 115 I=1,6
DO 115 J=1,6
D(I,J)=0.
115 CONTINUE

C(1,1)=1.
C(2,5)=1.
C(3,9)=1.
C(4,2)=1.
C(4,4)=1.
C(5,6)=1.
C(5,8)=1.
C(6,3)=1.
C(6,7)=1.
c   D  MATRIX (6x6) ************************************
D(1,1)=1.
D(1,2)=CN1
D(1,3)=CN1
D(2,2)=1.
D(2,3)=CN1
D(3,3)=1.
D(4,4)=CN2
D(5,5)=CN2
D(6,6)=CN2
D(2,1)=CN1
D(3,1)=CN1
D(3,2)=CN1
DO 30 I=1,6
DO 30 J=1,6
D(I,J)=COEF*D(I,J)
30 CONTINUE

DO 1000 N=1,8
```

```
DO 120 I=1,3
DO 120 J=1,3
AJAC(I,J)=0.
DO 120 K=1,20
SUM=COORD(J,K)*DSHP(I,N,K)
AJAC(I,J)=AJAC(I,J)+SUM
120 CONTINUE

DET=AJAC(1,1)*(AJAC(2,2)*AJAC(3,3)-AJAC(3,2)*AJAC(2,3))-
     1 AJAC(1,2)*(AJAC(2,1)*AJAC(3,3)-AJAC(3,1)*AJAC(2,3))+
     1 AJAC(1,3)*(AJAC(2,1)*AJAC(3,2)-AJAC(2,2)*AJAC(3,1))

CALL DLINRG(NJ,AJAC,NJ,AJINV,NJ)

DO 44 I=1,3
DO 44 J=1,3
AJ(I,J)=AJINV(I,J)
44 CONTINUE
DO 15 I=4,6
DO 15 J=4,6
AJ(I,J)=AJINV(I-3,J-3)
15 CONTINUE
DO 20 I=7,9
DO 20 J=7,9
AJ(I,J)=AJINV(I-6,J-6)
20 CONTINUE

DO 25 I=1,3
DO 25 K=1,20
II=1+3*(K-1)
DS(I,II)=DSHP(I,N,K)
DS(I+3,II+1)=DSHP(I,N,K)
DS(I+6,II+2)=DSHP(I,N,K)
25 CONTINUE

CALL MATMUL(C,AJ,CAJ,6,9,9)
CALL MATMUL(CAJ,DS,B,6,9,60)
CALL MATMUL(AJ,DS,G,9,9,60)

DETALL(N)=DET
DO 331 I=1,9
DO 331 J=1,60
GALL(I,J,N)=G(I,J)
331 CONTINUE

DO 35 I=1,6
DO 35 J=1,60
BT(J,I)=B(I,J)
35 CONTINUE

DO 37 I=1,3
DO 37 M=1,20
MM=I+(M-1)*3
AN(I,MM)=SHP(N,M)
```

```
37 CONTINUE

DO 38 I=1,60
DO 38 J=1,3
ANT(I,J)=AN(J,I)
38 CONTINUE

CALL MATMUL(BT,D,BTD,60,6,6)
CALL MATMUL(BTD,B,BTDB,60,6,60)
CALL MATMUL(ANT,AN,ANTN,60,3,60)
CALL MATMUL(ANT,FV,ANTF,60,3,1)

DO 39 I=1,60
DO 39 J=1,60
ANTNR(I,J)=ROE*ANTN(I,J)
39 CONTINUE

DO 40 I=1,60
PRF=DET*WT(N)*ANTF(I,1)
EFORCE(I)=EFORCE(I)+PRF
DO 40 J=1,60
PRST=DET*WT(N)*BTDB(I,J)
PRMAS=DET*WT(N)*ANTNR(I,J)
ESTIFF(I,J)=ESTIFF(I,J)+PRST
EMASS(I,J)=EMASS(I,J)+PRMAS
40 CONTINUE

1000 CONTINUE

RETURN
END

C ***********************************************************************
C SUBROUTINE FOR CALCULATING STRESS STIFFENING MATRIX
C ***********************************************************************
SUBROUTINE STRESS(EDISP,GALL,ESTSTIF,DETALL)
IMPLICIT REAL*8 (A-H,O-Z)
DIMENSION ESTSTIF(60,60),WT(8),
     1 G(9,60),GT(60,9),S(9,9),GTS(60,9),GTSG(60,60),
     1 EG1(3,9),EG2(3,9),EG3(3,9),CA(1,3),CB(1,3),CC(1,3),
     1 EG1G(3,60),EG2G(3,60),EG3G(3,60),
     1 EDISP(60,1),GP1(3,1),GP2(3,1),GP3(3,1),
     1 S1A(3,3),S1B(3,3),S1C(3,3),S11(3,3),
     1 GALL(9,60,8),DETALL(8)

DATA WT/8*1./
ELAS=20.6E10
ANUE=.3
GEE=ELAS/((1.+ANUE)*2.)

DO 52 I=1,3
DO 52 J=1,9
EG1(I,J)=0.
EG2(I,J)=0.
EG3(I,J)=0.
```

```
52 CONTINUE

DO 154 I=1,60
DO 154 J=1,60
ESTSTIF(I,J)=0.
GTSG(I,J)=0.
154 CONTINUE

DO 50 I=1,3
GP1(I,1)=0.
GP2(I,1)=0.
GP3(I,1)=0.
50 CONTINUE

DO 30 I=1,3
DO 30 J=1,3
S1A(I,J)=0.
S1B(I,J)=0.
S1C(I,J)=0.
S11(I,J)=0.
30 CONTINUE

DO 58 I=1,9
DO 58 J=1,9
S(I,J)=0.
58 CONTINUE

EG1(1,1)=ELAS
EG1(2,2)=GEE
EG1(2,4)=GEE
EG1(3,3)=GEE
EG1(3,7)=GEE

EG2(1,2)=GEE
EG2(1,4)=GEE
EG2(2,5)=ELAS
EG2(3,6)=GEE
EG2(3,8)=GEE

EG3(1,3)=GEE
EG3(1,7)=GEE
EG3(2,6)=GEE
EG3(2,8)=GEE
EG3(3,9)=ELAS

CA(1,1)=1.
CA(1,2)=0.
CA(1,3)=0.

CB(1,1)=0.
CB(1,2)=1.
CB(1,3)=0.

CC(1,1)=0.
CC(1,2)=0.
```

```
CC(1,3)=1.

DO 1000 NP=1,8

DO 139 I=1,9
DO 139 J=1,60
G(I,J)=GALL(I,J,NP)
139 CONTINUE

DO 136 I=1,9
DO 136 J=1,60
GT(J,I)=G(I,J)
136 CONTINUE

CALL MATMUL(EG1,G,EG1G,3,9,60)
CALL MATMUL(EG1G,EDISP,GP1,3,60,1)
CALL MATMUL(GP1,CA,S1A,3,1,3)

CALL MATMUL(EG2,G,EG2G,3,9,60)
CALL MATMUL(EG2G,EDISP,GP2,3,60,1)
CALL MATMUL(GP2,CB,S1B,3,1,3)

CALL MATMUL(EG3,G,EG3G,3,9,60)
CALL MATMUL(EG3G,EDISP,GP3,3,60,1)
CALL MATMUL(GP3,CC,S1C,3,1,3)

DO 54 I=1,3
DO 54 J=1,3
S11(I,J)=S1A(I,J)+S1B(I,J)+S1C(I,J)

S(I,J)=S11(I,J)
S(I+3,J+3)=S11(I,J)
S(I+6,J+6)=S11(I,J)
54 CONTINUE

CALL MATMUL(GT,S,GTS,60,9,9)
CALL MATMUL(GTS,G,GTSG,60,9,60)

DET=DETALL(NP)

DO 40 I=1,60
DO 40 J=1,60
PR=DET*WT(NP)*GTSG(I,J)
ESTSTIF(I,J)=ESTSTIF(I,J)+PR
40 CONTINUE

1000 CONTINUE

RETURN
END

c ***************************************************************************
c subroutine for matrix multiplication
c ***************************************************************************
SUBROUTINF MATMUL(A,B,C,I,J,K)
```

```
IMPLICIT REAL*8 (A-H,O-Z)
DIMENSION A(I,J),B(J,K),C(I,K)
DO 88 II=1,I
DO 88 KK=1,K
SUM=0.
DO 77 JJ=1,J
SUM=SUM+A(II,JJ)*B(JJ,KK)
77 CONTINUE
C(II,KK)=SUM
88 CONTINUE
RETURN
END

C ***************************************************************************
SUBROUTINE SHAPE(SHP,DSHP)
C ***************************************************************************
IMPLICIT REAL*8 (A-H,O-Z)
DIMENSION ZE(20),EE(20),ZT(20),F(24),SHP(8,20),DSHP(3,8,20),
     1 GP(2)
DATA GP/-0.577350269189626,0.577350269189626/

C the NODE numbering has been started for the bottom face with
c 1 at the left front end ***************************************

DATA ZE/1.,1.,-1.,-1.,1.,1.,-1.,-1.,1.,0.,-1.,0.,
     1 1.,0.,-1.,0.,1.,1.,-1.,-1./
DATA EE/-1.,1.,1.,-1.,-1.,1.,1.,-1.,0.,1.,0.,-1.,
     1 0.,1.,0.,-1.,-1.,1.,1.,-1./
DATA ZT/-1.,-1.,-1.,-1.,1.,1.,1.,1.,-1.,-1.,-1.,-1.,
     1 1.,1.,1.,1.,0.,0.,0.,0./

C for corner nodes  1 2 3 4 5 6 7 8 *****************************

M=0.
DO 4 J=1,2
DO 4 K=1,2
DO 4 L=1,2
M=M+1
F(M)=GP(J)
M=M+1
F(M)=GP(K)
M=M+1
F(M)=GP(L)
4 CONTINUE

LL=0.

DO 2000 N=1,8

LL=1+(N-1)*3
AZE=F(LL)
AEE=F(LL+1)
AZT=F(LL+2)

DO 55 I=1,8
```

```
SHP(N,I)=1./8.*(1.+AZE*ZE(I))*(1.+AEE*EE(I))*(1.+AZT*ZT(I))*
     1 (AZE*ZE(I)+AEE*EE(I)+AZT*ZT(I)-2.)
DSHP(1,N,I)=1./8.*ZE(I)*(1.+AEE*EE(I))*(1.+AZT*ZT(I))*
     1 (2.*AZE*ZE(I)+AEE*EE(I)+AZT*ZT(I)-1.)
DSHP(2,N,I)=1./8.*EE(I)*(1.+AZT*ZT(I))*(1.+AZE*ZE(I))*
     1 (2.*AEE*EE(I)+AZT*ZT(I)+AZE*ZE(I)-1.)
DSHP(3,N,I)=1./8.*ZT(I)*(1.+AZE*ZE(I))*(1.+AEE*EE(I))*
     1 (2.*AZT*ZT(I)+AZE*ZE(I)+AEE*EE(I)-1.)
55 CONTINUE
C for nodes with ZE=0.   10 14 16 12 ****************************
DO 99 I=10,16
IF(I.EQ.10)J2=I
IF(I.EQ.12)J2=I
IF(I.EQ.14)J2=I
IF(I.EQ.16)J2=I
SHP(N,J2)=1./4.*(1.-AZE**2)*(1.+AEE*EE(J2))*(1.+AZT*ZT(J2))
DSHP(1,N,J2)=-1./2.*AZE*(1.+AEE*EE(J2))*(1.+AZT*ZT(J2))
DSHP(2,N,J2)=1./4.*EE(J2)*(1.-AZE**2)*(1.+AZT*ZT(J2))
DSHP(3,N,J2)=1./4.*ZT(J2)*(1.-AZE**2)*(1.+AEE*EE(J2))
99 CONTINUE
C for nodes with EE=0.  9 11 15 13 ****************************
DO 90 I=9,15
IF(I.EQ.9)J3=I
IF(I.EQ.11)J3=I
IF(I.EQ.13)J3=I
IF(I.EQ.15)J3=I
SHP(N,J3)=1./4.*(1.-AEE**2)*(1.+AZT*ZT(J3))*(1.+AZE*ZE(J3))
DSHP(1,N,J3)=1./4.*ZE(J3)*(1.-AEE**2)*(1.+AZT*ZT(J3))
DSHP(2,N,J3)=-1./2.*AEE*(1.+AZT*ZT(J3))*(1.+AZE*ZE(J3))
DSHP(3,N,J3)=1./4.*ZT(J3)*(1.-AEE**2)*(1.+AZE*ZE(J3))
90 CONTINUE
C for nodes with ZT=0.  17 18 19 20  ****************************
DO 95 J4=17,20
SHP(N,J4)=1./4.*(1.-AZT**2)*(1.+AZE*ZE(J4))*(1.+AEE*EE(J4))
DSHP(1,N,J4)=1./4.*ZE(J4)*(1.-AZT**2)*(1.+AEE*EE(J4))
DSHP(2,N,J4)=1./4.*EE(J4)*(1.-AZT**2)*(1.+AZE*ZE(J4))
DSHP(3,N,J4)=-1./2.*AZT*(1.+AZE*ZE(J4))*(1.+AEE*EE(J4))
95 CONTINUE
2000 CONTINUE

RETURN
END

C ***********************************************************************
SUBROUTINE ELVOLUME(COORD,DSHP,VOLUME)
C ***********************************************************************
IMPLICIT REAL*8 (A-H,O-Z)
DIMENSION COORD(3,20),DSHP(3,8,20),AJAC(3,3),WT(8)

DATA WT/8*1./
VOLUME=0.

DO 1000 N=1,8

DO 120 I=1,3
```

```
      DO 120 J=1,3
      AJAC(I,J)=0.
      DO 120 K=1,20
      SUM=COORD(J,K)*DSHP(I,N,K)
      AJAC(I,J)=AJAC(I,J)+SUM
      120 CONTINUE

      DET=AJAC(1,1)*(AJAC(2,2)*AJAC(3,3)-AJAC(3,2)*AJAC(2,3))-
          1 AJAC(1,2)*(AJAC(2,1)*AJAC(3,3)-AJAC(3,1)*AJAC(2,3))+
          1 AJAC(1,3)*(AJAC(2,1)*AJAC(3,2)-AJAC(2,2)*AJAC(3,1))

      VOLUME=VOLUME+DET*WT(N)

      1000 CONTINUE

      RETURN
      END

C ***********************************************************************
      SUBROUTINE FORCE(VOL,FVEC)
C ***********************************************************************

      IMPLICIT REAL*8 (A-H,O-Z)
      DIMENSION XL(8),FRC(8),FVEC(3,42),VCOL(7),VRATIO(7,6),VOL(42),
          1 FELM(42),FCOL(7)
      DATA XL/0.,.14285,.2857,.4285,.5714,.7142,.857,1./
      PI=3.1415926

      DO 5 I=1,8
      FRC(I)=0.
      5 CONTINUE

      K=0
      DO 10 I=1,7
      VCOL(I)=0.
      DO 10 J=1,6
      K=K+1
      VCOL(I)=VCOL(I)+VOL(K)
      10 CONTINUE

      K=0
      DO 15 I=1,7
      DO 15 J=1,6
      K=K+1
      VRATIO(I,J)=VOL(K)/VCOL(I)
      15 CONTINUE

      BL=2.8
      A1=.34109902
      A2=.1620474
      A3=2.0524507E-2
      A4=-4.319239E-2

      R=.7
      ROE=7850.
```

```
c WS=0.
WS=2.*PI*5.
C WS=2.*PI*10.
C WS=2.*PI*15.
C WS=2.*PI*20.

A11=A1/BL**2
A12=A2/BL
A13=A3
A14=A4*BL
RN=R/BL

DO 18 I=1,8
XX=XL(I)
F1=A11*RN*(1.-XX)
F2=(A11+A12*RN)*(1.-XX**2)/2.
F3=(A12+A13*RN)*(1.-XX**3)/3.
F4=(A13+A14*RN)*(1.-XX**4)/4.
F5=A14*(1.-XX**5)/5.
FRC(I)=(F1+F2+F3+F4+F5)*ROE*WS**2*BL**4
18 CONTINUE

DO 24 I=1,3
DO 24 J=1,42
FVEC(I,J)=0.
24 CONTINUE

K=0
DO 20 I=1,7
FCOL(I)=FRC(I)-FRC(I+1)
DO 20 J=1,6
K=K+1
FELM(K)=FCOL(I)*VRATIO(I,J)
FVEC(1,K)=FELM(K)/VOL(K)
20 CONTINUE
RETURN
END
```

Appendix Q

COMPUTER PROGRAM FOR COMPUTING THE NATURAL FREQUENCY OF THE ROTOR-SHAFT SYSTEM

```
C  ************************************************************************
C  ************************************************************************
C  ********  THE PROGRAM FINDS THE NATURAL WHIRLING FREQ. OF THE     **
C  ********  ROTOR-SHAFT SYSTEM.                                     **
C  ********  ADDED MASS DUE TO WATER IS TAKEN INTO WATER.            **
C  ********  FORWARD/REVERSE WHIRL FREQ. ARE GOT.                    **
C  ********  SHEAR DEFLECTION EFFECTS HAVE BEEN CONSIDERED           **
C  ************************************************************************

C  ************************************************************************
C  NOMENCLATURE:-
C  ************************************************************************
C  EE1,EE2  = ROOTS OF THE EQUATION FOR THE ROTOR
C  AL       = ROOTS OF THE EQUATION FOR THE TAILSHAFT AND THE OVERHANG
C  Q1       = COEFFICIENTS OF THE DISPLACEMENT FUNCTION FOR T.SHAFT
C  FUN      = CHARACTERISTIC EQUATION
C  AMS      = MASS PER UNIT LENGTH OF SHAFT
C  AMR      = MASS PER UNIT LENGTH OF ROTOR
C  AMOMS    = AREA MOMENT OF INERTIA OF SHAFT
C  AMOMR    = AREA MOMENT OF INERTIA OF ROTOR
c  A,B,C    = NON-DIMENSIONAL LENGTH OF SHAFT SEGMENTS
C  ************************************************************************
C  ************************************************************************
DIMENSION RPS(6)
OPEN (UNIT=6,FILE='SHAFTFREQ.ANS',TYPE='NEW')
PI=3.1415927
DATA RPS/.1,1.,2.,3.,4.,5./

DO 30 I=1,6
OMEGA=2.*PI*RPS(I)
C  FIRST ITERATION**************************

W=1.
10 W=W+.01
CALL QFUNCTION(W,FUN,AL,EE1,EE2,OMEGA,Q1,Q2,Q3,Q4,EFS)
IF(ABS(FUN).EQ.FUN)GO TO 20
GO TO 10
C SECOND ITERATION**************************

20 W=W-.001
CALL QFUNCTION(W,FUN,AL,EE1,EE2,OMEGA,Q1,Q2,Q3,Q4,EFS)
IF(FUN.LT.ABS(FUN))GO TO 100
GO TO 20

100 WRITE(6,*)OMEGA*W,Q1,Q2,Q3,Q4,AL

30 CONTINUE
IF(EFS.LT.1.)WRITE(6,*)'REVERSE  WHIRL'
IF(EFS.GT.1.)WRITE(6,*)'FORWARD  WHIRL'
STOP
END


C ***************************************************************
SUBROUTINE QFUNCTION(W,FUN,AL,EE1,EE2,OMEGA,Q1,Q2,Q3,Q4,EFS)
```

```
C ****************************************************************
PI=3.1415927
ELAS=20.6E10
SHEAR=ELAS/(2.*1.3)
RAD=.35
RROT=2.*RAD
AN=W/OMEGA

ALEN=16.
BLEN=2.
CLEN=4.*RAD
TLEN=ALEN+BLEN+CLEN
A=ALEN/TLEN
B=BLEN/TLEN
C=CLEN/TLEN

C ****************************************************************
C FORWARD/REVERSE   WHIRL
C ****************************************************************
EFS=1.-2./AN
c EFS=1.+2./AN
C ****************************************************************

C ****************************************************************
C SHEAR DEFLECTION EFFECT
C ****************************************************************
C AK=0.
AK=1./.9
C ****************************************************************

C ****************************************************************
C ADDED MASS DUE TO WATER
C ****************************************************************
C ROE=7850.
ROE=7850.*1.25
C ****************************************************************

C ****************************************************************
C DEGREE OF FIXITY
C ****************************************************************
STIF=0.
C STIF=1.E+5
C ****************************************************************

AREA=PI*RAD**2
AROT=PI*RROT**2
AMS=ROE*AREA
AMR=ROE*AROT
AMOMS=AREA*RAD**2/4.
AMOMR=AROT*RROT**2/4.

ZETA1=ROE*AMOMR/AMR
ZETAR=ELAS*AMOMR/(AMR*OMEGA**2*TLEN**4)
ZETAS=ELAS*AMOMS/(AMS*OMEGA**2*TLEN**4)
```

```
C1=ZETA1*W**2*(EFS+AK*ELAS/SHEAR)/(ZETAR*TLEN**2)
C2=W**2*(AK*ZETA1*ROE*OMEGA**2*W**2*EFS/SHEAR-1.)/ZETAR

DISC=(C1**2-4.*C2)**.5

EE1=((-C1+DISC)/2.)**.5
EE2=((C1+DISC)/2.)**.5
  AL=(W**2/ZETAS)**.25

ALB=AL*B
ALA=AL*A
SL=SIN(ALB)
CL=COS(ALB)
SHL=SINH(ALB)
CHL=COSH(ALB)

SA=SIN(ALA)
CA=COS(ALA)
SHA=SINH(ALA)
CHA=COSH(ALA)

ALP1=-(2.*AL*SHA+STIF*(CHA-CA))/(2.*AL*SA+STIF*(CHA-CA))
ALP2=(STIF*SHA-STIF*SA)/(2.*AL*SA+STIF*(CHA-CA))

W1=ALP1*SA+ALP2*(CA+CHA)-SHA
W2=ALP1*CA-ALP2*(SA+SHA)+CHA

ANU=EE2/AL
GAM=EE1/EE2
BETA1=EE1*C
BETA2=EE2*C

CB=COS(BETA2)
SB=SIN(BETA2)
CHB=COSH(BETA1)
SHB=SINH(BETA1)

GM3=GAM**3
GM2=GAM**2
PH1=GM3*CB*CHB+GM2*SB*SHB
PH2=GM3*CB*SHB+GM2*SB*CHB
PH3=GM2*CB*SHB-GM3*SB*CHB
PH4=GM2*CB*CHB-GM3*SB*SHB

CN1=1.+ANU**2
CN2=1.-ANU**2
CN3=1.-(GAM*ANU)**2
CN4=1.+(GAM*ANU)**2

TH1=CN1*PH3*CL-ANU*(CN1*PH1+GAM*CN3)*SL+
     1 CN2*PH3*CHL-ANU*(CN2*PH1+GAM*CN4)*SHL
TH2=-((CN1*PH4+CN3)*CL-ANU*CN1*PH2*SL+
     1 (CN2*PH4+CN4)*CHL-ANU*CN2*PH2*SHL)

TH3=TH2/TH1
```

```
R1=.5*(CN1*PH3*TH3+CN1*PH4+CN3)
R2=.5*ANU*((CN1*PH1+GAM*CN3)*TH3+CN1*PH2)
R3=.5*(CN2*PH3*TH3+CN2*PH4+CN4)
R4=.5*ANU*((CN2*PH1+GAM*CN4)*TH3+CN2*PH2)

X1=R1*SL+R2*CL
X2=-R2*SL+R1*CL
X3=R4*CHL-R3*SHL

C ****************************************************************
C EIGEN VECTOR CALCULATION
C ****************************************************************
A1=1.
A4=A1/(PH1*TH3+PH2)
A2=A4*(PH3*TH3+PH4)
A3=TH3*A4

P1=X1*A4
P2=X2*A4
P3=X3*A4
P4=-P2

Q3=2.*P2/(ALP1*SIN(ALA)+ALP2*(COS(ALA)+COSH(ALA))-SINH(ALA))
Q1=ALP1*Q3
Q2=ALP2*Q3
Q4=-Q2

FUN=(X1+X3)*W1-2.*X2*W2

RETURN
END
```